Adaptive Resource Allocation for Wireless Body Sensor Networks

---

A thesis submitted in partial fulfilment of the requirements for the degree of

Doctor of Philosophy

presented by

Ehsan Tabatabaei Yazdi

Supervising Committee:

Dr. Andreas Willig (Senior Supervisor)

Professor Krys Pawlikowski (Associate Supervisor)

Examining Committee:

Associate Professor Nevil Brownlee (Oral Examiner)

Professor Ahmet Sekercioglu (International Examiner)

University of Canterbury

July, 2014

Abstract

Wireless Body Sensor Network (WBSN) technologies are one of the main research fields in the health care and entertainment industry. These technologies aim to one day become mature enough to improve the quality of human life. For example, WBSN technologies are able to control and monitor the health status of a patient at all times, alert patients or practitioners about abnormal physical health status that otherwise would have been ignored or remained unnoticed by the patient, give enough time to the patient to seek medical care, and thus help to cure illness before symptoms become visible or the physical health of the patient becomes critical. They allow elderly and chronically ill people to maintain their independence without need for constant supervision or the presence of caregivers.

WBSNs are an attractive proposal for such scenarios due to the ease of installation, their small size, low cost, low power consumption and low maintenance. Although WBSNs have significant benefits, their characteristics create numerous challenges, namely: network mobility in urban environments, interference caused by other technologies sharing the same frequency band, and most importantly, limited resources such as finite power supply, computational power, storage capacity and communication capabilities.

This thesis investigates adaptive resource allocation embedded into IEEE 802.15.4-based WBSNs with the aim to address the interference problem while reducing the overall energy consumed. In particular, the primary goal of this thesis is to maintain a reliable data communication between sensor nodes and their corresponding coordinator node by physical-layer resource allocation (frequency, and transmit power). Furthermore, our secondary goal is to increase the overall lifetime of the network by optimising energy consumption of the WBSN nodes. All these require the pro-

tocol running on the WBSN to be not only energy-efficient, robust and reliable, but also *adapt* to an ever changing interference background. To achieve these goals, an adaptive scheme embedded into real WBSN nodes to cope with interference changes within a variety of interference conditions is introduced.

All proposed schemes in this thesis are compared in different case studies, demonstrating the behaviour of each scheme under varying levels of interference source density and interference traffic intensity. Issues and challenges pertaining to reliability, energy-efficiency and robustness are addressed and investigated by conducting comprehensive simulation studies. Beyond this, some of the most promising of the proposed schemes are also evaluated via an experimental implementation to further validate the simulation results in a real life scenario and to assess the feasibility of embedding the proposed schemes on existing WSN nodes.

In the first stage, the IEEE 802.15.4 standard is compared with the so-called *genie* scheme. The genie scheme is a hypothetical scheme designed to illustrate the upper bounds of what is achievable in terms of successful data transmission when a WBSN is faced with an ever changing interference background and when all the WBSN nodes have global information of the channel quality for all available frequencies. An important conclusion from this study is that frequency adaptation *can* lead to an 80% increase in the fraction of successfully delivered data packets when compared with the no-adaptation scheme (IEEE 802.15.4 standard).

Next, periodic frequency adaptation schemes are explored. Finally, a further class of frequency adaptation schemes called *Lazy* schemes is proposed. The presented results suggest that the Lazy scheme is the most suitable adaptation approach for WBSNs to be used in harsh urban environments, as the Lazy scheme shows comparable performance to the genie scheme in terms of transmission success rates while reducing the overall consumed energy. To improve the Lazy scheme, different coordinator discovery schemes are proposed. However, contrary to our predictions, the performance evaluation results reveal that the proposed passive coordinator

discovery schemes lead to insignificant improvements in the overall successful data communication rates and energy consumption of the WBSNs. The relative performance trends between the IEEE 802.15.4 standard, a periodic adaptation scheme and the Lazy scheme are also confirmed experimentally by measurements. For these experiments an implementation of these schemes has been developed.

Finally, after implementation of the proposed Lazy scheme on existing WSN nodes, the effects of transmit-power variation and coupling variation of transmit-power with frequency adaptation is evaluated for interference mitigation in WBSNs. The simulation results showed that the upper bound of transmit-power adaptation alone has a significantly lower performance improvement than the frequency adaptation in environments with high WiFi interference. Furthermore, coupling maximum transmit-power with frequency adaptation, increases the data communication reliability and also reduces the overall energy consumption of the sensor nodes, by lowering the orphaning time, for scenarios with high WiFi interference.

Finally, the effects of coupling variation of transmit-power with frequency adaptation for interference mitigation in WBSNs are evaluated. The simulation results show overall that for high-interference scenarios frequency adaptation alone has a much stronger impact on performance than transmit power alone. Furthermore, employing frequency adaptation and using the maximum transmit power increases the data communication reliability and at the same time reduces the overall energy consumption of the sensor nodes. The results shown in this thesis suggest that the Adaptive-Lazy scheme shows significant improvements over the existing IEEE 802.15.4 standard and the Lazy scheme without transmit-power adaptation in scenarios with varying interferer densities and intensities. There is a strong prospect for the proposed scheme to be used in WBSN applications.

Publications

Related Journal and Conference Publications:

Yazdi, E.T. and Willig, A. and Pawlikowski, K., "Frequency Adaptation for Interference Mitigation in IEEE 802.15.4-Based Mobile Body Sensor Networks". *Computer Communications*, volume 53, number 0, pages 102-119, 2014.
URL http://www.sciencedirect.com/science/article/pii/S014036641400245X

Yazdi, E.T. and Moravejosharieh, A. and Willig, A. and Pawlikowski, K., "Coupling Power and Frequency Adaptation for Interference Mitigation in IEEE 802.15.4 Based Mobile Body Sensor Networks: Part II", In *2014 IEEE International Conference on Australasian Telecommunication Networks and Applications Conference (ATNAC)*, 2014. (Accepted)

Yazdi, E.T. and Willig, A. and Pawlikowski, K., "Coupling Power and Frequency Adaptation for Interference Mitigation in IEEE 802.15.4 Based Mobile Body Sensor Networks", In *2014 IEEE* 9^{th} *International Conference on Intelligent Sensors, Sensor Networks and Information Processing (ISSNIP)*, pages 1-6, April 2014.

Yazdi, E.T. and Willig, A. and Pawlikowski, K., "Shortening Orphan Time in IEEE 802.15.4: What can be Gained?", In *2013* 19^{th} *IEEE International Conference on Networks (ICON)*, pages 1-6, December 2013.

Yazdi, E.T. and Willig, A. and Pawlikowski, K., "On channel adaptation in IEEE 802.15.4 mobile body sensor networks: What can be Gained?", In *2012* 18^{th} *IEEE International Conference on Networks (ICON)*, pages 262-267, December 2012.

Other Publications:

Moravejosharieh, A. and Yazdi, E.T. and Willig, A. and Pawlikowski, K., "Adaptive Channel Utilisation in IEEE 802.15.4 Wireless Body Sensor Networks: Continuous Hopping Approach", In *IEEE International Conference on Australasian Telecommunication Networks and Applications Conference (ATNAC)*, 2014. (Accepted)

Yazdi, E.T. and Moravejosharieh, A. and Kumar Ray, S., "Study of Target Tracking and Handover in Mobile Wireless Sensor Network", In *IEEE* 28^{th} *International Conference on Information Networking (ICOIN)*, pages 120-125, 10^{th} of February 2014.

Moravejosharieh, A. and Yazdi, E.T. and Willig, A., "Study of Resource Utilisation in IEEE 802.15.4 Wireless Body Sensor Network, Part II: Greedy Channel Utilisation", In 19^{th} *IEEE International Conference on Networks (ICON)*, pages 1-6. 11^{th} of December 2013.

Moravejosharieh, A. and Yazdi, E.T., "Study of Resource Utilisation in IEEE 802.15.4 Wireless Body Sensor Network, Part I: The need for enhancement", In *IEEE* 16^{th} *International Conference on Computational Science and Engineering (CSE)*, pages 1226-1231, 3^{rd} of December 2013.

Ali, S. and Yazdi, E.T. and Willig, A., "Investigations on passive discovery schemes for IEEE 802.15.4 based Body Sensor Networks", In *IEEE International Conference on Australasian Telecommunication Networks and Applications Conference (ATNAC)*, pages 89-94. 20^{th} of November 2013.

Abbasnejad, I and Zomorodian, M.J. and Yazdi, E.T., "Combination of multi-class SVM and multi-class NDA for face recognition", In 19^{th} *International Conference on Mechatronics and Machine Vision in Practice (M2VIP)*, pages 408-413, November 2012.

Yazdi, E.T. and Mohamed, A.A. and Zareei, M. and Wan, T., "Enhanced mobile lightweight Medium Access Control protocol for wireless sensor networks", In

IEEE Symposium on Wireless Technology and Applications (ISWTA), pages 152-155, September 2011.

Participation and Presentation in Local Conferences:

New Zealand Computer Science Research Student Conference (NZCSRSC), 24^{th} of April 2014. (Awarded the best paper award by a panel of academic judges.)

New Zealand Computer Science Research Student Conference (NZCSRSC), 15^{th} of April 2013.

Post Graduate Conference, 29^{th} of August, 2013.

Post Graduate Conference, 23^{rd} of August, 2012.

Post Graduate Conference, 1^{st} of September, 2011.

New Zealand Computer Science Research Student Conference (NZCSRSC), 18^{th} of April 2011.

Post Graduate Conference, 31^{st} of August, 2010.

Deputy Vice-Chancellor's Office
Postgraduate Office

UNIVERSITY OF CANTERBURY
Te Whare Wānanga o Waitaha
CHRISTCHURCH NEW ZEALAND

Co-Authorship Form

This form is to accompany the submission of any thesis that contains research reported in co-authored work that has been published, accepted for publication, or submitted for publication. A copy of this form should be included for each co-authored work that is included in the thesis. Completed forms should be included at the front (after the thesis abstract) of each copy of the thesis submitted for examination and library deposit.

Please indicate the chapter/section/pages of this thesis that are extracted from co-authored work and provide details of the publication or submission from the extract comes:

A subset of results presented in Chapter 4 is extracted from:

Tabatabaei Yazdi, Ehsan and Willig, Andreas and Pawlikowski, Krzysztof. "On channel adaptation in IEEE 802.15.4 mobile body sensor networks: What can be Gained?" In *18th IEEE International Conference on Networks (ICON)*, pages 262-267, December 2012.

Please detail the nature and extent (%) of contribution by the candidate:

This was my own research. I conducted the evaluation studies presented in the paper. I also analysed the results. Dr. Andreas Willig and Prof. Krzysztof Pawlikowski provided advice and reviewed the paper. My contribution is about 90%.

Certification by Co-authors:
If there is more than one co-author then a single co-author can sign on behalf of all
The undersigned certifys that:

- The above statement correctly reflects the nature and extent of the PhD candidate's contribution to this co-authored work
- In cases where the candidate was the lead author of the co-authored work he or she wrote the text

Name: Dr. Andreas Willig
Signature: 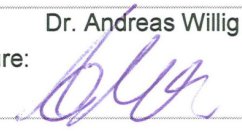 Date: 22/7/2014

Deputy Vice-Chancellor's Office
Postgraduate Office

UNIVERSITY OF CANTERBURY
Te Whare Wānanga o Waitaha
CHRISTCHURCH NEW ZEALAND

Co-Authorship Form

This form is to accompany the submission of any thesis that contains research reported in co-authored work that has been published, accepted for publication, or submitted for publication. A copy of this form should be included for each co-authored work that is included in the thesis. Completed forms should be included at the front (after the thesis abstract) of each copy of the thesis submitted for examination and library deposit.

Please indicate the chapter/section/pages of this thesis that are extracted from co-authored work and provide details of the publication or submission from the extract comes:

A subset of results presented in Chapter 5 is extracted from:

Tabatabaei Yazdi, Ehsan and Willig, Andreas and Pawlikowski, Krzysztof. "Shortening Orphan Time in IEEE 802.15.4: What can be Gained?" In *19th IEEE International Conference on Networks (ICON)*, pages 1-6, December 2013.

Please detail the nature and extent (%) of contribution by the candidate:

This was my own research. I conducted the evaluation studies presented in the paper. I also analysed the results. Dr. Andreas Willig and Prof. Krzysztof Pawlikowski provided advice and reviewed the paper. My contribution is about 90%.

Certification by Co-authors:
If there is more than one co-author then a single co-author can sign on behalf of all
The undersigned certifys that:

- The above statement correctly reflects the nature and extent of the PhD candidate's contribution to this co-authored work
- In cases where the candidate was the lead author of the co-authored work he or she wrote the text

Name: Dr. Andreas Willig
Signature: 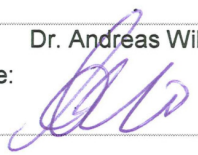 Date: 22/7/2014

Deputy Vice-Chancellor's Office
Postgraduate Office

UNIVERSITY OF CANTERBURY
Te Whare Wānanga o Waitaha
CHRISTCHURCH NEW ZEALAND

Co-Authorship Form

This form is to accompany the submission of any thesis that contains research reported in co-authored work that has been published, accepted for publication, or submitted for publication. A copy of this form should be included for each co-authored work that is included in the thesis. Completed forms should be included at the front (after the thesis abstract) of each copy of the thesis submitted for examination and library deposit.

Please indicate the chapter/section/pages of this thesis that are extracted from co-authored work and provide details of the publication or submission from the extract comes:

A subset of results presented in Chapter 7 is extracted from:

Tabatabaei Yazdi, Ehsan and Willig, Andreas and Pawlikowski, Krzysztof. Coupling Power and Frequency Adaptation for Interference Mitigation in IEEE 802.15.4 Based Mobile Body Sensor Networks. In 9th *IEEE International Conference on Intelligent Sensors, Sensor Networks and Information Processing (ISSNIP)*, pages 1-6, April 2014.

Please detail the nature and extent (%) of contribution by the candidate:

This was my own research. I conducted the evaluation studies presented in the paper. I also analysed the results. Dr. Andreas Willig and Prof. Krzysztof Pawlikowski provided advice and reviewed the paper. My contribution is about 90%.

Certification by Co-authors:
If there is more than one co-author then a single co-author can sign on behalf of all
The undersigned certifys that:

- The above statement correctly reflects the nature and extent of the PhD candidate's contribution to this co-authored work
- In cases where the candidate was the lead author of the co-authored work he or she wrote the text

Name: Dr. Andreas Willig
Signature: Date: 22/7/2014

Deputy Vice-Chancellor's Office
Postgraduate Office

UNIVERSITY OF CANTERBURY
Te Whare Wānanga o Waitaha
CHRISTCHURCH NEW ZEALAND

Co-Authorship Form

This form is to accompany the submission of any thesis that contains research reported in co-authored work that has been published, accepted for publication, or submitted for publication. A copy of this form should be included for each co-authored work that is included in the thesis. Completed forms should be included at the front (after the thesis abstract) of each copy of the thesis submitted for examination and library deposit.

Please indicate the chapter/section/pages of this thesis that are extracted from co-authored work and provide details of the publication or submission from the extract comes:

A subset of results presented in Chapters 4,5,6 and 7 are extracted from:

Tabatabaei Yazdi, Ehsan and Willig, Andreas and Pawlikowski, Krzysztof. Frequency Adaptation for Interference Mitigation in IEEE 802.15.4-Based Mobile Body Sensor Networks. *Computer Communications*, 2014. URL http://www.sciencedirect .com/science/article/pii/S014036641400245X

Please detail the nature and extent (%) of contribution by the candidate:

This was my own research. I conducted the evaluation studies presented in the paper. I also analysed the results. Dr. Andreas Willig and Prof. Krzysztof Pawlikowski provided advice and reviewed the paper. My contribution is about 90%.

Certification by Co-authors:
If there is more than one co-author then a single co-author can sign on behalf of all
The undersigned certifys that:

- The above statement correctly reflects the nature and extent of the PhD candidate's contribution to this co-authored work
- In cases where the candidate was the lead author of the co-authored work he or she wrote the text

Name: Dr. Andreas Willig
Signature: 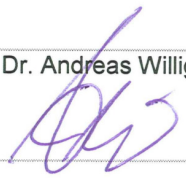 Date: 22/7/2014

Deputy Vice-Chancellor's Office
Postgraduate Office

UNIVERSITY OF CANTERBURY
Te Whare Wānanga o Waitaha
CHRISTCHURCH NEW ZEALAND

Co-Authorship Form

This form is to accompany the submission of any thesis that contains research reported in co-authored work that has been published, accepted for publication, or submitted for publication. A copy of this form should be included for each co-authored work that is included in the thesis. Completed forms should be included at the front (after the thesis abstract) of each copy of the thesis submitted for examination and library deposit.

Please indicate the chapter/section/pages of this thesis that are extracted from co-authored work and provide details of the publication or submission from the extract comes:

A subset of results presented in Chapter 7 is extracted from the paper:

Tabatabaei Yazdi, Ehsan and Moravejosharieh, Amirhosein and Willig, Andreas and Pawlikowski, Krzysztof. Coupling Power and Frequency Adaptation for Interference Mitigation in IEEE 802.15.4 Based Mobile Body Sensor Networks: Part II. In *IEEE International Conference on Australasian Telecommunication Networks and Applications Conference (ATNAC)*, 2014. (Under Revision)

Please detail the nature and extent (%) of contribution by the candidate:

This was my own research. I conducted the evaluation studies presented in the paper. I also analysed the results. Dr. Andreas Willig, Prof. Krzysztof Pawlikowski and Mr. Amirhosein Moravejosharieh provided advice and reviewed the paper. My contribution is about 90%.

Certification by Co-authors:
If there is more than one co-author then a single co-author can sign on behalf of all
The undersigned certifys that:

- The above statement correctly reflects the nature and extent of the PhD candidate's contribution to this co-authored work
- In cases where the candidate was the lead author of the co-authored work he or she wrote the text

Name: Dr. Andreas Willig
Signature: 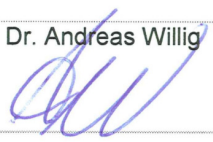 Date: 23/7/2014

Dedications

I dedicate this thesis to my parents, Dr. Hossein Tabatabaei Yazdi and Mahnaz Boroukhiyan, who are always supporting and encouraging me, and my sisters, Golsa and Nazi Tabatabaei Yazdi for their constant love, spiritual support and encouragement throughout my years of education.

Acknowledgements

I wish to express my sincere gratitude and indebtedness to Dr. Andreas Willig for his supervision, guidance and encouragement throughout this study. His invaluable suggestions and constructive criticism from time to time during the preparation of this thesis enabled the author to present the thesis in this form. My sincere gratitude is also due to Krzysztof Pawlikowski for his supervision and valuable suggestions throughout this study.

Thanks are due to Mr Peter Glassenbury, Professor Timothy David, Dr. Francois Bissey, Mr Phil Holland, Mr Joffre Horlor, Mr Adrian White, Mr Steven Sykes, Mr Dan Sun and Mr Tony Dale for their assistance they provided in the laboratory at various stages of the work.

I would like to thank my other committee members including but not limited to, Professor Antonija Mitrovic, Professor Tim Bell, Associate Professor Richard Green, Dr. Dong Seong Kim, Dr. Richard Lobb, Associate Professor Ray Hunt, Dr. Steve Weddell, Mrs Gillian Clinton and Mrs Alex Forster.

Finally, I would like to also thank my colleagues and dear friends including but not limited to, Mr Amirhosein Moravejosharieh, Mr Amir Shareghi Najar, Mr Dominic Winkler, Mr Masood Mansoori and Mr Jay Holland for their patience, support and encouragement during the course of this study.

Table of Contents

Abstract i

Publications v

Dedications xiii

Acknowledgments xv

Table of Contents xvii

List of Figures xxiii

List of Tables xxv

List of Terms and Abbreviations xxvii

List of symbols xxxiii

1. Introduction 1

1.1. Wireless Sensor Networks 1

1.2. Wireless Body Sensor Networks 2

1.3. Problem statement 4

1.4. Proposed solution 8

1.5. Methodology and Contribution 11

1.5.1. Performance measures 11

1.5.2. Hypotheses 12
1.5.3. Methodology and Contributions 13

2. Background and Literature Review **17**

2.1. Background 17
2.1.1. IEEE 802.15.4 17
2.1.2. IEEE 802.11 25
2.2. Impact of Interference on IEEE 802.11 systems 27
2.3. Impact of Interference on IEEE 802.15.4 systems 31
2.4. Cognitive Radio 33
2.5. Channel Adaptation 36
2.5.1. Coordinator discovery schemes 47
2.6. Transmit-Power Adaptation 52
2.7. Other Approaches 58
2.7.1. IEEE 802.15.6 60

3. System Model **63**

3.1. Network software and tools 63
3.2. Network Scenario and Topology 64
3.3. Propagation Model 66
3.4. WiFi Interference traffic model 66
3.5. WBSN model 69
3.6. Energy model 71

4. Frequency Adaptation **75**

4.1. Baseline Schemes 75
4.1.1. No-Adaptation Scheme 75
4.1.2. Genie Scheme 76
4.2. Frequency Adaptation Schemes 77
4.2.1. Periodic Schemes 79

4.2.2. Lazy Schemes . . . 82
4.3. Simulation-based Performance Evaluation . . . 83
4.3.1. Performance Metrics . . . 84
4.3.2. Non-adaptive schemes . . . 85
4.3.3. No-Adaptation and Genie Scheme . . . 89
4.3.4. Periodic Scheme . . . 91
4.3.5. Lazy Scheme . . . 95
4.3.6. Impact of Shadowing by the Human Body . . . 96
4.4. Discussion . . . 99

5. Orphan Recovery **103**
5.1. Considered Schemes . . . 103
5.1.1. Baseline Schemes . . . 103
5.1.2. Discovery Support Schemes . . . 104
5.2. Performance Metrics . . . 106
5.3. Simulation-Based Performance Evaluation . . . 107
5.4. Discussion . . . 110

6. Experimental Results **111**
6.1. Overview of Implementation . . . 111
6.2. Implementation in the nesC-TinyOS Environment . . . 113
6.2.1. Component Diagrams . . . 114
6.3. Experimental Setup . . . 116
6.3.1. Experimental Scenarios . . . 116
6.3.2. Experimental Components . . . 117
6.3.3. Performance Metrics . . . 120
6.4. Results . . . 121
6.5. Discussion . . . 133

7. The Influence of Transmit-Power on Performance **135**

7.1. Considered Schemes 135

7.1.1. Baseline Schemes 135

7.1.2. Transmit-Power Variation Schemes 136

7.1.3. A Joint Transmit-Power and Frequency Adaptation Scheme . 138

7.2. Simulation-Based Performance Evaluation 139

7.2.1. Performance Metrics 140

7.3. Performance Benefits of Transmit-Power Variation in Isolation 140

7.4. Performance Benefits of Coupling Transmit-Power with The Lazy Scheme 143

7.5. Transmit-Power Variation Schemes 146

7.6. A Joint Transmit-Power and Frequency Adaptation Scheme 148

7.7. Discussion 152

8. Conclusions **153**

8.1. Results and Findings 153

8.2. Evaluation of The Hypotheses 157

8.3. Future Works 157

REFERENCES **161**

A. Re-generating the IEEE 802.11 Transmit Spectral Mask **189**

B. Consumed energy calculations and examples **193**

C. The Influence of Packet Size on Performance **197**

List of Figures

1.1. Failed IEEE 802.15.4 transmissions at different power levels while walking along an urban shopping street [66]. 6

2.1. An example of an IEEE 802.15.4 super-frame structure [97, Sec. 5.1.1.1] 22
2.2. IEEE 802.15.4 and IEEE 802.11 spectrum usage in the 2.4 GHz ISM band. 26
2.3. An example of one WiFi channel overlapping the IEEE 802.15.4 spectrum. 27
2.4. Experimental testbed adopted by [19]. 30
2.5. The results for the percentage of failed transmission in [66]. 40
2.6. Noise floor, RSSI and LQI measurements of channel 18 [66]. 41
2.7. Noise floor within a window of ± 2 minutes around heavy transmission failures (starting at 0s) [66]. 42

3.1. WBSN and Interferer Deployment 65
3.2. IEEE 802.11 transmit spectral mask in the 2.4 GHz ISM band[2]. . . 68

4.1. Comparison of the three non-adaptive schemes where Δ is equal to 10 86
4.2. Comparison of the three non-adaptive schemes where Δ is equal to 100 87
4.3. Comparison of no-adaptation and genie schemes for $\Delta \in 10, 100, 300$. 90
4.4. Comparison of the periodic scheme where $\Delta = 100$ 92
4.5. Comparison of the periodic scheme where $\Delta = 300$ 93

4.6. Comparison of no-adaptation, periodic-measurement-MAX and Lazy scheme for $\Delta = 100$ 96
4.7. Comparison of no-adaptation, periodic-measurement-MAX and Lazy scheme for $\Delta = 300$ 97
4.8. Comparison of no-adaptation and Lazy scheme for $\Delta = 100$ and with additional node-dependent path loss 98
4.9. Comparison of no-adaptation and Lazy scheme for $\Delta = 200$ and with additional node-dependent path loss 99
4.10. Comparison of no-adaptation and Lazy scheme for $\Delta = 300$ and with additional node-dependent path loss 100

5.1. Comparison of the no-adaptation scheme with the different proposed coordinator discovery schemes added to the Lazy scheme where $\Delta = 300$ 108

6.1. NesC Component diagram for no-adaptation, periodic-random and Lazy schemes. 115
6.2. Scenario one. 118
6.3. Scenario two. 118
6.4. Spectrum utilisation over time for scenario one and for varying numbers of access points, from zero (top figure) to five (bottom figure). . 119
6.5. Spectrum utilisation over time for scenario two. 119
6.6. Summary experimental results for both scenarios. 121
6.7. Behaviour of the no-adaptation scheme for zero interferers, first scenario. 124
6.8. Behaviour of the no-adaptation scheme for one interferer, first scenario. 125
6.9. Behaviour of the periodic-random-1 scheme for zero interferers, first scenario. 126
6.10. Behaviour of the periodic-random-1 scheme for one interferer, first scenario. 127

6.11. Behaviour of the Lazy scheme for one interferer, first scenario. 128
6.12. Behaviour of the Lazy scheme for one interferer, first scenario. 129
6.13. Behaviour of the no-adaptation scheme with three interferers, second scenario. 130
6.14. Behaviour of the periodic-random-1 scheme with three interferers, second scenario. 131
6.15. Behaviour of the Lazy scheme with three interferers, second scenario. 132

7.1. Transmit-power variation scheme where data is generated every 1 s . 142
7.2. Transmit-power variation scheme where data is generated every 0.5s . 143
7.3. Transmit-power variation scheme where data is generated every 0.25s 144
7.4. Transmit-power variation scheme where data is generated every 0.125s 145
7.5. Comparison of Lazy_High with Lazy_Low where $\Delta = 10, 50, 100, 200$ and 300 146
7.6. Comparison of Lazy_High with Lazy_Low where data packets are generated every 0.5 second and $\Delta = 10, 50$ and 100 147
7.7. Comparison of Lazy_High with Lazy_Low where data packets are generated every 0.25 second and $\Delta = 10, 50$ and 100 148
7.8. Comparison of Lazy_High with Lazy_Low where data packets are generated every 0.125 second and $\Delta = 10, 50$ and 100 149
7.9. Percentage of energy consumed with respect to the Lazy_High scheme 150
7.10. Comparison of the Adaptive_Lazy scheme when data rate is 0.125 s . 151

A.1. Re-generated IEEE 802.11 transmit spectral mask with $f_c = 2412$. . . 190
A.2. A close-up of the IEEE 802.11 transmit spectral mask with $f_c = 2412$. 192

C.1. The influence of packet size on success rate where Δ=10, 50 and 100. 198

List of Tables

3.1. Simulation Parameters. 67

3.2. CC2420 parameter specification. 72

6.1. Lines of nesC code for implementation of different frequency adaptation schemes 114

7.1. Node lifetime 144

A.1. Different transmit-power off-set for different frequencies. 191

List of Terms and Abbreviations

A

ACI Adjacent Channel Interference.

AMR Automatic Meter Reading.

AP Access Points.

ARA Adaptive Resource Allocation.

ATPS Adaptive Transmit Power Scheme.

B

BCC Body Channel Communication.

BO Beacon Order.

BS Base Station.

C

CACCA Coexistence Aware Clear Channel Assessment.

CAP Contention Access Period.

CAPD Coordinator Assisted Passive Discovery.

CCA Clear Channel Assessment.

CCK Complementary code keying.

CFP Contention Free Period.

CS Carrier Sense.

CSMA Carrier Sense Multiple Access.

CSMA-CA Carrier Sense Multiple Access with Collision Avoidance.

D

DMMA Dynamic Multi-radio Multi-Channel media Access control.

DSSS Direct Sequence Spread Spectrum.

DTPC Dynamic Transmission Power Control.

E

ED Energy Detection.

F

FAN Fabric Area Networking.

FFD Full Function Device.

FHSS Frequency Hopping Spread Spectrum.

FID Fast on-line model IDentification.

FTPS Fixed Transmit-Power Scheme.

G

Genie The name "Genie" was selected for this scheme since the nodes in this network had to only ask the Genie to know which channel has the best quality at that given time with out delay costs. The Genie with its oracle knowledge of all 16 channels held time to calculate the channel quality of all existing channels and pick out the best channel.

GTS Guaranteed Time Slot.

H

HBC Human Body Communications.

Hyper-frame A hyper-frame is a set of subsequent super-frames, were at the end of the hyper-frame a decision is carried out.

I

IID Independent and Identically Distributed.

ISM Industrial, Scientific and Medical.

ITA Interferer-aware Transmission Adaptation.

L

LQI Link Quality Indicator.

LR-WPAN Low-Rate Wireless Personal Area Network.

M

MAC Medium Access Control.

N

NB Narrow-Band.

P

PAN Personal Area Network.

PER Packet Error Rate.

PHY Physical.

PI-AW Proportional-Integral with the Anti-Windup.

PLL Phase Locked Loop.

PLR Packet Loss Ratio.

PRR Packet Reception Rate.

PU Primary User.

Q

QoS Quality of Service.

R

RFD Reduced Function Device.

RFID Radio-Frequency IDentification.

RFS Random-Frequency-Selection.

RSSI Received Signal Strength Indication.

RX Receive.

S

SA-MAC Spectrum Agile Medium Access Control.

SD super-frame Duration.

SINR Signal to Interference plus Noise Ratio.

SIR Signal to Interference Ratio.

SNR Signal to Noise Ratio.

SO super-frame Order.

SU Secondary User.

T

TATPC Temperature-Aware Transmission Power Compensation.

TDMA Time Division Multiple Access.

TX Transmit.

U

UWB Ultra-Wide-Band.

W

WBAN Wireless Body Area Network.

WBSN Wireless Body Sensor Network.

WiFi Wireless Fidelity.

WLAN Wireless Local Area Network.

WRAN Wireless Regional Area Network.

WSN Wireless Sensor Network.

List of symbols

Δ In this study, Delta is a parameter used in the Poisson point process that indicates the density of the interferer devices.

λ Lambda indicts the average intensity interferer interference.

1. Introduction

This chapter introduces the main idea of this thesis. First, an overview of Wireless Sensor Networks (WSNs) will be presented. Next, a discussion about Wireless Body Sensor Networks (WBSNs) and their differences to WSNs is given. Then, the problem statement is presented, followed by a discussion of the solution approach. Finally, the methodology and thesis contributions are described, followed by the thesis outline.

1.1. Wireless Sensor Networks

WSNs are a well-established technology, typically used for control and monitoring purposes in many industrial and consumer applications [12–14, 35, 179]. Applications in which WSNs could be used include: (i) **Environmental Monitoring**: monitor and report the environmental conditions at sensors' locations to the base station in farms and forests [49, 76, 101, 123, 188]; (ii) **Automatic Meter Reading (AMR)**: reading electricity or gas meters within residential areas [17, 37, 38, 44, 63, 108, 120]; (iii) **Industrial Automation and Control**: WSNs could be used to control and monitor industrial processes and also to detect mechanical faults in hard-to-reach or harsh and hazardous environments and, if needed, to act accordingly [48, 78, 92, 156, 159]; (iv) **Inventory Management**: in big warehouses sensor nodes could be attached to items or shelves, to inform about any shortage of particular items or to identify the locations of items at any time (in

this area Radio-Frequency IDentification (RFID) systems are also commonly used) [110, 136, 140, 156, 167, 186]; (v) **Surveillance and Tracking**: sensors are also being used for detecting moving objects, and in security systems [27, 85, 107, 121, 122, 153].

WSNs consist of **nodes** that are wirelessly connected to each other, forming a network (typically multi-hop). Each node is able to connect to one or more nodes, depending on the type of node, its functionality, the application, and protocols used. The main components of a typical WSN node consist of digital circuitry, microcontroller, wireless transceiver, power source, and optional sensors and/or actuators. The size of WSNs varies from just a few to hundreds or thousands of nodes. Depending on the application and the protocols used, WSNs can form a simple single-hop **star topology** or more advanced **multi-hop mesh topologies**. Some of the challenges that need to be considered while designing and developing a WSN are scalability, robustness, network lifetime, energy consumption, fault tolerance, and mobility.

1.2. Wireless Body Sensor Networks

WBSNs target applications related to monitoring and processing of human vital signs for health and well-being, entertainment and tracking applications [31, 34, 98, 158]. The ultimate goal of WBSNs is to improve the quality of human life. For example, WBSN technologies could be used to seamlessly monitor the health status of elderly and chronically ill people without the need for constant supervision or presence of caregivers, allowing them to maintain their independence and freedom.

The major difference that separates classical WSNs [80, 145] from WBSNs is that WBSNs usually form small to medium-sized networks, and sensor nodes are at most one to two hops away from a coordinator node [39, 68]. The most common topology used for such networks is the star topology with only a single-hop between the sensor

node and the coordinator [14, 111, 171]. Another significant property of WBSNs is their group mobility. This means that, although each node in a WBSN has limited independent internal mobility, all sensor nodes and the coordinator node **move as a whole**, along with the movement of their human carrier [98]. This is also known as **network** or **group mobility**. Contrary to WBSNs, WSNs are usually static, medium to large-scale and multi-hop networks with very few mobile nodes [144, 157].

There are many protocols and standards that are used for WSNs and WBSNs [7, 16, 93, 97]. The IEEE 802.15.6 standard [7] is a standard specifically designed for WBSNs in 2012 which has been recently released. Although this is a very promising standard for WBSN applications, to the best of the authors knowledge, no WBSN node compatible following the specification of this standard is commercially available, both at the start and completion date of this thesis. A more popular, mature and well-established standard is the IEEE 802.15.4 standard [97]. The IEEE 802.15.4 standard is a Low-Rate Wireless Personal Area Network (LR-WPAN) standard that aims to increase the simplicity and reduce the network communication costs. This standard supports a wide range of applications such as WSNs and Personal Area Networks (PANs), for example WBSNs. The specification of this standard is limited to the Physical (PHY) and Medium Access Control (MAC) layers only. Due to its simplicity and popularity, the IEEE 802.15.4 standard is expected to remain a serious contender for WSNs and WBSNs. Thus, in this thesis, the IEEE 802.15.4 is considered as the benchmark protocol and further enhancements and genuine contributions are compared with this standard.

According to the IEEE 802.15.4 standard, the physical layer supports a total of 27 different frequency channels. Amongst these, 16 channels are in the 2.4 GHz Industrial, Scientific and Medical (ISM) band. This is arguably the most popular ISM band used by the IEEE 802.15.4 technologies, which is also shared with other technologies, for example WiFi and Bluetooth. Therefore, in this thesis, the 2.4 GHz ISM band with 16 available channels is considered.

Having to share the spectrum with other technologies – such as IEEE 802.11, IEEE 802.15.1 and other IEEE 802.15.4-based networks – implies that data transmission in WBSNs can be impacted by external interference, as documented in several publications addressing coexistence of IEEE 802.15.4-based networks with such technologies (See Section 2.3).

1.3. Problem statement

Both in WSNs and in WBSNs, scalability, robustness, network lifetime, fault tolerance, latency, throughput, and mobility are all important requirements that need to be addressed. However, the order of priority of some of these requirements is often different in WBSNs in comparison to WSNs. One of the most important criteria for a WBSN is to establish and maintain **reliable and timely data transfer** between the sensor nodes and the coordinator node, since these networks mainly deal with human vital signs. Being unable to send or receive critical human vital signs, or receiving the information with long delays, might be the difference between life and death. For example, it might be necessary to provide constant patient care and monitoring for an elderly or a chronically ill person. In order to maintain their independence without the need for constant supervision or the presence of caregivers, WBSNs provide a reasonably safe and low-cost solution with minimal maintenance. In such scenarios, the patients are free to go about their daily routines and, since many people live in densely populated urban environments such as shopping malls, hospitals, offices and residential communities, WBSNs are constantly being faced with an ever-changing interference background.

One of the major issues in wireless networks, in particular WBSNs, is interference caused by sharing the same radio spectrum with different overlapping networks and/or technologies. There are two scenarios where such problems are noticeable: (i) where two different networks using the same protocol cause interference to each

other; or (ii) other networks using different protocols and modulations, causing interference. In both of these cases, it is assumed that all included networks are using the same or overlapping frequency bands, and the distance between nodes of these two different networks is smaller than their radio transceiver's range. This thesis focuses entirely on the second case, i.e. external interference. In particular, the interference caused by stationary IEEE 802.11b-based Wireless Fidelity (WiFi) access points on IEEE 802.15.4 WBSN is considered. One of the consequences of sharing the same spectrum with other technologies is data transmission failure caused by external interference, which eventually results in network performance degradation as a whole [71, 95, 117, 129, 134, 166].

As an example, the effect of WiFi interference on WBSNs was measured in [66]. In one of the experiments conducted in this study, a WBSN was carried by a human carrier in an urban shopping street (see Figure 1.1). This figure illustrates the percentage of failed transmissions during a 26 minute period for different transmit power levels. The results reveal that the "interference landscape" changes significantly on time-scales of tens of second to minutes. This means that any radio and/or protocol parameter that was initially good may become sub-optimal in a matter of a few second.

Another important criterion for a WBSN is the **overall network lifetime**. Since most WBSNs operate on battery power, the overall power consumption becomes a major constraint for such networks. The radio transceiver consumes a large portion of the consumed energy by the WBSN device [80, Sec. 2.2.1] (not including the sensors and/or actuators). It is crucial to avoid keeping the radio device active – in Receive (RX) or Transmit (TX) – and to keep it in a low-power state – or sleep mode – as much as possible. External or environmental interference causes problems such as **data re-transmission** and in the worst condition **node orphaning** – an orphan node is a node that has lost connection and synchronisation with its coordinator, and needs to listen on a subset of available channels in order to find its corresponding

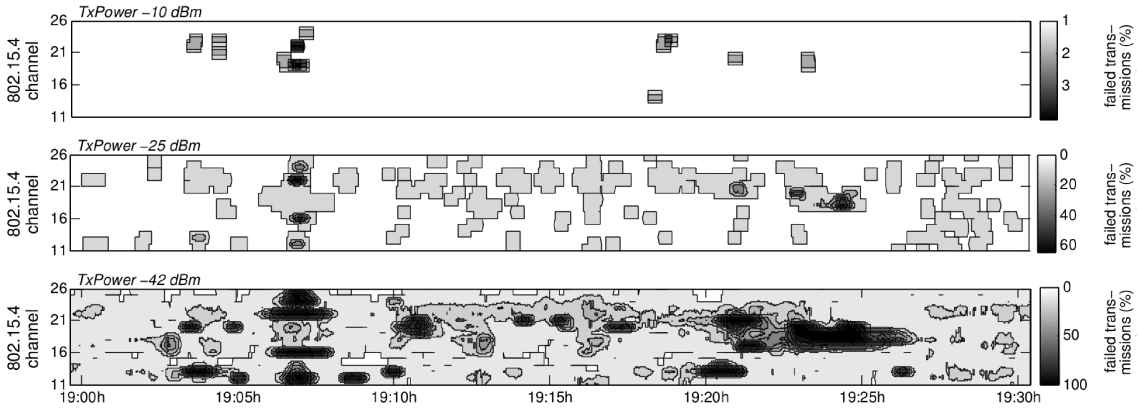

Figure 1.1.: Failed IEEE 802.15.4 transmissions at different power levels while walking along an urban shopping street [66].

coordinator node again. All this not only reduces the reliability and timely data transfer, it also reduces the network lifetime.

A basic IEEE 802.15.4-based WBSN is currently not able to avoid the interference caused by a WiFi device in the same coverage area. This is mainly due to the following factors: i) **Transmit-power**: a common transmit-power of a WiFi device is around 20 dBm, whereas the maximum available transmit-power for an IEEE 802.15.4-based WBSN device is in the order of 0 dBm[1], ii) **Bandwidth**: according to the 802.11 standard, the bandwidth of a WiFi channel in the 2.4 GHz ISM band is 22 MHz, which covers four frequency channels of IEEE 802.15.4. iii) **Coverage range**: because of the high transmit-power of WiFi devices their coverage area reaches 100 meter or more (in line of sight).

Therefore, it is logical for WBSNs to **adapt** by obtaining measurements of its surroundings (e.g. the current interference situation) and to adjust some of its operational parameters accordingly, in order to mitigate the interference problem. Within the scope of the IEEE 802.15.4 standard, there are physical and MAC layer parameters that can be adjusted.

The main adjustable parameters on the physical layer are the frequency channel

[1]This is the maximum transmit-power level available for popular and commonly used IEEE 802.15.4-compatible transceivers. Long-range IEEE 802.15.4-compatible transceivers are also commercially available with maximum transmit-power levels up to 10 dBm. However, such transceivers are application specific and not commonly used.

and the transmit-power. This layer also provides performance measures for the higher layers, such as Received Signal Strength Indication (RSSI), Energy Detection (ED) and Link Quality Indicator (LQI). These parameters could be used to evaluate the channel quality or the link quality. Based on the information gathered from the physical layer, higher layers of the WBSN could make changes to the network parameters and settings to try to minimise and/or avoid interference.

According to the IEEE 802.15.4 standard, on the MAC layer two operation modes are available, namely the beacon-enabled and non-beacon-enabled modes. This layer also provides two different access schemes, namely Time Division Multiple Access (TDMA) and Carrier Sense Multiple Access (CSMA) schemes. Guaranteed Time Slot (GTS) allocation is a TDMA technique used by the IEEE 802.15.4 standard to eliminate mutual interference caused by sensor devices in the same network. To minimise possible co-channel interference, this thesis uses Clear Channel Assessment (CCA) for Carrier Sense Multiple Access with Collision Avoidance (CSMA-CA), however this method of channel access does not prevent external interference from other technologies.

The relatively small time-scale of interference changes and group mobility of the network in harsh urban environments brings two main difficulties. The first obstacle is the small amount of time available for channel measurements. This increases the impact of faulty (or noisy) measurements, which can result in poor decision making. The second barrier is energy consumption. The energy consumed for these measurements, which may involve switching to various channels and listening on each one to estimate the energy or traffic load present, is non-negligible, and it is **not** a priori clear whether the energy spent for such measurements will pay off (for example by increasing the probability of successful data transmission and reducing the number of re-transmission attempts).

A further difficulty, which appears with introducing frequency adaptation, is when the frequency channel parameter is changed in situations with severe interference,

and some nodes in the network have low connectivity when the change is made. Wherever the decision is made within the WBSN, this decision – the time of switching and the newly selected frequency channel – must be communicated to the other nodes in the network. In a scenario with intense interference, some sensor nodes may not be able to receive the necessary information. These members, which in this thesis are referred to as orphaned nodes, can spend a significant amount of time and energy for searching and re-establishing connection to their corresponding coordinator.

To sum up, this thesis considers some of the current challenges for WBSNs coming from interference, such as reliable and timely data transfer, long node-orphaning durations caused by interference and the finite power source available for the network. We aim to investigate the feasibility of embedding an Adaptive Resource Allocation (ARA) scheme – more specifically, physical layer resources, such as transmit-power and frequency channel – into IEEE 802.15.4-based WBSNs. We investigate the reliability, energy efficiency, and robustness of the ARA as well as its implementation issues. **Such an adaptive scheme aims to provide reliable and timely data transfer despite the presence of WiFi interference, and to increase at the same time the overall lifetime of the network.**

1.4. Proposed solution

This thesis explores two possible physical-layer-based resource allocation approaches, namely, **frequency adaptation** and **transmit-power variation**. Setting a given frequency channel of a WBSN to a channel with no or less interference is a promising way to increase the reliability and timeliness of data transfer. In order to achieve this, a WBSN needs to consider the following steps:

1) Monitoring the current channel: The WBSN needs to frequently sample the quality of the current working channel. This stage is a crucial step, since the

human carrying the WBSN could be moving in densely populated urban environments with an ever-changing interference landscape. This stage needs quick and agile detection of the current channel status. If the human carrier enters the coverage area of an overlapping WiFi device in the vicinity, it is necessary that the WBSN recognises this interference source as early as possible before data transfer between the WBSN nodes is no longer possible.

2) Searching other channels: After the network is aware of the approaching interference source, it is important to scan all or a subset of available frequency channels to find the next working channel with the lowest interference level. In both phases (monitoring and searching phases), the time and energy it takes to estimate the channel quality and interference level is a major issue. An important question that needs to be answered is whether or not these extra costs pay-out in the long run to improve the performance of WBSNs. Choosing the appropriate link quality estimation methods is important. Commonly used methods are built on the following metrics: RSSI [10, 60, 105, 133], ED [25, 79, 148], LQI [51–53, 60], Packet Reception Rate (PRR) [60, 130, 170], Signal to Noise Ratio (SNR) [45, 59, 141, 161] and Signal to Interference plus Noise Ratio (SINR) [61, 87, 89, 139, 164]. All these link quality estimation methods need time to evaluate and give a valid estimation. Broadly speaking, the more time spent on channel evaluation, the more accurate the results can get. Although having accurate measurements aids to improve the channel selection process, it comes with higher costs. The longer the time spent scanning, the more energy is consumed and the longer it takes to find the next possible best channel. In a rapidly changing environment, WBSNs are then more at risk of packet loss or, in the worst case, connection loss. Finding the best link quality estimation method is out of the scope of this thesis and is left as one of the future work explorations.

3) Decision making and execution: Based on the information gathered in the searching phase, an unanimous decision needs to be made for selecting the next

working channel. This decision could be made in a distributed or centralised fashion. This thesis selects the centralised approach where the decision is made by the coordinator node. This assumption is made mainly to minimise the complexity and communication required for a decision making process. Furthermore, it is assumed that the coordinator is equipped with more resources compared to its sensor nodes. This decision – if made at a single point – then needs to be conveyed quickly to all devices in the WBSN network, before the interference levels increase so that communication between nodes is no longer possible. Some of the challenges that need to be addressed in this phase are: 1) Reducing the overall time for reaching this decision. 2) Coordinating all network devices to change their network parameters (Frequency channel and/or Transmit-Power) according to the chosen decision.

Actively monitoring the current state of the working channel and selecting the best channel with the lowest interference, when the current channel is no longer usable (because of high-interference), is one promising way to increase the reliability and timeliness of data transfer. However, this is not the only solution. Another possible solution is to modify or adapt the transmit-power of the nodes, which increases the SNR and thus increases the reliability of data transfer. This is a simpler solution in terms of implementation when compared to channel adaptation, but comes with potentially damaging side effects. One of the side effects of increasing the transmit-power is the increased signal strength and range. Although this increase benefits the current network in terms of improved SNR, it also causes interference for other nearby networks. This increase in the interference might result in neighbouring technologies reacting by increasing their transmit-power, respectively. The final outcome is not going to be satisfactory for the WBSN since the maximum transmit-power (0 dBm) of these devices is much less than the competing technologies such as WiFi (20 dBm). In addition, increasing the transmit-power could drain the battery, resulting in a shorter network lifetime.

Similar to frequency adaptation, transmit-power adaptation also needs the mon-

itoring, decision making and execution steps.

The aim of this thesis is to study:

Whether and how energy constrained WBSNs can reliably communicate in the unlicensed 2.4 GHz ISM band by avoiding and/or mitigating radio frequency interference caused by other technologies sharing the same spectrum, in particular WiFi interference, via frequency channel adaptation and transmit-power variation.

1.5. Methodology and Contribution

The objective of this research is to explore and investigate the possibilities of embedding adaptive resource allocation techniques to the existing well-established IEEE 802.15.4 standard, with the aim of enhancing the reliability and timely data transfer and improving the overall network lifetime of WBSNs.

This thesis consists of both primary and secondary research. The secondary research findings are presented in Chapter 2 and the primary research findings are presented in Chapters 4, 5, 6, and 7. Each chapter investigates a particular hypothesis (to be later explained in detail). This thesis considers a simple but realistic scenario where a WBSN connected to a moving human carrier experiences interference from stationary WiFi access points.

1.5.1. Performance measures

In order to evaluate and compare the different proposed schemes with each other and with the existing IEEE 802.15.4 standard, this thesis considers the following main performance measures:

i) **Success Rate**: This performance measure calculates the average percentage of data packets successfully transmitted from the sensor node to the coordinator node. The average is taken over all (equally loaded) sensor nodes. A data packet

is only considered as successfully transmitted when an acknowledgement packet is received by the sensor node.

ii) **Consumed Energy**: The average energy consumption of the sensor nodes and the coordinator node is calculated and compared separately. This thesis focuses on the energy consumption of the transceiver, the energy consumed by other components of a node is ignored.

iii) **Percentage of Time without PAN**: This is the percentage of time when the sensor nodes have lost synchronisation and connection to their PAN coordinator node. This performance measure is very important since during this time the sensor nodes need to spend considerable amount of energy to scan the whole spectrum and find their correspondent coordinator node, and during this time they are not able to transmit their data packets.

Other secondary performance measures are also considered that will be introduced in detail in later chapters.

1.5.2. Hypotheses

In the past decades, researchers have shown the effects of interference on both WSNs and WBSNs. This thesis explores the benefits of using ARA in WBSNs. This thesis uses simulation and experimentation to evaluate the following hypotheses:

- **Hypothesis 1**: By adaptively changing the current operating frequency of the WBSN to a channel with lower interference in environments with rapidly changing interference background, despite the energy costs of adaptation and the increasing risk of node orphaning, it is expected that the performance measures would be improved significantly.

- **Hypothesis 2**: By introducing channel adaptation schemes, the risk of node orphaning increases. Utilising coordinator-discovery techniques in high-interference

environments, WBSNs are expected to experience a shorter average node-orphaning duration. Shortening the orphan period enhances the network performance.

- **Hypothesis 3**: Frequency adaptation schemes can perform better when faced with external interference, in comparison to any ideal transmit-power adaptation schemes in isolation.

- **Hypothesis 4**: By coupling transmit-power with frequency adaptation in environments with varying WiFi interference, significant improvement of network performance could be gained, in comparison to either of them individually.

1.5.3. Methodology and Contributions

This thesis provides five main contributions:

1. The performance of the existing IEEE 802.15.4 standard (also referred to as the **non-adaptive scheme**) in a scenario where a pedestrian carrying a WBSN moves through a densely populated urban environment with high WiFi interference is explored. The non-adaptive scheme is then compared with an idealised frequency adaptation scheme called the **genie scheme**. Comparing the results of the non-adaptive and genie scheme illustrates the lower and upper bounds of what is achievable when frequency adaptation is added to the existing IEEE standard.

   The author of this thesis evaluates the performance of these schemes through simulation. For this study the transmit-power is fixed to the minimum available value presented by the well-known IEEE 802.15.4-compatible ChipCon CC2420 transceiver [149]. This is done to better demonstrate the effects of frequency adaptation in isolation. The simulation results of this study reveal that frequency adaptation schemes in isolation can provide substantial gains over the non-adaptive scheme.

2. Several frequency adaptation schemes are proposed in this thesis, amongst which the **Lazy scheme** is particularly attractive. This scheme not only achieves similar success rates as the genie scheme, but also increases the overall life-time of the network. Another attribute of this scheme is its simplicity, which makes it ideal for implementation on real WBSN devices. The Lazy scheme follows a simple approach: 1) The network remains on the same operating channel as long as it is "good enough"; 2) However, once the channel quality falls below a given threshold, the network searches all the available channels and selects the channel with the lowest interference level.

3. This thesis explores the node-orphaning problem in depth, which is the main cause of battery drainage and drop in success rate. In particular in the Lazy scheme when a new operating channel is selected and the network switches to the new operating channel, some sensor nodes might not get informed about this decision, due to high-interference levels. Hence, these nodes lose their synchronisation with their coordinator node and become orphans. In the absence of this information, sensor nodes have to scan all eligible channels. Currently the no-adaptation scheme does not provide much information for the orphan nodes to speed up the process of finding and associating with their network. According to the IEEE 802.15.4 standard, orphan nodes are to start scanning the subset of predefined channels specified by higher layers until they find and associate with their corresponding coordinator device.

   This study explores coordinator discovery schemes to reduce the orphan duration time of the Lazy scheme in high-interference scenarios. By providing the sensor nodes with additional information to make better decisions about the channels on which to search for the coordinator, this study proposes schemes that aim to help orphan nodes to shorten their orphan duration time.

   Although the proposed schemes are able to significantly reduce the number

of channels to be scanned before finding the right operating channel, to our surprise, the average overall time spent in the orphan state is **not** significantly reduced in scenarios with high-interference and/or interferer density. This was mainly due to orphan nodes failing to successfully receive the beacons of their corresponding coordinator on the new channels as well.

In the light of these findings concerning the node-orphaning problem, and since the orphaning duration in low-interference or low-interferer-density scenarios is negligible, this thesis concludes that additional mechanisms to rectify the node-orphan problem are **not** required to be included in any implementation.

4. To validate our simulation results, three schemes are implemented on commercially available IEEE 802.15.4-compatible WBSN devices and are compared with each other using real measurements. The Lazy scheme is compared with a blind frequency-hopping and the non-adaptive scheme. All three schemes use the available IEEE 802.15.4 stack [66] under the TinyOS operating system [67, 100]. The behaviour of these schemes is evaluated under two different WiFi interference scenarios.

   The results obtained not only confirm the relative performance trends already discovered in our simulations, but also substantiate the claim that the Lazy scheme in particular achieves excellent performance when faced to a changing interference background. Moreover, the feasibility of implementing the proposed schemes with minimal changes to the given IEEE 802.15.4 MAC protocol implementation is demonstrated. The proposed scheme is implemented with minor modification to the actual protocol implementation.

5. This thesis also explores performance gains of coupling transmit-power variation with frequency adaptation to mitigate interference in IEEE 802.15.4-based WBSNs. The non-adaptive and Lazy schemes are selected as the baseline schemes for this study. The performance of both schemes is evaluated when

the transmit-power of the network – both sensor and coordinator nodes – is set to the highest (0 dBm) and the lowest (-25 dBm) value – according to the IEEE 802.15.4-compatible ChipCon CC2420 transceiver [149]. This is done to better emphasise the effect of transmit-power in isolation. The results establish the performance bounds for transmit-power variation when WBSNs move through densely populated urban environments with high WiFi interference.

However, while maximising transmit-power improved the performance of both the non-adaptive and the Lazy scheme, transmit-power variation schemes alone do **not** outperform the Lazy scheme with minimum transmit-power. Our results suggest that in densely populated environments with high-interference, the coupling of maximum transmit-power with frequency adaptation schemes such as the Lazy scheme not only improves the success rate, but also, surprisingly, reduces the overall consumed energy of the network.

This finding motivated us to experiment with non-uniform allocation of transmit-power between sensor nodes and their corresponding coordinator node. Interesting results were observed, namely for schemes where sensor nodes were configured with maximum transmit-power the success rate was increased. Furthermore, for schemes where the coordinator node was configured with maximum transmit-power the consumed energy of the sensors was reduced while maintaining an acceptable high success rate.

Finally, a joint transmit-power and frequency adaptation scheme is proposed that utilises the pre-existing channel estimation information gathered by the Lazy scheme. The results showed the same level of success rate as produced by the coupling of maximum transmit-power with frequency adaptation approach, while consuming lower energy by the sensor nodes.

2. Background and Literature Review

2.1. Background

2.1.1. IEEE 802.15.4

The IEEE 802.15.4 [97] standard is a mature and popular technology designed for LR-WPANs. This standard was first released in 2003 [96]. Since its release, this standard has had many amendments, the most recent being the IEEE 802.15.4k, approved in August, 2013 [9]. This standard has recently attracted attention in the WBSN area. This thesis expects that due to the availability and variety of low-cost commercially available components the IEEE 802.15.4 standard will remain a serious contender in the WBSN area for quite some time to come – despite the recent approval of the IEEE 802.15.6 standard [7]. The specification of this standard is limited to the physical and MAC layers.

The standard divides WSN nodes into two classes: Full Function Devices (FFDs) and Reduced Function Devices (RFDs). RFDs have limited computational power, memory, power supply and are commonly used for sensing and/or actuating. According to the specifications of the standard, these devices are limited to communicate only with FFDs and implement only a subset of the functionalities that the standard prescribes. A FFD normally has access to more resources, allowing it to not only support all the capabilities of a RFD; but also, it could take the responsibilities of

a coordinator, repeater or a gateway node. In this thesis, we use the term **Sensor node** and **Coordinator node** for RFD and FFD devices, respectively. According to the specifications, WSN nodes are able to connect to each other and form a network using either a **star** or **peer-to-peer** topology. Furthermore, in a network, multiple sensors and coordinator nodes may exist, however, there can only be one PAN coordinator.

Physical Layer

The physical layer supports a total of 27 non-overlapping frequency channels, operating in three different bands. One channel is available in the European 868-868.6 MHz band, 10 channels are available in the 902-928 MHz ISM band, and 16 channels are specified in the 2400-2483.5 MHz ISM band. On the latter band, each channel is 2 MHz wide, and their centre frequencies are separated by 5 MHz. The channels are numbered from 11 to 26. This thesis is mainly interested in the 2.4 GHz ISM band, which is arguably the most popular and widely used frequency band. The other two frequency bands are restricted to certain countries or regions. At this frequency band, IEEE 802.15.4 offers a bandwidth of 250 kbps per channel and uses the Offset Quadrature Phase-Shift Keying O-QPSK modulation. It offers interference mitigation mechanisms, namely the Direct Sequence Spread Spectrum (DSSS) and the CSMA-CA scheme to co-exist with other technologies using the same frequency band.

This layer provides two measured parameters: RSSI/ED and LQI. RSSI is the estimated RF power received by the transceiver antenna. This value is reported as an 8-bit integer, giving it a dynamic and linear range between -100 to 0 dBm. RSSI and ED are used interchangeably in the CC2420 specifications. According to the CC2420 data-sheet the RSSI accuracy of this transceiver is $\pm 6dB$. RSSI could be used to estimate the background noise of the current operating channel without the need for receiving a packet. The LQI value is an estimate that is directly correlated

with the chip error rate. For the CC2420, the LQI value is calculated over the 8 symbols following the start frame delimiter [97, 149]. A similar process could be used to calculate the RSSI value. The calculated RSSI and LQI values are reported with every received frame. The RSSI value is used in CCA. According to the IEEE 802.15.4 standard CCA can be carried out in three different modes: 1) Channel is clear when the received energy is below the programmed threshold[1]. 2) Channel is clear when not receiving valid IEEE 802.15.4-based signals. 3) Finally, channel is clear when not receiving valid IEEE 802.15.4-based packets and the received energy is below the programmed threshold. This thesis uses the latter CCA mode for its channel assessments.

Medium Access Control Layer

The MAC layer allows or denies access to the physical medium (frequency channel) at a given time. This layer is responsible for device configuration, synchronisation, state transition (RX, TX and sleep mode) and re-transmission (if an immediate acknowledgement is not received), association and dis-association to the PAN coordinator, assigning GTS, and employing security mechanisms (to some extent).

The IEEE 802.15.4 only allows one PAN coordinator per network. The PAN coordinator is the primary controller responsible for determining network-wide parameters that are used for device synchronisation, coordination and addressing. Two network topologies are specified in the IEEE 802.15.4 standard, namely **Star** and **Peer-to-Peer** topology. In the **peer-to-peer** topology, FFDs may send and receive packets from any node that is within its communication range. In such networks, RFDs are only allowed to connect to FFDs that are within their communication range. Nodes may form a multi-hop network in which a set of nodes cooperatively maintains network connectivity. Peer-to-Peer networks are infrastructure-less and very flexible. Such networks may be used in applications such as search-and-rescue

[1]According to the CC2420 specification, this threshold is by default set to -77 dBm.

or data acquisition in farm and forests. In the **star topology**, nodes exchange packets via the coordinator node. Similar to peer-to-peer network, a sensor node is only able to connect to a PAN coordinator or a coordinator node that is within its communication range; no direct packet exchange is allowed between sensor nodes. If a data packet is required to be sent from one sensor node to another, this packet needs to be transferred through a coordinator node. These infrastructure-based networks are simpler in terms of control and management, making them suitable for WBSN applications. This thesis uses the star topology to connect the sensor nodes to the coordinator node. An extension of our approaches to multi-hope networks is part of future works.

The IEEE 802.15.4 standard specifies two operation modes: **beacon-enabled** and **non-beacon-enabled** mode. In the **non-beacon-enabled** mode, nodes use the un-slotted CSMA-CA mechanism to send their packets after a random back-off period. They perform a Carrier Sense (CS) operation on the current operating channel before sending a packet. If the channel is detected as busy, the node listens again after a random back-off period. In this mode, the destination node needs to be constantly listening or obtain some sort of synchronisation, which is not specified in the scope of the IEEE 802.15.4 standard. In scenarios where a star topology is used and the network is operating in the non-beacon-enabled mode, the coordinator node needs to be constantly listening for up-link traffic or down-link request packets. Since network lifetime is important in WBSNs, this thesis does not consider the non-beacon-enabled mode; instead the alternative beacon-enabled mode is employed.

The **Beacon-enabled** mode is the other mode that is specified in the standard. In this mode, the coordinators maintain synchronisation by periodically broadcasting beacon packets without performing a CS operation. This mode divides time into sub-sequent time durations called super-frames. The super-frame structure is illustrated in Figure 2.1. The start of a super-frame is indicated by the coordinator node via a beacon packet. The beacon packet includes network configuration

information and an indication of whether downlink data packets are pending. A beacon packet may also have a payload field. A super-frame is subdivided into two regions, namely active and inactive period. The active period is further divided into 16 time slots. Based on the MAC layer configuration, these time slots are divided into a Contention Access Period (CAP) and a Contention Free Period (CFP). During the CAP, nodes compete to send up-link packets to, and request pending down-link packets from their corresponding coordinator using a slotted variation of the CSMA-CA mechanism or by employing the ALOHA scheme. This thesis uses the CSMA mechanism.

The CFP is optional and follows the CAP. The CFP is further divided into smaller slots called GTSs. GTSs are dynamically assigned by the coordinator to a sensor node. A maximum of seven GTSs could be assigned, out of which more than one GTS may be allocated to a sensor node. During a GTS, a node can attempt to transmit and receive packets in a contention-free fashion – without the need for CS. Following the CFP is the inactive period. During this time, all nodes including the coordinator node can turn off their transceivers to save energy.

In this thesis, sensor nodes are mainly restricted to send up-link packets using CSMA-CA in the CAP period only. Preliminary studies discussed in Section 4.3.2 reveal that scenarios with external interference networks using CSMA in the up-link direction achieve higher packet success rates than networks using allocated GTSs. The networks using GTSs consumed marginally less energy as compared to networks using CSMA. Nevertheless, with interference the networks using allocated GTS are punished for not using carrier-sensing, with CSMA it becomes possible to avoid transmissions during interference bursts – to some extent. For similar reasons, this thesis, ignores the use of the ALOHA scheme. Furthermore, the inactive period is used in some of the proposed schemes in this thesis by the coordinator for channel measurements.

The length of the super-frame and the inactive period within a super-frame are

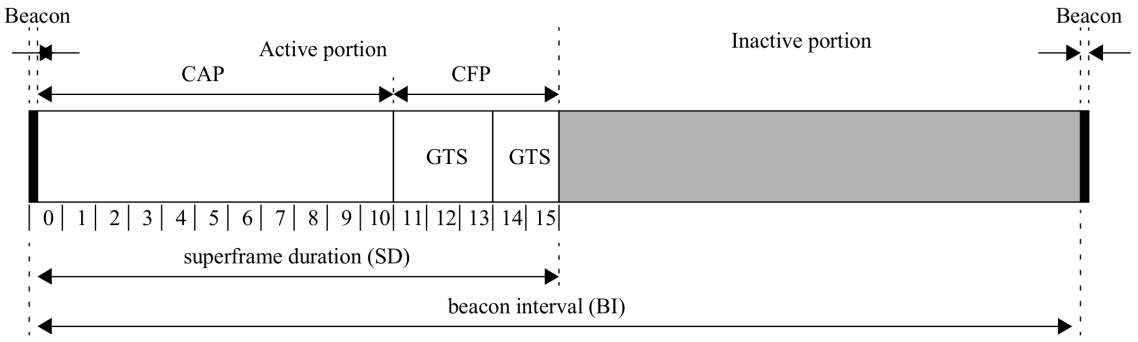

Figure 2.1.: An example of an IEEE 802.15.4 super-frame structure [97, Sec. 5.1.1.1]

configurable via two parameters: Beacon Order (BO) and super-frame Order (SO). According to the IEEE 802.15.4 standard, the inter-arrival time between beacon packets is calculated via Equation 2.1 [97, Sec. 5.1.1]:

$$BI = aBaseSuperframeDuration \times 2^{BO}, 0 \leq BO \leq 14 \tag{2.1}$$

where BI is the Beacon Interval and aBaseSuperframeDuration is equal to 60 channel symbols – if using the 2.4 GHz physical layer this duration is equal to 15.36 ms. The duration of the active period, also referred to as super-frame Duration (SD), is calculated using the following Equation 2.2 [97, Sec. 5.1.1]:

$$SD = aBaseSuperframeDuration \times 2^{SO} \tag{2.2}$$

where $0 \leq SO \leq BO \leq 14$. Figure 2.1 illustrates a simple example of a super-frame structure. In this example, SO is considered to be one unit smaller than BO; this implies that the SD is half the BI duration. Furthermore, two GTSs are assigned to sensor nodes.

In the beacon-enabled mode, sensor nodes are required to wake-up before the start of the super-frame and receive the beacon packet. When a sensor node does not receive aMaxLostBeacons[2] consecutive beacon packets, the sensor node may consider its synchronisation lost and change its state to an **orphan** node. An orphan

[2]According to the IEEE 802.15.4 standard aMaxLostBeacons is equal to four

node needs to re-associate with its corresponding PAN coordinator node before it is allowed to transmit or receive further data packets.

Sensor nodes are generally required to first discover beacon packets sent by their corresponding coordinator node before associating to a network. In scenarios where the network switches channels in order to mitigate external interference, sensor nodes are required to search all or a subset of available frequency channels and listening on them (see [84, 163]). In cases where nodes possess additional information that aids in narrowing down channels into which the PAN coordinator may have hopped, higher layers can elect a subset of channels, to both reduce the time spent in orphan state and the energy consumption (see Chapter 5). For non-adaptive networks, the higher layers may choose to confine the search to only the current operating frequency channel, in order to save time and energy.

After receiving the beacon packet, nodes then need to send association request control packets during the CAP. The coordinator may or may not grant the sensor node's association request. The same discovery process is repeated every time the sensor becomes orphaned. When an association request is granted, an associated node may choose to stay synchronised with its corresponding coordinator and track its beacons [97, Section 5.1.4.1]. In such cases, sensor nodes wake up shortly before the start of a super-frame and attempt to receive the beacon packet. Every time a beacon packet is successfully received, network parameters such as BO/SO, PAN ID, and other pending information in the beacon payload – if any – are forwarded to higher layers. In scenarios where a node has lost four beacon packets in a row, it concludes that synchronisation is lost and the higher layers are informed. This thesis assumes that nodes choose to maintain synchronisation. This is required when the higher layers adapt the BO/SO settings for realigning a PAN, or for adaptive schemes such as frequency adaptation schemes described in Chapter 4.

When a node fails to receive four consecutive beacons packets – due to external interference – it informs the higher layers about losing synchronisation with their

corresponding coordinator node. The higher layers decide to either re-set the MAC layer completely – forcing the node to start a new association procedure – or changing the nodes status to orphan mode. One way of finding neighbouring networks is by channel scanning – orphan channel scan. Another way for orphan nodes to re-locate their corresponding coordinator after losing synchronisation is by sending orphan-notification command packets and waits for a response from its PAN coordinator [97, Sec. 5.3.6]. This method is mainly used for non-beacon enabled networks, since it requires the coordinator to be active at all times. After sending the orphan-notification command packet, the sensor node listens at most for macResponseWaitTime. If it successfully receives a coordinator realignment command during the specified time, the sensor node would continue its normal routines as an associated sensor node. This approach is not used in this thesis, instead orphan nodes perform channel scanning and listen on every channel for the duration of one beacon period[3]. After re-locating the PAN coordinator, the node associates and continues track its beacon packets. This thesis refers to the time between losing four successive beacon packets and the next received beacon as the "time spent in orphan state" or "orphan duration time".

To sum-up, this section provided a brief overview of the well-established IEEE 802.15.4 standard. The popular IEEE 802.15.4-compatible CC2420 transceiver that operates in the 2.4 GHz ISM band has been selected as the physical layer. Furthermore, the MAC layer uses the beacon-enabled mode to communicate and save energy by sleeping during the inactive periods. According to the specifications of this standard, CSMA-CA is a mechanism that aids with the co-existence issues in the 2.4 GHz band. Nevertheless, due to extensive usage of this frequency band by other technologies (e.g. WiFi), WBSNs that are being used in densely populated

[3]This is done to circumvent a problem in the standard: in the beacon-enabled mode there is the risk of coordinator being in its inactive period when the orphan sends the orphan-notification command packet. By forcing the orphan nodes to listen for an entire beacon period, it is guaranteed that to receive at least one beacon – excluding scenarios where the beacon packet is not received successfully due to external interference or errors.

urban environments may experience an ever-changing interference landscape [66]. The following section gives an overview of the popular IEEE 802.11 standard – also known as WiFi.

2.1.2. IEEE 802.11

IEEE 802.11 is a Wireless Local Area Network (WLAN) standard [2], also referred to as WiFi. In the 2.4 GHz ISM band it operates in a total of 14 overlapping channels, each with a bandwidth of 22 MHz and a channel separation of 5 MHz – in IEEE 802.11b. A common transmit-power used by WiFi systems is 20 dBm, which leads to an approximate communication range of 100 metres (in a line of sight). Users of this technology connect to each other via Access Points (AP) or in an ad-hoc manner. The IEEE 802.11b version [2] supports DSSS for its spreading and Complementary code keying (CCK) as its modulation technique, with a data rate between 1 and 11 Mbps. IEEE 802.11g [4] is backwards compatible and supports DSSS; the main modulation scheme used in IEEE 802.11g is OFDM, which supports data rates between 6 to 54 Mbps. Another difference introduced in the IEEE 802.11g standard is the 20 MHz wide channel bandwidth. This allows up to four conflict-free WiFi networks to operate at the same location when choosing channels 1, 5, 9 and 13.

The previous version, IEEE 802.11b, with a channel width of 22 MHz is limited to three conflict-free channels only, namely channels 1, 7, and 13 (not including channel 14 with a central frequency of 2.484 GHz; this frequency range is only allowed in certain countries, e.g. in the United Kingdom). Figure 2.2, illustrates the spectrum usage of this standard and compares it with the IEEE 802.15.4. From the perspective of an IEEE 802.15.4-compatible device, all packets sent by a WiFi device – no matter which WiFi version or data rate is used – are considered as external noise. This thesis uses WiFi interference sources configured to operate with the IEEE 802.11b standard and at a data rate of 1 Mbps. This decision was

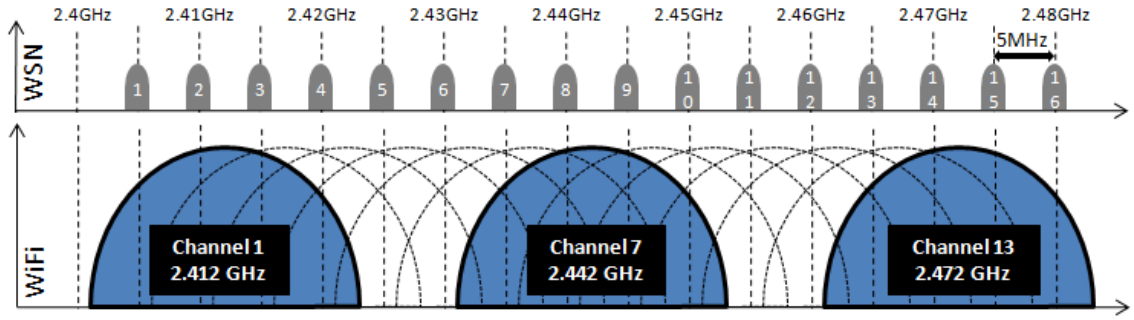

Figure 2.2.: IEEE 802.15.4 and IEEE 802.11 spectrum usage in the 2.4 GHz ISM band.

made to introduce interference on a larger portion of the bandwidth and to generate interference where the interference bursts lasts longer using conventional WiFi APs.

An example of channel interference caused by overlapping of only one IEEE 802.11 channel over the IEEE 802.15.4 spectrum in the 2.4 GHz ISM band is shown in Figure 2.3. This figure presents a more detailed view of the interference caused by a single WiFi device over an IEEE 802.15.4 network. In other words, when a WiFi AP is operating on channel 7 and transmits at full capacity, and the IEEE 802.15.4 network is in close proximity to the interferer source (AP), four of the 16 IEEE 802.15.4 channels would perceive noticeable disturbance caused by the AP's spectral mask – creating a shadow over channels 7, 8, 9 and 10, shown in red. Furthermore, out of the remaining channels, four channels would also suffer from partial interference caused by Adjacent Channel Interference (ACI) [23]: channels 5, 6, 11 and 12 shown in orange. In other words, one WiFi channel overlaps directly with four IEEE 802.15.4 channels, and creates side band interference or ACI for the neighbouring two channels on either side [23, 62, 160]. The impact of ACI on IEEE 802.15.4-based networks is presented in [152]. This study shows that ACI has a noticeable negative impact on IEEE 802.15.4-based network PRR. Nevertheless, to simplify the analysis, ACI is ignored in our simulation model.

To sum up, in a scenario where a single WiFi device is transmitting at full transmission capacity and in close proximity to an IEEE 802.15.4 network, the IEEE 802.15.4 network would be limited to utilising only half of the total available chan-

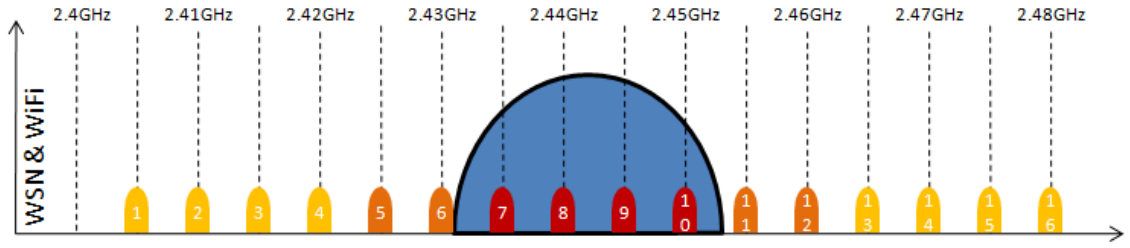

Figure 2.3.: An example of one WiFi channel overlapping the IEEE 802.15.4 spectrum.

nels with no interference. The effects of external interference on IEEE 802.15.4-based devices are later presented in Section 2.3.

2.2. Impact of Interference on IEEE 802.11 systems

Howitt and Gutierrez studied the impact of IEEE 802.15.4 on 802.11.b devices [71]. They proposed an analytical method based on [70] to analyse the coexistence impact of these two technologies. In this study, the collision probability is considered to be the probability of one IEEE 802.11b packet getting impacted by one or more IEEE 802.15.4 packets. Nevertheless, collision of IEEE 802.11b packets with IEEE 802.15.4 packets does not necessarily result in packet loss because of the vastly different transmit-power levels. This probability represents the Packet Error Rate (PER) of IEEE 802.11.b devices. This study was limited to a special scenario where only the packets transmitted from IEEE 802.11b-based APs were assumed to have an impact on neighbouring WSN nodes. Their study proved that unless the 802.11 Base Station (BS) is also located near the IEEE 802.15.4 devices (with high activity levels), IEEE 802.15.4 networks have minor to no impact on the performance of IEEE 802.11b devices.

Mutual interference of IEEE 802.11b and IEEE 802.15.4 was analysed by Shin et al. in 2007 [143]. The authors proposed a scenario where in the future devices

would use both these technologies on the same hardware device. They assume that the distance between the two radio transceivers would be less than one metre. In their simulation analysis they looked at PER, transmission delay and throughput as their performance measures. The performance of both these technologies (on each other) was analysed based on their distance and the centre-frequency-offset between them. In their simulation scenarios the transmit-power used by IEEE 802.11b and IEEE 802.15.4 devices was set to 30 mW ($\approx$ 14.77 dbm) and 1 mW (= 0 dbm), respectively. Based on the simulation results they obtained, if the distance of an IEEE 802.15.4 device is more than eight metres to an IEEE 802.11b device, the PER of the IEEE 802.15.4 is less than 10^{-5}. Similarly, the distance between these two networks needs to be less than four metres so that the PER of the IEEE 802.11b goes above 10^{-5}. The simulation results also showed that if the centre-frequency-offset between the two technologies is more than 7 MHz at a seven metre distance, the PER of IEEE 802.15.4 is less than 10^{-5}. The authors clearly show the IEEE 802.15.4-based devices have less impact on the performance of WiFi devices than vice versa.

A very similar simulation-based study was conducted by Yoon et al. in 2006, that looked at PER of 802.11b networks under the influence of WSNs [181]. They showed that if the distance between these heterogeneous networks is more than four metres, the measured PER measured of IEEE 802.11b-based networks would be over 10^{-4}. They also proposed optimal packet lengths for different distances between the two networks. Performance analysis of the IEEE 802.11b network under the influence of multiple WSN devices was conducted using simulation by Yoon et al. in 2007 [182]. In this study, they used PER and throughput as their performance metrics. The results show that, regardless of the number of WSN interference sources, the performance of the IEEE 802.11b devices is not affected if the distance between the two technologies is greater than six metres.

An experimental study conducted by Angrisani et al. in 2008 presented useful

information about coexistence issues between IEEE 802.11b and IEEE 802.15.4 networks [19]. Their ultimate goal in this experimental study was to deduce useful information to optimise the network design and setup in common real-life coexistence conditions. By taking into account the coexistence issues of these two technologies and adopting appropriate interference avoidance solutions (such as frequency or transmit-power adaptation), interference effects could be drastically reduced. The authors of this research considered the effects on the Packet Loss Ratio (PLR) when WiFi is affected by IEEE 802.15.4 interference and vice versa. This study is a continuation of their previous work, where they used cross-layer measurements to assist with the coexistence of these two technologies [18].

Figure 2.4 illustrates the adopted testbed used in this experimental study. In this experiment, Tmote Sky sensor nodes were randomly distributed in a circle with a radius of r=2 metres. At the centre of this circle a notebook equipped with a WiFi adapter was placed. This notebook was connected to an AP placed at a d=13 metre distance. Many interesting findings were derived from these experiments. Some of these findings are as follows: The WiFi's PLR has a direct relationship with WiFi's duty cycle λ_{WiFi}. It is shown that for λ_{WiFi} greater than 70% the PLR remains the same with or without the presence of WSN interference. Another dependent factor is the size of WiFi packets. The packet size of 1112 bytes is suggested by the authors of this study which also agrees with the recommendations of [181]. An even more interesting result is that the direction of interference has no effect on the PLR. Nevertheless, when packets are transmitted from a source which is in close proximity to WSNs, the interference experienced at the destination is mainly due to channel occupation, whereas, in the case where the AP is transmitting and the receiving WiFi device is near WSN devices, the interference experienced is mainly caused by packet collision or channel errors. Finally, the increase in the intensity of WSN interference has negative impacts on both PLR and Signal to Interference Ratio (SIR). The authors also confirm that the predominant effect of interference is

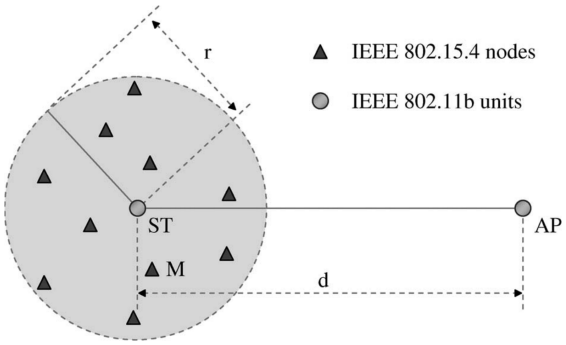

Figure 2.4.: Experimental testbed adopted by [19].

from IEEE 802.11 based networks to IEEE 802.15.4 technologies.

Contrary to the research presented so far in this section, where all results suggest that because of the vast difference between the transmission powers of these two technologies the impact of IEEE 802.15.4 on IEEE 802.11 is negligible, Pollin et al. proved that in many cases IEEE 802.15.4 has significant impact on the performance of IEEE 802.11b devices [128]. One of the key points that the authors of this measurement-based study consider is the listen-before-send mechanism that both these networks employ as their interference mitigation mechanism. This research shows that because of the vast difference between the duration of channel sensing – 20 μs for WiFi and more than 320 μs for WSN – the IEEE 802.15.4-based networks have a greater impact on the performance of WiFi networks. They experimentally tested this hypothesis and proved that even in cases where listen-before-send is enabled in IEEE 802.15.4-based networks, the WiFi network suffers from over 80% throughput degradation. Moreover, this research also illustrates the importance of validation through experimentation.

As presented above, despite the asymmetric transmission powers of IEEE 802.15.4-based WSNs and IEEE 802.11, IEEE 802.15.4 devices can have significant impact on the performance of IEEE 802.11 devices. Nevertheless, since the focus of this thesis is on WBSNs – that are worn by humans living in densely populated urban environments – and these networks deal with human vital signs, having reliable and timely data transfer is of utmost importance. Furthermore, according to the

experimental studies done by Angrisani et al. in [19], the duty cycle and distance of WBSNs need to be fairly high and near, respectively, to have serious effect on the performance of WiFi devices.

2.3. Impact of Interference on IEEE 802.15.4 systems

Shin et al. in 2005 analysed the impact of IEEE 802.11b interference on the IEEE 802.15.4 performance [142]. They looked at the PER of WSN devices as their performance measure. In their simulation analysis they used two WiFi and two WSN devices all placed at a one metre distance from each other. The distance between the two networks was varied. The results revealed that if the distance between the two networks goes beyond eight metres the interference of IEEE 802.11b network on WSNs is negligible and the PER is smaller than 10^{-6}. Furthermore, if the centre frequencies of these two technologies are 7 MHz apart from each other at a four metre distance, the interference of the WiFi network on IEEE 802.15.4-based networks is negligible and could be ignored.

An experimental study done by Petrova et al. in 2007, showed the interference impact of the IEEE 802.11g/n on IEEE 802.15.4-based sensors [125]. The purpose of this measurement-based research was to show the impact that the IEEE 802.11g/n-based devices have on industries with existing IEEE 802.15.4-based networks. In their experimental study they used two configuration setups. In the first setup they evaluated the impact of different traffic loads on WSNs and in their second setup they illustrated the impact of directionality of IEEE 802.11n on the two sensor nodes. As expected, the IEEE 802.15.4-based devices had a very poor packet delivery ratio when faced with medium to high WiFi traffic loads. Another interesting observation showed that due to the sensitivity threshold setting in the IEEE 802.15.4 devices, the impact of IEEE 802.11n-based interference on non-overlapping channels is still

destructive for WSN packets. The results obtained with their directional experiment show that, based on the angle that the WSNs are placed in, a maximum difference of 50% is observed in the packet delivery ratio. The authors of this work conclude that special attention is needed for selecting the frequency channels that these two networks are operating on.

Ko et al in 2009 performed empirical studies in a medical environment – in particular at the emergency room of the Johns Hopkins Hospital, Baltimore, United States. In this pilot study they monitored the vital signs of ambulatory patients in the hospital's emergency room waiting to be seen by the doctors. The sensor units used for this study collected the heart rates and blood oxygen levels of the patients before transmitting this information to the base station using IEEE 802.15.4-based radio systems. Their results showed that hospital conditions are more intense in terms of noise levels and have more bursty links in comparison with other indoor environments. In addition, they experienced that the quality of the channel remains stable for only short periods in time – tens of second. Despite the previous belief [102, 146] that high LQI values have a direct relationship with achieving high PRRs, this study showed that high LQI is necessary but not sufficient. This phenomenon could be explained since LQI values are recorded only when a packet is successfully received, therefore the LQI value returns a somewhat biased representation of the quality of the channel compared to the PRR value. Although the link condition of the emergency room was measured to be high, the authors managed to achieve an end-to-end delivery ratio of over 99%, using their routing protocol. They illustrated that in harsh environments like hospitals, wireless medical sensing applications are able to perform well [90].

A more recent experimental study done by Wykret et al. illustrated the impact of other WSN, WiFi, Bluetooth and microwave-ovens, on IEEE 802.15.4-based networks [166]. The findings of this experiment showed that co-channel interference from other WSNs not only affected the networks with the same operating chan-

nel, but also on neighbouring channels caused by adjacent channel interference. The effects was most pronounced when WiFi interference was introduced. Since Bluetooth devices employ a frequency hopping mechanism all WSN channels were affected equally. Microwave-oven interference showed the most impact on the middle WSN channels, starting from channel 15 up-to channel 24.

All studies mentioned in this section unanimously stress the severe negative impact of external interference, in particular of IEEE 802.11-based devices, on IEEE 802.15.4-based networks. In WBSNs where network reliability and timely delivery of information is of utmost importance, strategies that mitigate the external impact of such interference sources are crucial. Cognitive radio is a recent research field that allows a radio device to dynamically adapt and schedule its resources to improve coexistence, utilise un-used operating channels and reduce external interference.

2.4. Cognitive Radio

By sensing the spectrum, detecting the vacant bands and adjusting the communication parameters, cognitive radio improves the overall spectrum utilisation in both licensed and unlicensed bands [11]. In the case of licensed bands, Primary Users (PUs) that are given license to operate on the allocated frequencies have priority over Secondary Users (SUs). SUs are only permitted to utilise the free frequency bands if they do not cause interference to other neighbouring PUs. In the case when a PU starts its communication, SUs must perform the following three steps:

1. Spectrum Sensing: detecting alternative free bands.

2. Spectrum Decision: determine the next operating frequency band.

3. Spectrum Handoff: adjusting the operating parameters in a way that the current communication is continued on the newly selected band.

The same techniques could be employed for unlicensed bands. An example of using cognitive radio in WSN devices operating on unlicensed frequency bands such as the 2.4 GHz ISM band is dynamic or opportunistic spectrum access of WSNs to efficiently cooperate with other heterogeneous networks operating on overlapping frequency bands [69]. Opportunistic access to multiple potential channels can reduce the probability of packet loss and collision in comparison with fixed channel selection schemes [69]. Apart from increasing the reliability of the network, cognitive-radio-capable networks consume less energy by decreasing the number of packet transmissions. Moreover, adapting to varying channel conditions aids in increasing the overall network lifetime. In scenarios with overlapping homogeneous networks, dynamic spectrum management helps with efficient coexistence of these networks in both communication performance and resource utilisation aspects. Finally, cognitive-radio-capable networks are able to overcome and adapt to varying spectrum regulations applied to specific regions or countries.

The IEEE 802.22 standard [6], the first cognitive radio Wireless Regional Area Network (WRAN) standard, introduces an infrastructure-based approach with central coordination which allows SUs the usage of the TV broadcast bands in both VHF and UHF range. Some of the advantages of using the white spaces allocated in the TV broadcast bands for applications used in hard-to-reach and low-population areas or rural environments are the reasonable antenna size, and good non-line-of-sight propagation characteristics of these bands [147]. The VHF/UHF frequency band ranges from 54 to 862 MHz, depending on the location across the globe. Without a centralised control infrastructure, synchronisation of fixed and mobile sensor networks operating on a given spectrum is a harder task in WSNs. One of the fundamental problems in cognitive-aware WSNs is the design of accurate and fast channel estimation techniques used to sense the spectrum [22].

In the case of WSNs, much research has been done to find the potential white spaces in the spectrum without an allocated coordinator or infrastructure similar

to IEEE 802.22 [113–115]. Moravejosharieh et al. classified the channel utilisation into three – white, grey and red – regions, which represent if a given channel is idle, being used by one user or overlapped with two or more neighbouring WSN nodes, respectively. The authors studied the percentage of channel utilisation as the network density increases. Preliminary schemes are proposed (blind, Idealised, Initial choice and Greedy) to detect the existence of overlapping neighbouring networks without the need for a centralised coordination infrastructure. Their Greedy scheme enabled the WSNs to adapt their schedule in order to minimise the red region. While this thesis introduces frequency adaptation schemes, which result in switching to a channel with the lowest interference, the aforementioned Greedy scheme assists WSNs to utilise that specific frequency more efficiently. Nevertheless, this scheme has its drawbacks, namely in scenarios where the number of networks per channel exceeds the channel capacity, arrival of additional networks would result in their starvation in terms of channel access.

Users of unlicensed frequency bands where no PU is defined, in order to coexist with other neighbouring heterogeneous networks, employ different strategies; one of which is choosing a modulation scheme. Following are two examples of popular spread spectrum techniques used by some of the 2.4 GHz users:

1. Frequency Hopping Spread Spectrum (FHSS): The IEEE 802.15.1 [3, 5] standard, widely known as Bluetooth, is a popular wireless PAN technology which employs FHSS as its modulation scheme. This standard has a total of 79 frequency channels in the 2.4 GHz ISM band. Each channel has a bandwidth of 1 MHz and a channel separation of 1 MHz. The hopping kernel operates by selecting a segment of 64 adjacent channels out of the 79 available channels. Then, it will start hopping on 32 different channels randomly – following a pseudo-random sequence known by both transmitter and receiver – without reusing the same selected channels, while transmitting its data. Next, a different segment of 64 channels is selected where this process repeats itself. This

modulation scheme increases the resistance of devices in such networks against narrow-band interference. Furthermore, if the pseudo-random sequence used for this frequency hopping scheme is unknown, real time transmission interception of such communication is difficult. Finally, spreading technologies like FHSS better utilise the entire available spectrum, as compared to other modulation schemes used by IEEE 802.15.4 or IEEE 802.11.

2. Direct Sequence Spread Spectrum (DSSS): Another technique used to spread the carrier signal over a wide bandwidth is DSSS. Using this modulation scheme the transmitted signal utilises more bandwidth than the information signal. By multiplying the transmitted data signal with a pseudo-random sequence of binary "chips", the original signal is spread over a much wider band. Although the resulting signal looks like white-noise, by correlating the signal with the same pseudo-random sequence, the original data can be recovered. Benefits of using this modulation scheme are: resilience against jamming, enhancing the signal-to-noise ratio (by adding more chips per bit), and sharing the same channel with multiple users using different pseudo-random sequences. This modulation scheme is used by both IEEE 802.11 and IEEE 802.15.4 devices.

Other strategies that increase network reliability and reduce the energy consumption of the network are introduced in following sections.

2.5. Channel Adaptation

Channel adaptation has been used in wireless technologies for many years. Many studies have shown dynamic spectrum access and opportunistic channel selection techniques that significantly impact on the overall performance of the network [40, 66, 117, 129]. Some studies suggest graph colouring schemes to pre-assign different channels to nodes and networks to mitigate channel interference and to efficiently

distribute the traffic loads [41, 165] – mainly used in static scenarios. While these schemes increase the performance in scenarios with high traffic demand, they are not robust to environments with external interference or dynamic network topologies.

More recent studies introduce the use of multiple radio transceivers on a single sensor node [36, 106, 185]. There are many protocols that support multi-radio, which could be categorised in two groups namely, schemes that use one radio channel for control purposes and the others for data transfer [168, 184], and schemes that utilise all channels to increase the data throughput or act as relay nodes [88, 168]. In applications such as WBSNs where sensor devices are placed inside the human body and the expected network lifetimes are up to 10 to 15 years [151], Body Channel Communication (BCC) and Fabric Area Networking (FAN) are introduced to both increase the reliability of the connection and also to reduce the energy cost of communication [180]. Following are brief summary of some of these schemes.

An interesting approach to minimise the impact of WiFi interference on IEEE 802.15.4-based WSNs was suggested by Pollin et al. in 2006 [129]. The primary goal was to propose a distributed technique to address the coexistence of the two network protocols. The average delay between the times a sensor data packet is generated and when the data packet is received by a fixed sink node is considered as their primary performance measure. Another performance metric investigated in this work is the energy consumption. The authors used a simple line topology in their simulation scenario to connect sensor nodes to each other. Three schemes were considered: the first is the Random-Frequency-Selection (RFS) scheme, in which sensor nodes randomly switch to a new channel – following a uniform distribution – every period. The data is sent to the node located closest to the sink node if both nodes have selected the same operating frequency. The advantage of this scheme is that no coordination is needed and this scheme is easily scalable. Nevertheless, the average delay in this technique is expected to be large, since the neighbouring nodes need to be also on the same frequency channel to be able to forward the data

packet to the sink node.

The second scheme proposed in their work is the Scanning-Based approach, where the quality of the channel is measured based on the number of beacon packets received on the given channel. The last scheme is the Learning-Based scheme, which uses the Q-learning algorithm introduced in [162] to select the channel with the maximum rewards. Simulation results illustrated that the Learning-Based approach not only outperformed the Scanning-Based scheme in some scenarios, but also the energy consumption was reduced by a factor of two. Timmers et al. in 2008 further improved the Learning-Based algorithm which suffered from over-exploration when steady-state was reached [150]. To achieve a better balance between exploration and exploitation, simulated annealing was employed to gain more effective heuristic optimisation. The results show that the proposed adaptive-simulated-annealing approach clearly outperforms the reward-based scheme, by reaching an optimal steady-state and having a faster convergence. The main differences of their work to ours is that the proposed schemes are not designed for scenarios with constantly changing interference where a steady-state is not reached. Furthermore, in our scenario the network has group mobility.

One simple approach to overcome the interference caused by neighbouring WiFi devices is channel hopping. The idea is to switch the network to a different channel that has no or less background noise created by overlapping technologies. Musaloiu-E and Terzis in 2008 compared four RSSI-based channel interference estimation mechanisms, namely cardinality, max, mean and threshold-based RSSI measurement schemes [117]. The cardinality value represented the variation in the sampled RSSI values, whereas the Max RSSI value only shows the maximum observed RSSI value measured during a given sampling window. The Mean RSSI estimation value represented a smooth curve, illustrating the average RSSI value observed over a given duration. The threshold-based RSSI value presents the number of RSSI observations obtained where the sampled value was above a preconfigured threshold

representing the noise-floor (in this case, -90 and -87 dBm).

The main advantage of these channel-estimators is their simplicity and their ability to differentiate between noisy and ideal channels. Musaloiu-E and Terzis attempted to avoid interference using channel hopping. Their results showed a significant drop in the packet loss rate from 58% to less than 1%. In their approach they assumed that channels 25 and 26 of the IEEE 802.15.4-based radios are interference free. Although this assumption is true for some countries, it is not a reliable approach: for example, in Asia IEEE 802.11-based devices are allowed to use those frequencies. Another limitation of this work is that they only looked at stationary nodes.

In [66], Hauer et al. experimentally measured the dynamics and changes in noise floor along with the packet RSSI and LQI values while moving in a densely populated urban environment full of WiFi interferers. This study illustrated that in low-powered WBSN devices with resource restrictions, external interference is typically the primary cause of a substantial percentage of packet loss. In this study, noise floor – represented as Signal Strength Indication Noise (SSInoise) – is in fact the value of RSSI sampled between data transmissions. Hauer et al. showed that a single SSInoise value is not a reliable source for detecting the presence of an interference source. This study also pointed out that as the distance between the sensor nodes and the interference source decreased, the LQI values show higher variation, whereas the RSSI values remain unaffected or with insignificant variation. They experimentally measured the interference in urban environments, and this gave a clear insight into how noise floor, RSSI and LQI react to interference. The authors' aim was to empirically demonstrate the correlation between WBSN packet reception performance and the activities of actual WiFi interference. Furthermore, in order to find a potential trigger for changing the operating frequency channel of WBSN as an interference mitigation strategy, the authors explored the use of cross-channel quality correlation and trends.

In their experimental approach, they used two Tmote Sky [43] nodes placed ap-

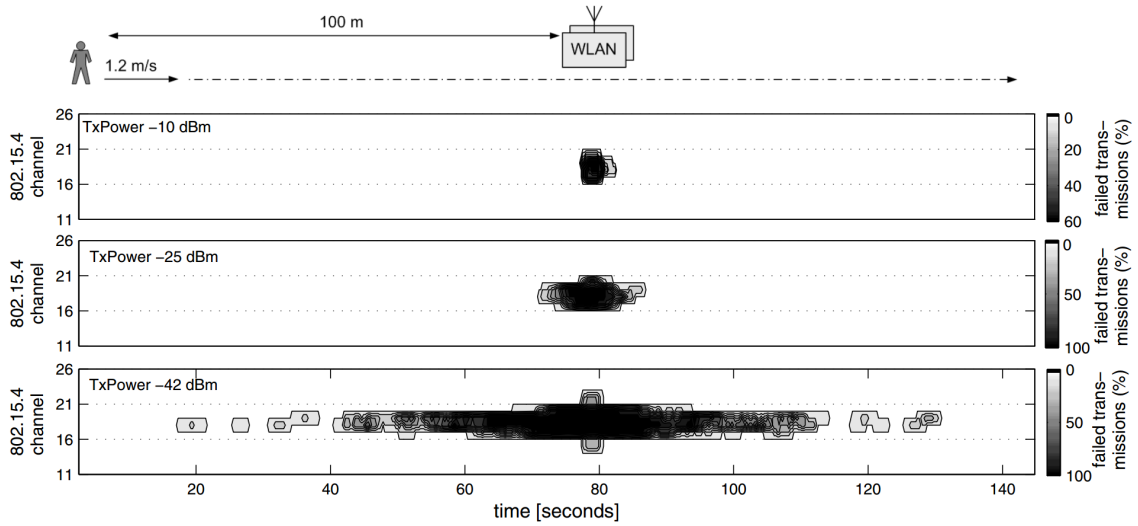

Figure 2.5.: The results for the percentage of failed transmission in [66].

proximately 1.5 metres apart from each other on a human body. For the purpose of their experiment they used two physical links to synchronise the two sensor nodes and also to get feedback from the devices on a laptop computer. For each experiment they transmitted 32 data packets followed by an acknowledgement packet without the use of CCA. This process was repeated for different transmit-powers and for all available 16 channels. In their first experiment they connected two laptops using an IEEE 802.11b ad-hoc network connection (on channel 7) to transfer a large file between them. They placed the laptops in the middle of the field close to each other and asked a human to carry the sensor nodes from one end of the field to the other in a straight line crossing over the laptops. Figure 2.5 illustrates the effects of WiFi interference on WBSN packet delivery for all 16 channels and with different transmit-power levels. It is interesting to point out that at roughly 10 metre distance from the WiFi interference source, when transmitting at -25 dBm, very few packets were successfully transmitted on IEEE 802.15.4 frequency channels overlapped by channel 7 of IEEE 802.11. This distance further increases to over 75 metre when transmitting at -42 dBm.

Additionally, results shown in Figure 2.6 represent the noise floor, RSSI and LQI measurements recorded for channel 18 of the IEEE 802.15.4 frequency channels with

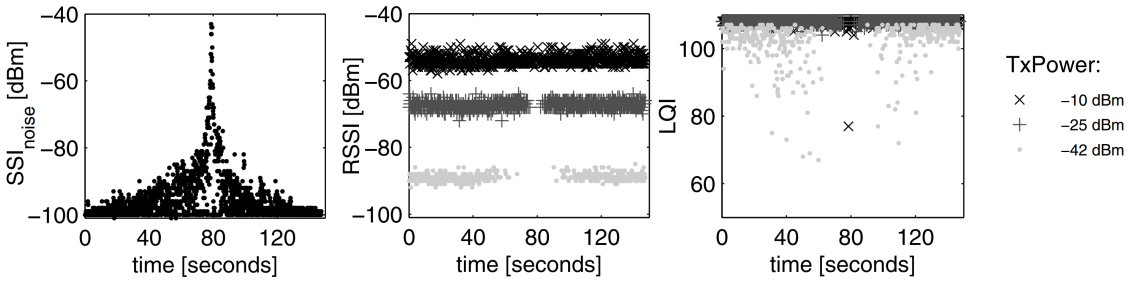

Figure 2.6.: Noise floor, RSSI and LQI measurements of channel 18 [66].

different transmit-power levels. Both RSSI and LQI measurements obtained from the received packets stop when the interference source is at close proximity to the WSN nodes. Unlike RSSI and LQI, SSI_{noise} measurements are obtained even if the nodes are near the interference source. However, the authors pointed out that it is not possible to rely on a single SSI_{noise} measurement since, as can be seen in Figure 2.6, during 80 second there are SSI_{noise} samples that are equal to the noise floor (-100 dBm) – mainly because the sample was taken between WiFi packet transitions. In addition, the authors also found "some correlation in time and frequency, sometimes lasting for a few tens of second up to multiple minutes and spanning over multiple consecutive 802.15.4 channels" [66, Sec. 4.2] where communication between the sensor nodes was not possible. This finding clearly indicates that for high-risk applications that deal with human vital signs in WBSNs, it is important to detect these interference sources and accordingly switch the frequency channel or transmit-power to maintain a reliable connection between the sensor nodes and their coordinator node.

Furthermore, Hauer et al. gathered trace information from three different environments (shopping street, urban residential and office environment on different days and times). Using these traces they calculated the minimum number of channel hops needed to successfully transmit all data packets, using an ideal channel hopping scheme that has information about future channel quality. Their results showed that for a transmit-power of -10 dBm there is at any time at least one channel that could be used and get a 100% success rate. For -25 dBm the number of channel

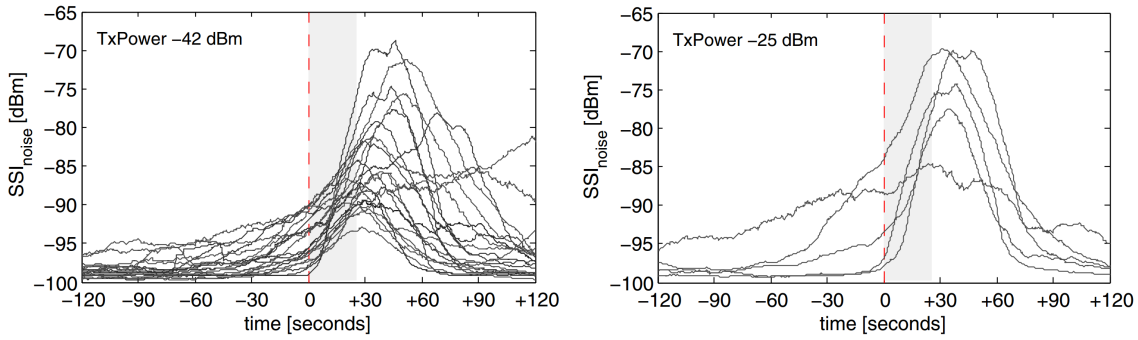

Figure 2.7.: Noise floor within a window of ±2 minutes around heavy transmission failures (starting at 0s) [66].

hops increased to roughly three hops. In the case of -42 dBm over 50 channel hops were required, which meant on average every two second.

Another experimentation done by the authors revealed that a substantial increase in SSI_{noise} is usually followed by escalated packet loss [66, Sec. 5.2]. For their experiment they extracted about 1000 samples starting two minutes before experiencing significant link degradation and two minutes after. Figure 2.7 illustrates the averaged SSI_{noise} values calculated using a moving-average of 26 second. The trends show similarities for both transmit-power levels. The bell-shaped trend suggests that the human is passing an interference source. Looking closer to the results, 13 second before and after the zero second point there is a significant rise in the noise floor. The authors believe by incorporating noise floor history and using more developed statistical techniques it would be possible to forecast the link quality of a given channel.

Chowdhury and Akyildiz [41] acknowledged the severe impact of external interference on the performance of IEEE 802.15.4-based WSN. They attempted to approach this problem by proposing an Interferer-aware Transmission Adaptation (ITA) scheme that adjusts the operating channel, packet inter-arrival time and duty-cycle of the network depending on the detected interference patterns. In this study they proposed an interference classification mechanism that encompasses an off-line measurement phase – where the reference spectral characteristics of different

well-known external interference sources such as WiFi and microwave devices are obtained – and an online matching phase – where the detected spectrum shape is cross-referenced with the existing recorded patterns. The sensor nodes then leverage the information stored to appropriately select the optimal frequency channel, packet inter-arrival time and the network sleep and wake durations. The results showed roughly 60% improvement in terms of energy consumption for nodes using the ITA scheme compared to classic approaches, while preserving packet loss to the minimum. The authors also evaluated the performance on the interferer network and found no noticeable performance degradation when using the ITA scheme. However, this approach may not have the same performance in scenarios with WBSNs moving in a rapidly changing interference landscape. Also, for applications that deal with human vital signs, changing the packet inter-arrival time and duty-cycle of the network may not be optional.

A Spectrum Agile Medium Access Control (SA-MAC) Protocol was proposed by Ansari et al. in [20]. This scheme uses a lightweight heuristic channel selection algorithm. SA-MAC attempts to evaluate each channel in the channel pool by assigning a weight. A sensor node used the preamble-sampling principle to detect the channel state (namely idle, being used or has interference) and increases the weight by one, two and three units, respectively. The channel with the minimal interference is elected to be the operating channel by sorting the calculated channel weights. The authors attempted to further improve their scheme by keeping record of the channel history. Nonetheless, scanning all available channels consumes both time and energy. To mitigate this, Ansari et al. introduced a threshold variable which is used to subdivide the available channels. Using this strategy, sensor nodes only scanned a small subset of available channels, thus consuming less energy and time. In the case where the weight of the subset of channels exceeded the preconfigured threshold new channels are introduced. Both analytical and experimental results showed that this protocol maintains a high packet success ratio in the presence

of heavy interference. However, in their experiment only stationary nodes were considered which is the main difference compare to our study. Furthermore, in our approach channel switching is only made if the current channel quality drops below a given threshold rather than constantly switching to the channel with the lowest interference.

In [21], Ansari et al. improved their scheme by allowing spectrum occupancy characteristics recorded in a table to be shared amongst other neighbouring sensor nodes. They used bit vectors representing if a given channel has a weight higher than the preconfigured threshold. At the receiver end, the sensor increases its table by one unit if a particular channel has a weight higher than the threshold; otherwise the receiver node decreases the weight by one unit. By using bit vectors to represent neighbourhood channel maps they not only minimised the communication overhead, but also increased the accuracy of channel estimation by utilising neighbourhood channel estimation information. Their results revealed that their scheme increased the network performance by 10% in comparison to random channel selection scheme, reaching a success ratio of approximately 95% for scenarios with cyclic or permanent interference. For scenarios with random interference SA-MAC performed 4% better that the random selection scheme, reaching a success ratio of 91 % in comparison to 87 % in the case of random selection scheme.

Single fixed channel approaches are commonly used in WSN applications, mainly due to their simplicity and low power consumption [50]. However, nowadays many low-power sensor network nodes are equipped with radio transceivers capable of operation on multi-channels and/or multi-bands [22, 54, 69, 88, 106, 166, 168]. One of the objectives of multi-channel MAC protocols is to increase the throughput of network. The drawback of such protocols is that under light channel interference they are less energy-efficient in comparison to single-channel protocols. In [88], Kim et al. proposed an energy efficient multi-channel MAC protocol for WSNs, called Y-MAC, capable of achieving high performance while being energy-efficient

for both moderate and high traffic conditions. Although using multiple transceivers on a WBSN device increases the total performance gains and reduces the energy consumption, the main goal of this thesis was to keep costs, complexity and size of the sensor devices as small as possible by using commercially available and popular WBSN devices.

Wykret et al. used RSSI measurements to select the best channels in the 2.4 GHz and 900 MHz bands and operate on the channel with the lowest noise-floor [166]. In case the nodes lost their link connection the sensor nodes would return to a predefined control channel (in this case channel 11). The experimental results showed a 97% PRR. The main drawback of this approach apart from additional energy costs of having an extra radio receiver was the reduced bandwidth of the 900 MHz radio. Clearly, such assumption (considering the control channel) is the major difference to what is proposed in our study.

Liu and Wu in [106] proposed a Dynamic Multi-radio Multi-Channel media Access control (DMMA) protocol to further increase the robustness and throughput of the network. In their study they implemented their proposed protocol on a WSN node with 4 radio transceivers. In order to reduce the energy consumption of sensor nodes, their DMMA protocol uses a sleeping-based mechanism. In their approach they assigned a dedicated fixed channel for control and synchronisation and the remaining channels for data transfer. The DMMA scheme is able to detect interference using carrier-sensing and selects alternative idle channels for data transfer. Their experimental results disclose that DMMA outperforms traditional CSMA approaches significantly. In the case where three interference sources were introduced their DMMA scheme achieved over 98% average delivery ratio compared to 70% in the case of CSMA-based schemes. Nevertheless, as the available frequency channels for such devices are finite and overcrowding of the spectrum is unavoidable, guaranteeing a dedicated interference free control channel is very difficult and in some cases impractical. Another drawback of using multi-radio platforms is the increasing cost

of nodes in the network.

After illustrating the destructive impact of WiFi devices on WSNs used in medical environments, Hou et al. proposed the use of a hybrid sensor device that not only has the IEEE 802.15.4 physical radio layer, but also the IEEE 802.11 [69]. The authors of this experimental study identified two schemes in which the IEEE 802.11 radio would be able to intervene and create windows when other neighbouring WiFi devices would sleep and would allow WSN packets to be sent. The first method involves sending an arbitrary IEEE 802.11 packet that indicates this packet is unusually long. Unfortunately, this method did not work since most commercially available WiFi devices ignored this rogue packet. The second method introduced by Hou et al. employed the use of request-to-send and clear-to-send (also referred to as RTS/CTS). Using this method the authors blocked all neighbouring IEEE 802.11-based devices from transmitting packets for a specific duration of time. Using this hybrid solution the authors showed an approximate successful transmission of 99%. Although sending RTS/CTS packets prevents IEEE 802.11-based devices to transmit, since the duty cycle of WSN devices is low and they usually carry small but critical information, this jamming would not have serious effects on the performance of the WiFi devices.

In 2008 Xu et al. proposed channel surfing strategies to assure the availability of WSN services in dynamic networks with low degree of node mobility [168]. In their study, they explored **coordinated channel switching** and **spectral multiplexing**. For coordinated channel switching, the entire sensor network switches its operation channel to enhance the reliability of the network; while in the case of spectral multiplexing only sensors located in the jammed region changed their operation channel where the boundary nodes act as relay between the different spectral zones. To trigger the channel switching mechanism, in the coordinated channel switching strategy each sensor node autonomously examines the loss of its neighbours, and using a broadcast-assisted channel switching mechanism, the newly selected operating

channel is rapidly switched with low latency. The authors explored both synchronous and asynchronous approaches to simplify the scheduling problem of sensor nodes operation on multiple channels. The proposed schemes were implemented on a testbed with 30 sensor network nodes. For their evaluation they chose network-recovery time and protocol-overhead as their two main performance metrics. They concluded that their proposed channel surfing strategies can rapidly and effectively correct network connectivity in jamming/interference scenarios. Although the authors of this work proposed a coordinated channel switching approach that triggers all nodes in the network to switch their operating channel in order to mitigate external interference, their scheme does not address mobility or severe variation of interference landscape.

2.5.1. Coordinator discovery schemes

Unlike channel adaptation, discovery schemes are not categorised as interference mitigation strategies. They address the case when despite the channel adaptation capabilities of the network, the excessive background-noise causes nodes to lose synchronisation to their coordinator. Neighbour or coordinator discovery schemes play an important role in reducing the orphaning duration and increasing the overall network lifetime. Neighbour and coordinator discovery has received significant attention from the research community in the past few years. Nevertheless, the issue of sensor nodes recovering their synchronisation with their coordinator – after becoming orphaned due to external interference – is not well considered. Studies conducted on neighbour and coordinator discovery techniques, attempt to reduce the packet loss rate, energy consumption and latency [56, 77, 83, 84, 137]. Neighbour discovery and collecting a list of surrounding networks is essential for other applications and protocols such as topology-control algorithms, medium access and routing protocols [30, 64, 137].

Some common similarities found in most neighbour discovery schemes are: (1) time is sub divided into slots and, (2) two nodes operating on the same frequency

channel could discover each other only if they are awake in overlapping time slots. Discovery schemes could be further divided in to single channel [77, 86, 174] and multi-channel [15, 83, 84, 163] discovery problems.

The IEEE 802.15.4 standard [96] presents active and passive discovery techniques for both beacon-enabled and non-beacon-enabled mode networks. This thesis is mainly interested in the passive discovery technique for beacon-enabled networks because active discovery is not allowed there. Generally, a sensor device is required to discover both the operating channel and the beacon period to establish a connection with its corresponding coordinator. However, in our study only channel discovery is performed and the beacon period is assumed to be known. As explained before in Section 2.1.1, orphan nodes may passively listen to the channel until they receive a beacon packet from their corresponding coordinator node. Choosing the correct operating frequency channel is crucial in this process, and is assigned to the higher layers. Another important factor to consider in IEEE 802.15.4-based neighbour discovery schemes is the duration that nodes spend listening on each channel. Different networks may use different beacon-intervals. In order to minimise the packet loss rate, energy consumption and latency, selecting the optimal listening duration and subset of channels to be scanned is crucial.

The SWEEP strategy proposed in [163] further expands the passive discovery technique of the IEEE 802.15.4 standard [96], by introducing varying discovery periods. In other words, by scheduling the listening periods of the sensor network node, this search strategy reduces the network discovery time. Implementation of this scheme needs no modification to the existing MAC layer of the standard. The authors assessed the performance of both targeted and untargeted passive discovery scenarios. The evaluations of the targeted discovery scheme – where nodes are attempting to find a pre-assigned coordinator with known PAN ID – concludes that elevating the success rate of discovery, significantly increases the energy consumption of the nodes. For the untargeted scenario – where the objective of a node is to

discover any coordinator in the vicinity in the shortest amount of time – the results revealed that remaining on the same channel for longer duration increases the performance. They conclude that discovery of networks with longer beacon intervals is very rare and most of the times they remain hidden from the sensor nodes. However, this thesis is mostly interested in targeted coordinator discovery approaches.

Karowski et al. [83] expanded the SWEEP strategy [163] by proposing two optimised discovery strategies, called OPTimised (OPT), and SWitchOPTimised (SWOPT). The authors later proposed a simplified discovery scheme named SUBOPT [84], which requires less memory. The OPT scheme outperformed the SWEEP by rapidly switching channels and remaining on a given channel for a duration time equal to the smallest beacon interval – $BI = 2^0 \times BSD$ where $BSD = aBaseSuperframeDuration$. The SWOPT scheme improved the OPT strategy, reducing the number of channel switches by selecting the minimum duration spent on a given channel to a preconfigured value equal to the minimum beacon interval used by neighbouring networks – $BI = 2^{minimum_beacon_order} \times BSD$. The sub-optimal algorithm SUBOPT gives the same result as SWOPT with less complexity if the total number of channels to be scanned is odd. In the case where the number of channels is even this algorithm is not able to discover all networks.

The three main assumptions made in this study are: 1) No channel switching duration is considered – in other words, the time required for the transceiver to change the operation frequency channel is assumed to be negligible. 2) The beacon transmission/reception time is not considered – this is done by assuming that the beacon packet length is equal to zero. 3) No collision or fading is assumed. All three assumptions are made solely to better illustrate the performance of neighbour discovery in ideal conditions. The main performance measures considered in this study are: the duration time to discover the first network, the average time of discovery and the time it takes to find the last network. The results for OPT and SWOPT were compared against the IEEE 802.15.4 standard passive discovery and the SWEEP

strategy. The cross validation of analytical, simulation and experimentation results of average discovery duration showed similar correlation and trends. Their results showed that the proposed schemes discover networks with smaller beacon orders faster.

In [26, 56] Bashir et al. proposed a Coordinator Assisted Passive Discovery (CAPD) scheme which attempts to decrease the discovery time of both mobile and static devices by altering the duty cycle of the coordinators. This scheme was designed for scenarios where an end device is constantly moving and needs to find a network to transfer its information to. The main two steps of CAPD scheme are to detect mobile nodes and to reduce the beacon order of the coordinator. To detect the mobility of a given node they consider the variation in the LQI value of the received packet. Finally, a decrease-beacon-interval command message is broadcasted by the coordinator associated to the mobile node to all other neighbouring networks. The neighbouring networks reserve the option to immediately reduce their duty cycle, – risking synchronisation loss of their existing sensor nodes – or after the expiry of the current beacon interval. The simulation analysis results reveal that the proposed scheme not only elevates the success rate of association, but also significantly reduces the time mobile nodes spend finding and re-associating with a new network.

In many location tracking applications, it is important for mobile nodes to actively discover all surrounding networks in the shortest amount of time and with minimal energy consumption. As illustrated in [26], while networks with long duty cycles consume less energy, they have higher latency in terms of transmission and reception. Contrary, short duty cycles have the advantage of providing lower discovery latency with the added energy cost. Kandhalu et al. in [77], proposes an optimal trade-off solution named U-Connect for neighbour discovery. U-Connect is a deterministic neighbour discovery scheme which addresses both symmetric and asymmetric coordinator discovery problems. As mentioned earlier in this section, in order for sensor nodes operating on the same frequency channel to discover one

another, they need to be active in overlapping time slots. U-Connect forces nodes to become active at time slots numbers that are multiples of prime numbers. By choosing prime slot durations nodes are guaranteed to eventually have overlapping slot durations, hence discovering each other. To solve the problem of nodes choosing the same prime number, Kandhalu et al. prompted nodes to remain active for slightly longer than half the prime period. Their performance metric used for validation of this study was the product of power and latency.

They compared their proposed scheme with existing protocols such as Disco [55] through both simulation and experimentation. Disco was an asynchronous neighbour discovery and rendezvous scheme proposed by Dutta and Culler, in 2008. Using this strategy ad-hoc nodes are able to discover each other without the need for any synchronisation. This is done by selecting a pair of prime numbers where the mutual sum is equal to the desired duty-cycle. Ad-hoc nodes use these numbers to turn their radio transceiver on and start their packet transmission and reception whenever the internal-timer-counter of the device is dividable by either prime numbers. According to the Chinese Remainder Theorem node discovery time is guaranteed to be bounded in time. Although this scheme was initially designed for ad-hoc networks, Kandhalu et al. implemented this strategy for WSN. Their results showed that U-Connect achieved an order of magnitude lower latency for a preconfigured duty cycle compared to existing discovery schemes.

A neighbour discovery technique called EasiND was proposed by Huang et al. in [73]. Based on the quorum system [28], this scheme can bound the discovery latency for multi-channel WSN scenarios with low power consumption. For multi-channel WSN scenarios with mobile nodes, the authors also proposed an optimal asynchronous neighbour discovery scheme based on different duty-cycle sets that minimised power consumption with bounded discovery latency. The proposed EasiND scheme allows sensor nodes with no prior clock synchronisation knowledge of other neighbouring devices or network to discover and adapt to their operation

frequency and duty-cycle. In their theoretical analysis they showed over 33% improvement of the product of power and latency in comparison to the U-Connect scheme. Their implementation results revealed up to 86% drop in the average discovery latency compared to the U-Connect scheme.

2.6. Transmit-Power Adaptation

Transmit-power adaptation is not a new topic. Much research has been done in this field. Existing solutions proposed in this area could be categorised into four classes: 1) Network-level solutions: here the transmit-power of the whole network is selected and assigned to all nodes in the network [119, 138]. 2) Node-level solutions: each node independently selects a transmit-power to operate and communicate with its neighbouring nodes [91]. 3) Neighbour-level solutions: the transmit-power is independently selected for each neighbour [29, 169]. 4) Packet-level solutions: depending on the type and priority of the packet the transmit-power is selected for each packet transmission [102].

Lin et al. in 2006 introduced a unique adaptive transmit-power control protocol called ATPC. The authors acknowledged that the link quality between low-powered WSN nodes varies noticeably over time and in different environments. Although theoretical studies and simulations present the fundamental basics of a solution, nevertheless these solutions may not be applicable in the physical world. Lin et al. find that static network configurations, such as transmit-power, might not be effective in the real world. Based on the link-quality history, their proposed solution builds individual link models to find the correlation between transmit-power and link-quality for all neighbouring nodes.

The proposed ATPC supports packet-level transmit-power control for upper layers. This unique feature allows higher layers to differentiate the transmission of packets with higher priority from lower priority by changing their transmit-power

and reduce the overall transmit-power of the network. To increase the speed of their online link-quality analysis, they used RSSI or LQI as an estimate for the desired PRR. Based on the off-line correlation they found between the RSSI or LQI, and the PRR, to reach a given quality of PRR they identified a lower bound for RSSI and LQI; this correlation was later disproved by [90].

Lin et al. experimentally illustrated that introducing transmit-power adaptation not only increases the end-to-end packet reception rate from less than 50% to over 98% throughout a three day experiment with both fair and rainy conditions; but also their proposed solution consumed 25% less energy in comparison to a network-level solution with maximum transmit-power settings. Lin et al. later expanded their work in 2009 by proposing a hierarchical framework for their ATPC scheme. This study mainly focused on enhancing the energy efficiency and success rate of the network in the link-layer. The authors relied on the same shortcomings of the ATPC, counting on the correlation between RSSI/LQI and PRR.

An adaptive transmit-power scheme proposed by Rukpakavong et al. in [137] utilises the hello packet used in neighbour discovery to estimate the distance and the appropriate transmit-power for a given neighbouring node. Unlike [102], in [137] the sender broadcasts a single hello packet with maximum transmit-power. All neighbouring nodes reply back to the sender using a unicast message with maximum transmit-power. The RSSI value of the source is saved in neighbour table and updated every 20 second. After the information in the neighbour table is collected, the device is able to send packets to the desired destination with the minimum transmit-power level greater or equal to the computer prediction. The results revealed no significant difference in terms of packet reception rate when comparing the adaptive scheme with the maximum transmit-power scheme. However, their experiments showed a 50% reduction in terms of energy consumption.

More recently, Nandi and Kundu introduced the Adaptive Transmit Power Scheme (ATPS) designed for square-grid WSNs affected by multipath fading [118]. Their

study focused on static networks with resource-constrained devices. This scheme increases the lifespan of the network by adjusting the transmit-power of the nodes depending on the node density and channel conditions. Considering the sensing range of nodes and maintaining a pre-configured signal detection probability level, this scheme maintains an acceptable Quality of Service (QoS). The authors investigate the impact of node density, packet length and channel fading on energy efficiency for both the adaptive transmit-power based and Fixed Transmit-Power Scheme (FTPS). The results showed that in the case of FTPS, detection probability dropped as the node spatial density decreases; this leads to shorter sensing range. However, for nodes using the proposed ATPS scheme, the transmit-power adapted to the node's spatial density and channel conditions. Simulation results revealed that energy consumption of ATPS is less than that of FTPS in scenarios with moderate to high node spatial density.

Hackmann et al. introduced an adaptive and robust topology-control protocol, also known as ART, in 2008. In this study, three fundamental questions were answered. The first question explored whether topology control is beneficial. To answer this question they observed the PRR, sequence number of packets received, RSSI and LQI of each node in the network with different transmit-power levels. Their results showed that when maximum transmit-power was used, the network had full connectivity, however, when operating with minimum transmit-power, the topology of the network has partitioned into smaller clusters of high-quality links. This change also resulted in the reduction of energy consumption of the network.

The second fundamental question illustrated that transmit-power has an impact on contention. This was shown by randomly selecting 10 nodes out of all the nodes in the network to simultaneously transmit packets while monitoring the PRR of other nodes in the network. The experiment was repeated for different transmit-powers between -25 and 0 dBm. The results showed that as the transmit-power increased the PRR also increased. This trend continued until reaching a peak at

-7 dBm. After this point, increasing transmit-power resulted in negative effects on the PRR. This is mainly due to the trade-offs between link-quality and contention. The authors also confirmed that link-quality estimators such as RSSI and LQI are not always robust indicators for evaluating the PRR. The proposed ART protocol assigns the selected transmit-power directly based on the calculated PRR of that link. This is done by calculating the PRR of a given link over a window of time and comparing it with a pre-assigned application-specified target. Using a light-weight heuristic feedback mechanism, the transmit-power of the device is automatically adjusted.

The results showed that using this scheme 75% of the nodes would achieve a delivery rate of higher than 90% as compared to 61% when all nodes are transmitting at maximum transmit-power. To show how contention affects the ART protocol, a similar scenario was used. The results showed that the PRR of the un-optimised ART is not statistically different when compared with maximum transmit-power, both achieving an approximate PRR of 83%. However, the APT nodes consumed 5% less energy that the maximum transmit-power scheme. The optimised APT scheme performed roughly 20% worse than the maximum transmit-power scheme. This was mainly due to many nodes rapidly changing their transmit-power, which directly affects the link-quality [64].

MPC is a Model Predictive Control method proposed by Witheephanich and Hayes in 2009 [164]. This closed-loop transmit-power control approach proved that RSSI can be used as a feedback signal to reduce the energy consumption of the device while maintaining an acceptable QoS performance. They experimentally tested their approach for both static and hybrid scenarios with one and two mobile nodes. Their results illustrate nearly a 50% reduction in energy consumption compared to other baseline schemes.

In 2010, Qian and Zhenzhou [72] proposed an MAC-based protocol that adaptively adjusts the transmit-power of the WSN device. They named this scheme Adaptive

Transmit Power MAC which was originally based on the S-MAC protocol [178]. To reduce the energy consumption of the network, the proposed scheme calculates the distance between the sender node and the destination node according to the received signal strength measurements. The appropriate transmit-power is then automatically selected based on the calculated distance and the propagation model.

In [58], Fu et al. proposed a practical transmit-power control protocol called P-TPC in 2012. Based on the experience gained from [64, 102, 103, 164], their P-TPC scheme employed approaches from control-theory to achieve robustness against complex and dynamic wireless properties and save the energy of resource-constrained WSNs. P-TPC keeps a record of the total number of transmissions and failures and, based on the pre-assigned data generation of the sensor nodes, calculates the PRR of a given link. This receiver-oriented approach uses probe packets to initialise and update the link model based on the calculated PRR. By combining a theoretical link model with real-time parameter estimation techniques, this scheme updates the appropriate transmit-power for a given link.

The P-TPC protocol comprises to two main building-blocks: a Fast on-line model IDentification (FID) and a Proportional-Integral with the Anti-Windup (PI-AW) controller. The FID calculates the PRR and updates the model between transmit-power and PRR. This component also initialises and re-configures the PI-AW. The PI-AW selects the appropriate transmit-power based on the current PRR and the pre-assigned application-specified target PRR. The changes to the transmit-power follow a non-linear curve presented by the proportional-integral control algorithm with an anti-windup element. This approach was compared with three existing base-line schemes: ART[64], ATPC [102, 103] and MPC[164]. In their first experiment they looked at single-link results. Interestingly, the ART showed the slowest reaction to link quality changes. This outcome could be attributed to its simple heuristic approach of updating the transmit-power one unit at a time. The ATPC scheme only reacted once to the link quality changes.

These results illustrate the shortcomings of this scheme. Since ATPC based its approach on the correlation of RSSI on PRR, however, their results are inconsistent with previous empirical studies that prove RSSI is not a reliable index for PRR. Comparison of MPC and P-TPC reveals that both approaches perform well when faced with varying link quality. Nevertheless, MPC, having a more complex optimisation algorithm showed slightly better performance than P-TPC's approach. This slight performance improvement of the MPC scheme comes with a complexity and energy cost which is not practical for implementation on resource-constrained WSN nodes.

Temperature shifts in harsh environments such as deserts [42] – the temperature difference between night and day – or urban areas [116] – where the isolation between indoor and outdoor environments result is a huge and sudden temperature difference – is one of the causes of link quality degradation [24]. Maintaining full connectivity in adaptive transmit-power schemes is difficult and requires control packet overhead, when compared with schemes with fixed transmit-power set to maximum. An efficient transmit-power control protocol was proposed by Lee and Chung [99]. This aims to explore the impact of temperature variation on WSN link quality and to compensate these changes by introducing an efficient temperature-aware scheme. This scheme reduces the feedback overhead of existing adaptive transmit-power scheme by incorporating a closed-loop feedback process.

Furthermore, by adaptively adjusting the transmit-power level of the network, it prolongs the network lifetime while maintaining an acceptable QoS. Their experimental evaluations portrayed irregular variations of link quality caused by temperature fluctuations over time (a 5^oC drop in temperature results in over 5 dBm increase in noise floor). This variation escalated as the distance between the nodes increased. They compared their closed-loop Temperature-Aware Transmission Power Compensation (TATPC) scheme with The Dynamic Transmission Power Control (DTPC) protocol presented in [75]. The experimental results revealed that although DTPC

is more energy-efficient due to its adaptive transmit-power algorithm, the TATPC scheme showed over 5% higher PRR than DTPC. This is mainly because of taking into consideration the temperature variation of the environment.

2.7. Other Approaches

Four coexistence mechanisms are introduced by the IEEE 802.15.6 standard which offers interference mitigation strategies while dealing with neighbouring Wireless Body Area Networks (WBANs) [7] [Section 6.13].

The first coexistence mitigation mechanism is called **beacon shifting**. In this mechanism the hub selects a beacon shifting sequence that is not being used by its neighbouring WBANs. By transmitting beacon packets at different time offsets, the hub mitigates potential repeated beacon collisions with neighbouring WBANs operating on the same channel. The hub informs other nodes and other neighbouring WBANs of its chosen beacon shifting sequence by including this information in its beacon packets. However, this mechanism is not applicable for frequencies below 405 MHz.

Channel hopping is another mechanism used in this standard. This mechanism is only allowed for WBANs with physical layers that operate in Narrow-Band (NB) – excluding the Medical Implant Communication Service (MICS) band or the Frequency Modulation Ultra-WideBand (FM-UWB) enabled physical layer. In this mechanism a hub will hop to another channel after a fixed number of beacon periods. According to the standard, the hub includes both the selected channel hopping state and the next channel hop fields in both its beacon frame and in its connection assignment frame. To avoid interference, the hubs choose a channel-hopping sequence that is not being used by other neighbouring hubs.

The final two coexistence mechanisms introduced by this standard are the **Active super-frame-interleaving** and **B2-aided time-shifting** mechanisms used

for beacon-enabled and non-beacon-enabled mode WBANs, respectively. These mechanisms are available for all frequency bands excluding frequencies between 402 and 405 MHz. According to the standard, by using these mechanisms one or more WBANs may share the same operating channel. The basic idea of these two mechanisms is to negotiate either a common active super-frame-interleaving or a time-shifting parameter between the neighbouring WBANs. After sending a command-active-super-frame-interleaving-request frame and receiving the acknowledgement frame, a command-active-super-frame-interleaving-response frame is sent to indicate the acceptance or rejection of the request. In sum, the above-mentioned approaches aim to alleviate the issues caused by channel coexistence and their impact on WBSN performance. It is suggested to consider these approaches in combination with the transmit-power variation and frequency adaptation schemes proposed in this thesis for future enhancement of both IEEE 802.15.4 and IEEE 802.15.6 protocols.

Although both IEEE 802.11 and 802.15.4 technologies operating in the 2.4 GHz ISM band employ CSMA-CA as one of their collision avoidance schemes, this mechanism is specifically designed to increase the reliability of heterogeneous technologies. Regrettably, this technique is not as effective when faced with other technologies. Hou et al. state that "CSMA/CA schemes implemented by 802.11 do not recognise the transmission efforts of ZigBee devices" [69]. In other words, packets transmitted by IEEE 802.15.4-based devices are not detectable by the IEEE 802.11 networks. One approach introduced by Tytgat et al. is called Coexistence Aware Clear Channel Assessment (CACCA) [154]. This scheme introduces an extra back-off delay for nodes of one technology to coexist with other technologies. By looking deeper in the CCA mechanisms of IEEE 802.15.4 and 802.11, Tytgat et al. proposed a shorter CCA duration and receive-mode-to-transmit-mode switching duration. This alteration in the IEEE 802.15.4-based devices alone reduced the PER by 24%. The CACCA was also added to both technologies, reducing the percentage of packets

lost by approximately 99%. This approach increased the energy consumption of the WSN nodes by 8% and the WiFi devices by 2%.

2.7.1. IEEE 802.15.6

In February 2012, the IEEE Standards Association introduced the IEEE 802.15.6 standard for WBANs [7]. This standard was designed to provide reliable wireless communication for extremely low-power devices used in close proximity to or inside the human body. It supports the following three physical layers: NB [4], Ultra-Wide-Band (UWB)[5], and the Human Body Communications (HBC)[6] physical layer. According to the IEEE 802.15.6 standard, a WBSN is capable of operating on at least one of 241 available frequency channels. Amongst these, 230 channels are available in the NB, 10 frequency channels are available in the UWB, and one channel is available in the HBC range. This standard also supports a wide range of data rates, starting from 75.9 kbps up to 10 Mbps.

The MAC layer specification permits a network to form a star topology with only one hub. The number of nodes ranges from zero to mMaxBANSize. With the aid of relay-capable nodes, end devices are able to be placed either one hop or two hops away from their corresponding hub. In this standard, time is divided into super-frames. A super-frame structure is bounded by beacons. The beacon period and time slot allocation are selected by the hub. The hub is also able to shift the offsets of the beacon periods. These networks are able to operate in one of the following three access modes [7, Sec. 6.3]: 1) Beacon mode with beacon periods (super-frames), 2) Non-beacon mode with super-frames, and 3) Non-beacon mode without super-frames.

Although this standard is specifically aimed and designed for WBANs [94], this

[4]A compliant device with a NB-compatible physical layers shall be able to operate in one or more of the following frequency bands: 402-405 MHz, 420-450 MHz, 863-870 MHz, 902-928 MHz, 950-958 MHz, 2360-2400 MHz, and 2400-2483.5 MHz.

[5]The 10 frequency channels are divided into two groups: 1)Low band (3494.4, 3993.6, and 4492.8 MHz) 2) High band (6498.6, 6488.8, 7488.0, 7987.2, 8486.4, 8985.6, 9484.8 and 9984.0 MHz).

[6]A HBC-compatible transceiver operates in the 21 MHz frequency band.

thesis decides not to use this technology simply because this standard has just recently been introduced and – to the best knowledge of the author – no commercially available hardware exists (at the time when this thesis was submitted) that is compatible with the specifications of this standard.

3. System Model

This chapter describes the system model for Chapters 4, 5 and 7.

3.1. Network software and tools

Simulation software and/or tools have been used as a cheaper and risk free alternative for experimenting with new ideas. Implementing a new idea using an abstract computer model enables researchers to test their proposed schemes in different controlled scenarios.

This thesis performed a thorough search in order to find a simulation tool, which could model overlapping of IEEE 802.15.4 and IEEE 802.11 frequency channels. Amongst the existing and well-known network simulators available, OPNET [112] and QualNet [131] provide the most powerful features required for this research. Unfortunately, these simulation tools are commercial products and require licensing and registration before using them. Furthermore, modification access to the source code is limited or not available for such tools. An alternative option is the use of open-source network simulators, for example NS2 [109] or OMNET++ [155]. This thesis surveyed several simulation libraries operating on top of OMNET++, such as: MiXiM [1], INET Framework [8] and Castalia [32].

After comparing all the simulation tools mentioned above, Castalia [32] seems the most suitable package for our needs and expectations [74]. This open-source network simulator was originally designed for WSNs and WBANs. Amongst other

models and protocols this simulation software fully supports both the IEEE 802.15.4 physical and MAC layer specifications. The package works on top of the OMNET++ platform [32] – which is also an open-source software.

The main drawbacks of this package are: i) lack of WiFi traffic support and ii) not keeping track of all 16 IEEE 802.15.4 channels simultaneously, which is needed for this research. Nevertheless, since Castalia is an open-source network simulator, it was possible to add the extra features. This thesis uses Castalia version 3.2 – the current and most up-to-date version available – for generating the simulation results presented in later chapters. For the purposes of this thesis, Castalia has been extended to support simultaneous access to all 16 IEEE 802.15.4 channels. This helps keep track of and monitor all the oncoming traffic from all available channels. This extra feature not only allows simultaneous access to and knowledge of all channels, but also helps produce more accurate and realistic results[1]. An interference traffic model for generating WiFi traffic has been added to this simulation package as well. This extension enables the WiFi device to send WiFi packets simultaneously on four IEEE 802.15.4 channels with different transmit-powers according to the WiFi standard's spectral mask. More detail regarding the interference traffic model is given in Section 3.4.

3.2. Network Scenario and Topology

This thesis uses a simple scenario in which a human carrier walks on a straight line in a field where external interference is caused by randomly distributed WiFi APs. The human carrier is assumed to be carrying a WBSN, consisting of one PAN coordinator and four sensor nodes. The sensor nodes are carefully placed on the human body forming a star topology, where sensor nodes are equidistant from each

[1] In the current version of Castalia (version 3.2), packets sent to a channel different from the current working channel of the device are ignored. In such a case, if that device decides to switch to a different channel, Castalia would completely ignore any previously sent packets or packets that are currently being sent and are causing interference. This assumption was made by the authors of Castalia to simplify the problem and to reduce the simulation time.

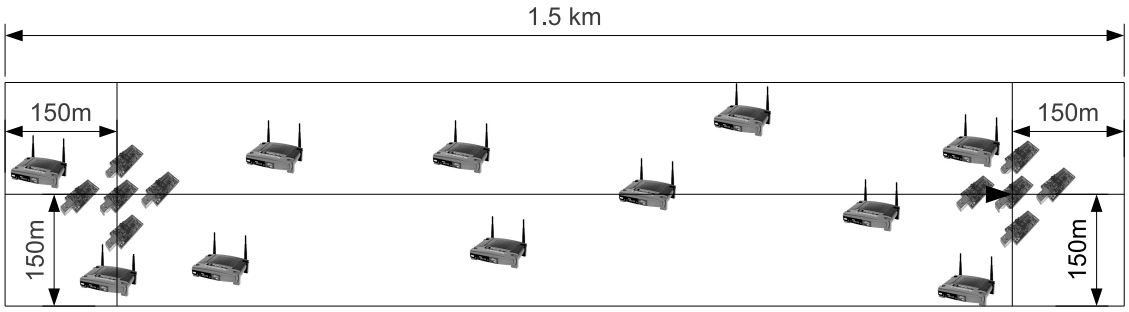

Figure 3.1.: WBSN and Interferer Deployment

other on a circle of one meter radius with the PAN coordinator node at the centre of the circle (see Figure 3.1). Throughout this thesis, the combination of four sensor nodes and their corresponding PAN coordinator are interchangeably referred to as WBSN or human carrier. Moreover, in order to focus on the impact of interference in isolation, for the majority of the results presented in this thesis, other impairments such as shadowing caused by the human body are ignored. Nevertheless, the effects of human body shadowing are considered and discussed in Section 4.3.6.

The considered playground is a 300 meter by 1500 meter field, where the human carrier walks at a constant pace of 5 km/h [57, 183] – an average walking speed of a pedestrian – from one side of the field (location (150 m, 150 m)) to the other end of the field (location (1350 m,150 m)) on a straight line. With this arrangement, the human carrier stays away from the boundaries of the playground field. To further simplify the problem, this thesis does not consider any obstacles on the path of the human carrier.

In order to create interference, a random number of fixed stationary WiFi APs is placed in the field at randomly chosen locations. The location of each AP is independent of other APs and is selected according to a uniform density. The number of WiFi APs placed in the field is derived following a Poisson distribution, where Δ is the average density – number of APs – in the field[2].

[2]This deployment forms a Poisson point process, see [81, Sec. 1.3] and [82, Chap. 16].

3.3. Propagation Model

This thesis uses a standard log-distance model with shadowing as a path loss model [132] for both its WiFi interference sources and the WBSN. The path loss for distance d is calculated using Equation 3.1 [32, Sec. 4.1.1]:

$$PL(d) = \begin{cases} PL_0 + 10 \cdot \gamma \cdot \log_{10}(d/d_0) X_\sigma & d > d_0 \\ PL_0 & d \leq d_0 \end{cases} \tag{3.1}$$

where PL_0 is the path loss at reference distance d_0 (which in this thesis is assumed to be 1 m), and γ is the path loss exponent, typically chosen between two and six. This thesis uses the default value of $\gamma = 2.4$ suggested by the simulation package. In [187], Zuniga and Krishnamachari conducted an experimental study with mica2 motes, which explained the observed PRR with the lognormal shadowing channel model. This shadowing model is appropriately used by the simulation package. The shadowing term X_σ is a zero-mean Gaussian random variable with $\sigma = 4$ (which is again the default value provided by the simulation package). The relatively low value for γ gives a very high impact of the WiFi interferers on the WBSN. The propagation parameters and other relevant parameters are summarised in Table 3.1.

3.4. WiFi Interference traffic model

To simulate a device that mimics a WiFi interference source in Castalia, small modifications were made to the existing physical layer model of this simulator. Namely, for every WiFi packet generated in the application layer of a given WiFi device, instead of sending one WiFi packet that overlaps with four IEEE 802.15.4 channels in the physical layer, it generates four identical packets, which are sent simultaneously on four neighbouring IEEE 802.15.4 frequency channels. Any packet transmitted by a WiFi interferer affects only the four IEEE 802.15.4 channels that are directly overlapping with the WiFi spectrum mask. This thesis do not consider adjacent

channel interference, which is 30 dBm below the main lobe.

The transmit-powers for these four packets differ from each other depending on the transmit spectral mask of the IEEE 802.11 Standard. Figure 3.2 illustrates the transmit spectral mask of a WiFi transceiver. At the centre frequency, the received signal strength is 0 dB and as it gets further away from the centre, the signal strength declines until it reaches another side band. In order to simulate the effects of the WiFi interference nodes, this thesis applies an offset to the TX power of the individual WiFi packets sent on different frequency channels of the IEEE 802.15.4 standard with respect to the transmit spectral mask of the IEEE 802.11 standard given in Figure 3.2.

Using the formula given in Figure 3.2, this thesis calculates and simulates the differences in transmit-power between the four overlapped channels. For more information on how these values have been calculated see Appendix A.

Each WiFi AP in this thesis is independent of other APs. Their operating frequency channel is randomly selected and pre-assigned using a uniform distribution at the beginning of every simulation run. According to the IEEE 802.11b specifica-

Main Application Layer Parameters		
Packet Inter-arrival Time	1	s
Start-up Delay	5	s
Data Payload	Uniform(64,102)	bytes
Main IEEE 802.15.4 MAC Parameters		
Max Frame trials	10	
Max Lost Beacons	4	
Packet Validity Time (Expiration date)	8 * 122.88 = 983.04	ms
Frame Order	61.44	ms
Beacon Order	122.88	ms
Beacon Time Out	3	ms
Buffer size	32	
initialSwitchCount (see Section 4.2)	4	
Buffer size	16	
Main IEEE 802.15.4 Physical layer Parameters		
TX power	-25	dBm
Data Rate	250	kbps
Main Path Loss Model Parameters		
Loss at reference distance PL_0	55	dB
Path loss exponent γ	2.4	

Table 3.1.: Simulation Parameters.

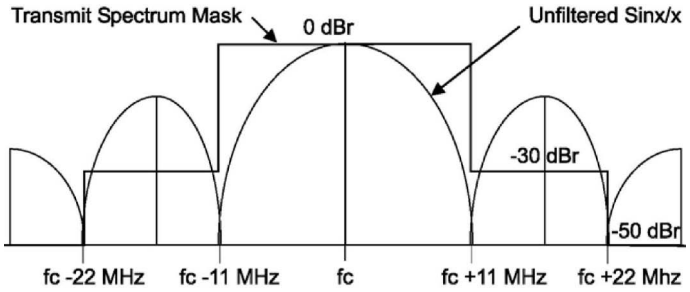

Figure 3.2.: IEEE 802.11 transmit spectral mask in the 2.4 GHz ISM band[2].

tions, WiFi channels start from channel 1 (2412 MHz) to channel 13 (2472 MHz) – channel 14 (2484 MHz) is also available; however, operating in this frequency channel is only permitted in certain regions and countries [2]. This thesis looks at the first 13 channels. This assumption is made so that all 16 available IEEE 802.15.4 channels would be affected by external interference. Moreover, all WiFi interferer nodes are assumed to operate with a transmit-power of 20 dBm. In addition, although the IEEE 802.11 standard has control messages and a CS mechanism, in this thesis, an individual WiFi AP generates its traffic independently withoutperforming carrier-sensing before sending its data packet.

The size of the packets generated by the interferer device are a sequence of Independent and Identically Distributed (IID) random variables, following a uniform distribution between 64 and 1500 bytes. The WiFi APs transmit their data at a data rate of 1 Mbps (IEEE 802.11b)[2]. As mentioned before in Section 2.1.2, the selected IEEE 802.11 version and data rate makes no difference for IEEE 802.15.4-based devices, and any packets sent by the WiFi device is considered as external noise. The inter-arrival times between WiFi packets are also IID random variables following an exponential distribution. The average inter-arrival times between WiFi packets are chosen in such a way that a prescribed traffic intensity of $\lambda = 0\%, 10\%, 20\%, \ldots, 70\%$ is obtained.

Clearly, this traffic model is not a realistic WiFi model, but an artificial traffic model, and it is a topic of future research to consider more realistic traffic and to also consider interactions between the APs that would be achievable by performing

a CS operation. Nevertheless, this thesis chooses a more simple and naive traffic model – without any carrier-sensing – ensuring the intended traffic intensity λ indeed occurs faithfully on the channel and that WBSNs do not have any influence on the operation of the AP's. This is regarded as a conservative and worst-case traffic assumption.

3.5. WBSN model

This thesis considers a WBSN with four sensor nodes connected to one coordinator node. The nodes are connected in a star topology, using the beacon-enabled IEEE 802.15.4 MAC layer. In this arrangement the coordinator periodically sends beacon messages to all neighbouring sensor nodes. After receiving these beacon packets, devices first associate themselves to the coordinator – and if specified in the configuration of the sensor nodes, they may also try to request a GTSs. This thesis generally does not use GTS for up-link or down-link traffic, and nodes may use the CAP period to transmit or receive their packets[3]. In this study a sensor device generates data packets at one-second intervals[4] – this value represents a common data traffic load expected for representative WBSN-based applications [104, 124, 151].

The lengths of the packets generated by the sensor nodes are IID random variables, generated from an uniform distribution between 64 and 102 bytes. The coordinator responds to a successfully received packet from a sensor node with an acknowledgement packet. If the sensor node does not receive an acknowledgement packet from its coordinator node (for example due to external interference), it performs up to nine re-transmissions (giving a total of 10 trials per frame).

Sensor nodes maintain their synchronisation by listening to and receiving the coordinator's beacon packets. If a device does not receive four successive beacons, it becomes an orphan node. This would force the orphan node to listen continuously

[3]The only exception of allocating GTSs is enabled while obtaining preliminary results reported in Section 4.3.2

[4]This number could later be adjusted to different scenarios or applications (see Section 7).

to the current channel until it receives a beacon message from its PAN coordinator node, and then it re-associates. In scenarios where frequency adaptation schemes are employed, orphan nodes scan through a list of channels to find beacon packets and re-associate (See Chapter 4). This can for example happen when the coordinator has chosen to switch to another channel in response to excessive interference but the device has not received any of the beacons announcing this decision. The beacon order and the super-frame order have been fixed to values of 3 and 2, respectively, corresponding to a beacon period of $\approx$ 122.88 ms and an active period of $\approx$ 61.44 ms duration. Table 3.1 gives a more detailed overview of the parameters used in this thesis.

There are cases in the IEEE 802.15.4 protocol where packets queue up in the MAC or PHY layer of the sensor network device. One such situation is when a node looses its PAN connection due to excessive interference. In such scenarios, the application layer of the sensor node continues to generate data packets every second – regardless of it being in the orphan state. This thesis follows the IEEE 802.15.4 standard and sets the "packet validity timer" to eight times the beacon period (corresponding to $\approx$ 983.04 ms), which is just below one second. Thus, if the data packet is not successfully acknowledged before the timer expires, the MAC layer drops the data packet from its buffer. This effectively ensures that the current data packet is removed from the MAC layer before the next data packet arrives. The packet validity timer is independent of the maximum number of frame re-transmissions. Each packet is allowed a maximum of 10 re-transmission attempts before being discarded, which is fairly typical for periodic traffic. An application example would be where the transmitted data is only valid for a given duration of time, in this case just less than one second.

3.6. Energy model

A sensor node comprises of different components, consuming different levels of energy, namely the transceiver unit, the sensing unit, the processing unit, etc. Previous studies reveal that a considerable percentage of WBSN node's energy is consumed by its transceiver unit [33, 126, 127]. The energy model used in this thesis only considers the power consumption of the transceiver unit, and the power consumed by other hardware components of a WBSN node is ignored.

The energy model used in this thesis uses the characteristics of the well-known IEEE 802.15.4-compliant ChipCon CC2420 transceiver [149], with a supply voltage of 3.3 V. The physical layer manages the transition between the different transceiver states (Receive, Transmit and Sleep state). According to the CC2420 specifications, at receive state, the transceiver draws 18.8 mA and at the idle and power down mode, it only draws approximately $426\mu A$ and $20\mu A$, respectively. The transmit-power supported by the CC2420 transceiver has a range of steps starting from -25 dBm to a maximum of 0 dBm and the current consumption of each transmit-power level varies between 8.5 mA and 17.4 mA, respectively[5].

In this thesis the transmit-power level is fixed to -25 dBm – this is the lowest transmit-power supported by this transceiver[6]. However, in scenarios where shadowing effects of the human body are considered (see Section 4.3.6), or where transmit-power variation is considered (see Chapter 7), other transmit-power levels up to 0 dBm are also used – this is the maximum transmit-power level supported by the CC2420 transceiver.

The CC2420 transceiver has four operational states: transmit, receive, idle, and

[5]The official transmit-modes stated in the CC2420 data-sheet are 0,-5,-10,-15 and -25 dBm, which consume 17.4, 14, 11, 9.9 and 8.5 mA, respectively [149]. This transceiver also supports other transmit-power levels like -42 dBm that are not officially declared in the specifications of the provided data-sheet [66].

[6]Other transmit-power levels are achievable by manually changing the TXCTRL.PA_LEVEL parameter of the CC2420 transceiver. However, they are not not specified in the data sheet of this transceiver [149]. For example in [66], experimental measurements revealed that a transmit-power of -42 dBm is achievable by setting the value of TXCTRL.PA_LEVEL to two.

sleep. In the simulation model presented in this thesis, the time a node spends in either state is recorded. In other words, if at t_1 the transceiver changes its state to s_x and remains in that state till t_2, the device has spent the duration time of $(t_2 - t_1)$ in state s_x. To compute the total energy consumption of a given device, this time is then multiplied with the average power consumption of each state (obtained from the data sheet [149]). The time and power required for RSSI measurements (as they are carried out to assess channels), and the time and power needed to switch between channels after adaptation decisions, are also taken into account. The current consumption of a WBSN device in all transceiver states, including the duration time of a single RSSI measurement[7], and the time needed to switch between channels[8], are presented in Table 3.2.

In the beacon-enabled MAC all nodes sleep during the inactive part of the superframe. To get a clearer understanding of how different schemes affect the consumed energy of a WBSN device, sensor nodes are forced to go to sleep immediately after receiving the beacon packet from the coordinator if the sensor node has no packets

[7]According to the CC2420 data sheet [149], a single RSSI measurement, which is averaged over 8 symbols, takes 128μs to calculate. However, in order to be sure that the registered value is valid, it is recommended to wait for twice that duration. Therefore, this study considers that the radio transceiver of a given node remains in the RX state for 256μs waiting for one RSSI measurement result.

[8]Moreover, according to the CC2420 data sheet [149], a Phase Locked Loop (PLL) lock time duration (192μs) is the duration needed for a node to switch between channels. In this study, for a node to switch to another channel the radio transceiver of a given node needs to remain in RX mode for one PLL lock time duration.

CC2420 Parameter		
RX mode	3.3 V * 19.7 mA	65.01 mW
TX mode -25 dBm	3.3 V * 8.5 mA	28.05 mW
TX mode -15 dBm	3.3 V * 9.9 mA	32.67 mW
TX mode -10 dBm	3.3 V * 11 mA	36.3 mW
TX mode -5 dBm	3.3 V * 14 mA	46.2 mW
TX mode 0 dBm	3.3 V * 17 mA	57.42 mW
Sleep IDLE mode	3.3 V * 426 μA	1.4058 mW
Sleep Power Down mode	3.3 V * 20 μA	0.066 mW
Duration time		
RSSI Measurement time	256	μs
PPL (Phase Locked Loop) time	192	μs

Table 3.2.: CC2420 parameter specification.

to transmit or receive. Appendix B explains in depth the steps taken for calculating the total considered energy along with simple examples.

4. Frequency Adaptation

This chapter describes the frequency adaptation schemes proposed and compared in the first part of our study. A subset of the results presented in this chapter has been published in [172] and [177].

4.1. Baseline Schemes

Two schemes are considered as baseline schemes, namely, the **non-adaptive** and the **genie** schemes, which represent the lower and upper bound of what is achievable, respectively. The lower bound is represented by the current existing IEEE 802.15.4 standard and the upper bound is represented by a hypothetical frequency adaptive scheme capable of dynamically switching the current operating channel to the channel with the lowest interference level.

4.1.1. No-Adaptation Scheme

This thesis uses the existing non-adaptive IEEE 802.15.4 standard as its baseline scheme. The non-adaptive IEEE 802.15.4 standard scheme itself comes in three different modes.

1. **non-adaptive CAP mode**: In this mode, the sensor nodes carry out their initial associations, and any up-link or down-link traffic is handled during the CAP period of the super-frame. GTSs are not utilised or assigned.

2. **non-adaptive GTS mode**: In this mode, the sensors carry out their initial associations and requests for GTS slots in the CAP period. But all other up-link or down-link transmissions are carried out in their allocated GTS slot.

3. **non-adaptive CAP+GTS mode**: the sensors, similar to the previous mode, carry out their initial associations and requests for GTS slots in the CAP period. However, this mode allows sensor nodes to transmit and/or receive packets in both their allocated GTS and during the CAP period. No priority is given to either opportunity. In other words, if data packets are available and the sensor node is in the CAP period it will attempt to send its data packet as soon as possible.

In the non-adaptive scheme the coordinator does not change its channel throughout the simulation. Hence, there is no frequency adaptation. Clearly, this scheme does not require or perform any additional activities like for example channel quality measurements.

The coordinator picks its initial channel randomly at the beginning of every simulation run and never changes it. When a device becomes orphaned, it remains on the same operating channel and resumes operation when it detects the next beacon packet.

This thesis compares the three existing non-adaptive schemes with each other. This is done to find out which non-adaptive scheme performs best in the presence of external interference. Based on the results given in Section 4.3.2, the non-adaptive CAP scheme is selected as the bench mark for non-adaptive schemes, which is referred to as the **no-adaptation** scheme.

4.1.2. Genie Scheme

The second baseline scheme is the **genie** scheme. This scheme is a hypothetical scheme, enabling all WBSN nodes to measure the instantaneous RSSI levels on all

channels simultaneously. The purpose of designing this hypothetical scheme is to show the potential upper bound of what is achievable if nodes in the network are given oracle knowledge of their surrounding environment – like channel quality – and based on this information they are able to switch their operating frequency in an ideal way (simultaneously synchronise, without any costs except energy). It is assumed that all nodes measurements are noise-free, identical and instantaneous[1].

This thesis takes into account the energy costs required by these measurement and channel adaptation processes. The corresponding energy costs are related to the activities of 16 parallel transceivers being used for each device on the network. In addition, before transmitting a new packet, either from the coordinator node or a sensor node, all devices in the network automatically switch to the best channel (in this scenario the best channel is the channel with the least energy – the assumption that all measurements are identical lets the members unanimously agree on the next best channel), without any signalling delay or signalling costs. This scheme approximates ideal adaptation without any of the involved risks like wrong decisions resulting from measurement noise, or failure of sensors to take notice of coordinators decisions.

4.2. Frequency Adaptation Schemes

In our framework frequency adaptation is carried out entirely by the PAN coordinator. More precisely, the PAN coordinator performs measurements on the current channel or on other channels to judge their quality, makes the decision to change the frequency, determines the frequency to hop to, and notifies the remaining nodes about the decision. This thesis assumes that the SO is strictly smaller than the BO, so that there is an inactive period in each frame during which the coordinator

[1]Performing RSSI measurement takes time (See Table 3.2). However, in simulation, it is possible to not take into account the time it takes to measure all 16 channels, the time it take to switch to a new channel, and any related synchronisation issues. These assumptions are made to transform a typical WBSN to a network with genie capabilities.

carries out the channel measurements. For these measurements it is assumed that the coordinator measures the energy level without trying to demodulate a signal [7]. In the terminology of the IEEE 802.15.4 standard the coordinator performs RSSI measurements, as only this mode can detect the presence of other technologies.

Since the MAC layer of the IEEE 802.15.4 standard does not foresee a service (or associated command frames) for channel adaptation, this thesis uses the beacon payload field. The IEEE 802.15.4 beacon frame can carry a variable-length payload which is utilised for frequency adaptation. The precise usage depends on the adaptation scheme, but for all schemes at least two fields are included, put together into one byte: a four-bit field indicating the next channel to switch to (*nextChannel*), and a four-bit field (called *switchCount*) counting down the number of beacons to be transmitted on the current channel before switching to the channel indicated in *nextChannel*. The second field allows to use several beacon frames to announce the new channel before switching, which in heavy interference situations can help to notify all associated devices. Further fields might be present, depending on the scheme.

Another parameter used in this thesis is the *initialSwitchCount*. This variable represents the number of super-frames before the network switches its operating frequency to the next channel. In other words, when the coordinator (currently on channel c_o) has made a decision to switch to a new channel c_n, it writes the value c_n into the *nextChannel* field of the next beacon and initialises its *switchCount* field with the value stored in the configuration parameter *initialSwitchCount*. The coordinator transmits *initialSwitchCount* beacons on channel c_o and then switches to channel c_n. The *switchCount* field is counted down while transmitting the beacons on c_o. After switching to c_n and before any new switching decision is made, the coordinator writes c_n into the *nextChannel* field and the value 0 into the *switchCount* field.

4.2.1. Periodic Schemes

In the class of periodic adaptation schemes the coordinator decides about the next channel periodically, after a fixed number of super-frames, which is referred to as a **hyper-frame**. For this study the hyper-frame length is fixed to ten super-frames[2]. In other words, the operating frequency channel could be changed every ten super-frames.

Periodic Random Scheme

The first periodic adaptation scheme that is investigated in this thesis, is the **periodic-random scheme**. In this scheme, the PAN coordinator randomly selects a channel using a uniform distribution and independent of previous choices. There are no channel measurements involved in this scheme. The extra energy costs for channel switching, which occurs when the previous and the next channel are different, are considered in the calculation of the total energy consumption.

For both practical and simulation implementation of this scheme, a pseudo-random number generator for generating a sequence of numbers that represent future channels is used. In this scheme the PAN coordinator informs the sensor nodes, during the association stage, about its current **seed** number, Hyper-frame size and the offset to the next Hyper-frame. Having this information, sensor nodes are able to switch channels and maintain synchronisation with their coordinator even if they loose three consecutive beacon packets[3]. Furthermore, the coordinator updates the sensor nodes about its current seed number and offset to the next Hyper-frame by including this information in the beacon packets[4].

This thesis presents two variations of the periodic-random scheme, where the

[2]In this thesis other hyper-frame lengths have also been considered.

[3]After losing four consecutive beacon packets, sensor nodes become orphaned and the information regarding the seed number and offset to the next channel hop is ignored. The sensor nodes are forced to scan all available channels in order to find and re-associate with its corresponding coordinator node.

[4]A similar technique is used by [135].

length of the Hyper-frame is 1 and 10, respectively. This allowed us to validate our hypothesis that reducing the Hyper-frame length – the duration time spent on a given channel – increases the success rate. In other words, the faster the network switches its operating channel, the smaller the chance of being affected by the possible external interference present on the operating channel – this is true if the next operating channel is without interference.

Periodic Measurement Scheme

Similar to the periodic-random scheme, the **periodic-measurement scheme** also changes its operating channel at the end of each Hyper-frame. However, in this scheme the WBSN coordinator takes RSSI measurements of all 16 channels during the inactive period of each super-frame, and based on the measurements taken in the last ten super-frames, at the end of the sixth super-frame of a Hyper-frame it makes a decision about the best channel for the following Hyper-frame. The decision is based on the observed RSSI values and is communicated to the sensors over the remaining four[5] super-frames.

For channel evaluation, this thesis employs the schemes proposed in [117]. Since in this study the coordinator makes the decision, it is also solely responsible for collecting RSSI measurements from all available channels. For this, the coordinator remains active and in RX mode during the inactive period of a super-frame while all sensor nodes are in sleep mode. According to the IEEE 802.15.4 standard there should not be any activity or interference from the nodes in the same WBSN during this period. The coordinator takes eight RSSI samples from each channel during the inactive period of the super-frame. This, multiplied by the sample set size, which is equal to the number of super-frames in a hyper-frame (10), gives a total of 80 RSSI samples per channel. These RSSI measurements are assumed to be noise-free[6],

[5] see *initialSwitchCount* parameter in Section 3.5

[6] In other words, if two independent devices located at the same location take RSSI measurements at the same time they will both get the same RSSI value.

but the energy required to take these samples and to switch to all 16 channels is accounted for. If the newly selected channel is different from the current operating channel, the simulation model also calculates the cost of channel switching that the sensor incurs. This extra measurement cost is calculated to be ≈ 2.33 mJ per channel switch (for the breakdown of this calculation see Appendix B).

After the decision is made the information about the next channel switch is then added into n subsequent beacon packets – in this study $n = 4$. Starting from the $(n+1)^{th}$ super-frame the coordinator and all sensor nodes that successfully received at least one of the past n beacon packets, switch to the newly assigned frequency channel. In this approach there is a possibility that a sensor node may not receive any of n beacon packets and thus is not notified of channel switching decisions. In such scenarios the coordinator and all the sensor nodes that had received one of these beacon packets would have switched to the newly assigned channel. The nodes that did not receive any of the beacon packets – due to external interference – would be left behind in the same channel. These nodes would become orphan nodes and forced to spend a substantial amount of time and energy on scanning all available channels in search of finding and associating to its corresponding PAN coordinator.

Next is the description of the three periodic-measurement schemes proposed in this thesis:

Periodic-Measurement-Max Scheme

This scheme looks for the maximum observed RSSI value out of the last ten measurement sets as a summary statistic for a given channel, and the decider chooses the channel with the smallest maximum RSSI value (in the figures the scheme is denoted as *periodic-measurement-max* scheme).

Periodic-Measurement-Mean Scheme

Another performance measure suggested by [117] is to calculate the average observed RSSI value of the measurements obtained on each channel. The coordinator selects the channel with the smallest mean RSSI value (this scheme is referred to as *periodic-measurement-mean* scheme).

Periodic-Measurement-Cardinality Scheme

This scheme selects the channel with the lowest RSSI variation. As described in [117], this scheme counts the number of unique RSSI measurements obtained for each channel. The channel with the lowest score is selected by the coordinator. The idea behind this choice is that channels with no or little interference are more likely to be stable – in terms of energy level detected in the channel – thereby having a smaller cardinality score.

4.2.2. Lazy Schemes

The general idea for the class of Lazy schemes is that the WBSN stays on the same channel as long as it is good enough – thus the name Lazy. Channel switching happens only when the measured channel energy exceeds a pre-assigned threshold[7]. More specifically, in the **Lazy** scheme the coordinator takes RSSI measurements on all channels during the inactive periods of each super-frame. Similar to the periodic-measurement-MAX scheme (see Section 4.2.1), the coordinator collects the last ten sets of RSSI readings from each channel. In this scheme, the channel quality is represented by the maximum of those readings. The results presented in Section 4.3.4 show that in the presence of external interference the periodic-measurement-Max scheme outperforms other periodic-measurement schemes (Mean and Cardinality). Therefore, for the Lazy schemes only the channel quality estimation of the periodic-

[7]The Lazy scheme does not depend crucially on this choice alone and other criteria could be used as well (e.g. when PER is increased).

measurement-Max scheme is used, with the exception that a channel switch is only carried out if the maximum RSSI value of the current channel exceeds a threshold of -90 dBm, and if there is another channel with a lower maximum RSSI value. Various thresholds have been explored, however, only the results for -90 dBm are shown in this thesis. This variable could be tuned according to the application and surrounding environment. Using higher values (e.g. -87 dBm [46]) would increase the tolerance, which is suitable for environments with high noise floor. However, increasing the threshold would allow less time for the coordinator to inform the sensor nodes about the decision to switch the operating channel. This thesis finds -90 dBm an acceptable threshold value that gives enough time for the network to detect and decide on the next channel before the channel conditions reach a state where communication is no longer possible.

4.3. Simulation-based Performance Evaluation

This study utilises an extended version of Castalia[8] to extract the necessary results and graphs (see Section 3.1). The schemes described in this chapter are evaluated for varying values of the average number of interferer density Δ and the interferer traffic intensity λ. An individual interferer picks its operating channel randomly according to a uniform distribution over the allowed channels. For each combination of Δ and λ, a considerable number of replications were performed to reach a maximum relative error of 5% or less, at a 95% confidence level for the success rate. A simple simulation scenario and topology is considered, as explained in Section 3.2. For every simulation run a new WiFi deployment is generated. Each replication simulates a human walking at a constant speed of 5 km/h from one end of the simulation field to the other. This process takes approximately 14.4 minutes in simulated time. To achieve a relative error of 5% or less, each simulation scenario has been replicated at least 100 times or in some cases more. The results obtained from different attempts

[8]Castalia version 3.2 [32]

are averaged and only these averages are reported. In order to avoid visual clutter in the figures, the error bars are removed.

4.3.1. Performance Metrics

To compare the different schemes presented, this study looks at two core and three additional performance measures.

The first core performance measure considered for evaluating the schemes is the **success rate** (percentage of successfully acknowledged transmissions). This is the average percentage of up-link packets that the coordinator has successfully received (possibly after retransmissions) and for which the sender has successfully received an acknowledgement, see Section 1.5.1

The second and equally important core performance measure is the **energy consumption** of sensors and/or the coordinator node, consumed by the transceiver, as the carrier walks once from left side to the right side of the scenario field. The average energy consumption of the sensor nodes is plotted separately from the average energy consumption of the coordinator node. The main focus of this thesis is on the sensor nodes since in many scenarios the coordinator node will have more energy available than the sensor nodes. The unit of consumed energy is the Joule, see Section 1.5.1.

In addition to these two core performance measures, the following performance measures are used to explain the relationship between trends:

i) **Percentage of expired transactions**: This illustrates the average number of packets generated by the application layer of the sensor nodes which were not successfully transmitted and dropped, due to exceeding the maximum time a given packet is valid (packet validity time = 983.04 ms).

ii) **Percentage of time without PAN**: This is the percentage of time during which sensor nodes are orphaned. If a node does not receive four consecutive

beacon packets it concludes that synchronisation has been lost and becomes an orphan node. During this period, sensor nodes cannot transmit or receive any data packet, instead they are required to continuously scan all or a subset of channels to find and re-associate themselves with their corresponding coordinator node. This consequently, results in higher PLR and energy consumption (see Section 1.5.1).

iii) **Fraction of channel hops**: This trend shows the fraction of channel hops the coordinator has made in order to mitigate the external interference by switching channels.

4.3.2. Non-adaptive schemes

According to the IEEE 802.15.4 standard, explained in Section 2.1.1, the sensor nodes are allowed to transmit their up-link traffic during the active period of the super-frame. In other words, either during the CAP or during the assigned GTSs or both. This section looks at the three different available schemes that the IEEE 802.15.4 standard specifies. The aim of this study is to observe which of the three schemes performs best when faced with external interference. The three non-adaptive schemes are named as follows: **non-adaptive CAP**, **non-adaptive GTS** and **non-adaptive CAP+GTS**. Figures 4.1 and 4.2 compare these schemes with different interferer node density of Δ and interferer traffic intensity of λ.

As illustrated in Figure 4.2a the consumed energy of the coordinator remains stable for all values of Δ and λ. However, the consumed energy of the sensor nodes increases as the density of interferers and the intensity of the interferer traffic increases (see Figures 4.1a and 4.2b). This is partly due to the increase in packet re-transmissions needed for a successful packet reception by the coordinator and successful reception of acknowledgement from the coordinator. Furthermore, due to the drop in channel quality, the probability of sensor nodes losing four consecutive beacon packets sent by the coordinator increases. Thus, the percentage of time

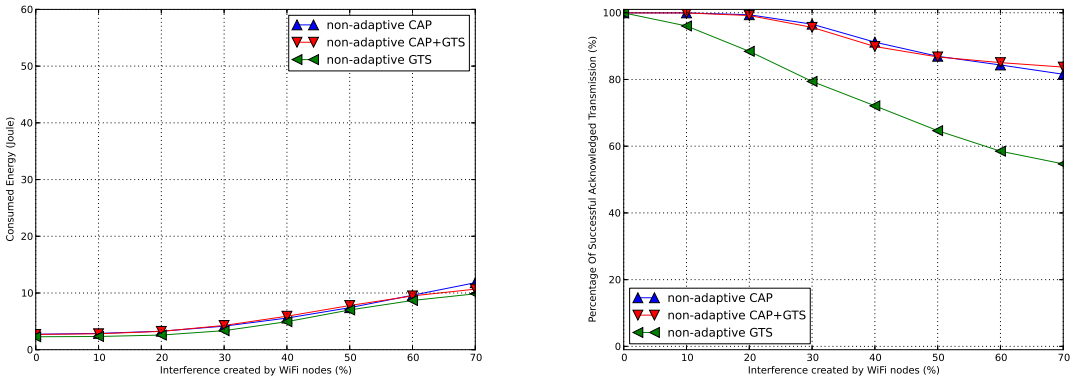

(a) Energy consumed by sensor nodes (b) Success rate

Figure 4.1.: Comparison of the three non-adaptive schemes where Δ is equal to 10

that the nodes spend without a PAN connection increases. Therefore the sensor nodes need to remain active for a longer time to re-associate to their corresponding coordinator. This increases the time that the sensor nodes need to remain active, resulting in higher energy consumption by the sensor nodes.

As expected, the consumed energy of the coordinator node for all three schemes and all Δ and λ values has remained at a **constant value, just under 30 Joule**[9]. The reason is that *the coordinator has no adaptation capability and it selects a channel only once at the beginning and remains on that channel for the remainder of its lifetime. Also, since transmission and reception requires roughly about the same power, although the increase in interference would result in higher probability of packet re-transmissions, the overall energy consumption seems to remain unchanged.* The coordinator transmits a beacon message and remains active for the whole duration of the active period. Afterwards, the coordinator turns its transceiver off until the start of the next super-frame. This action of the coordinator is the same for all three schemes, and does not change for different Δ and λ values (refer to figure 4.2a).

However, the energy consumed by the sensor nodes varies depending on the density

[9]An average AA battery contains approximately 9 to 11 kJ depending on the type of battery (Lithium Ion, NiMH, Nickel-Cadmium, Carbon-zinc etc.)

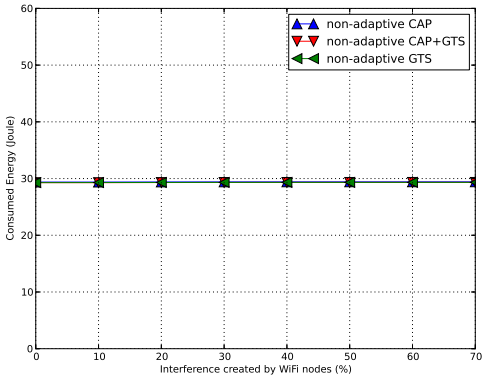

(a) Energy consumed by the coordinator

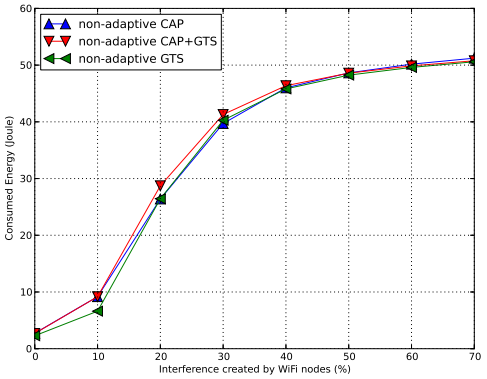

(b) Energy consumed by sensor nodes

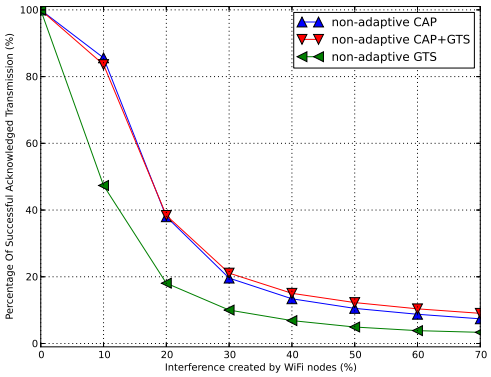

(c) Success rate

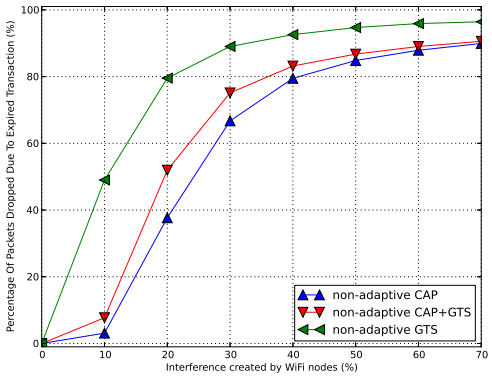

(d) Percentage of expired transaction

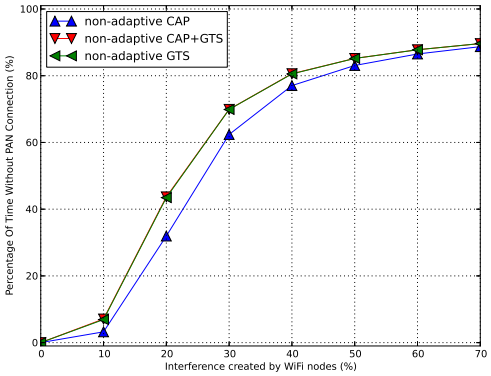

(e) Percentage of time without PAN

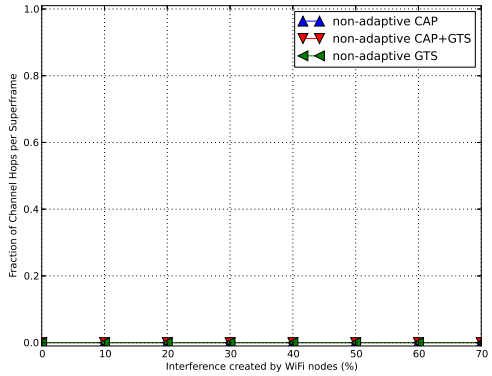

(f) Fraction of channel hops

Figure 4.2.: Comparison of the three non-adaptive schemes where Δ is equal to 100

and traffic intensity of the external interferer sources (refer to Figures 4.1a and 4.2b). In both of these figures, despite the different density of the interferer nodes, when the traffic intensity of the WiFi interferer nodes is at 0% utilisation, they all roughly consume around 3 Joule of energy. However, this trend changes as the traffic

intensity increases. Observing the results of the CAP scheme and interferer traffic intensity of $\lambda = 20\%$, the energy consumed by the sensor nodes start from roughly 3 Joule for $\Delta = 10$ to over 25 Joule for $\Delta = 100$ (see Figures 4.1 and 4.2).

The percentage of successfully transmitted packets is illustrated in Figures 4.1b and 4.2c. These figures indicate that the CAP scheme performs better as the traffic intensity and the density of the interferer nodes increase. The results show that the GTS scheme has the worst tolerance to external interference compared with CAP and CAP+GTS. This is expected since the IEEE 802.15.4 assumes that during an allocated GTS, no device except the allocated device is allowed to transmit during that time slot. Furthermore, no CS is carried out during this time slot. Figures 4.2d and 4.2e show the percentage of expired transactions and the percentage of time that the nodes spent without having a PAN connection. In Figure 4.2e, it could be seen that the non-adaptive CAP scheme has a noticeable lower time without PAN than the other two schemes (CAP+GTS and GTS). This is mainly because after sensor nodes become orphaned and after finding their coordinators beacon packet, in the CAP only scheme sensor nodes have a longer CAP period to re-associate with their coordinator than in the other two schemes[10].

The figure depicting the percentage of time that the nodes spent without having a PAN connection suggests a direct relationship with the consumed energy of the sensor nodes. The figures for the percentage of packets dropped due to expired transactions show a invert relationship with the percentage of packets successfully received and acknowledged by the coordinator. Both of these trends are expected: when the sensor nodes are orphaned and are scanning the channel to find a beacon packet and re-associate to their coordinator, they can not transmit their data packets on time – before getting expired – and they consume more energy for constantly being in receive mode.

As illustrated in Figure 4.2f, since neither of these three schemes has any channel

[10]When GTS slots are assigned, the active period is divided in to two portions: CAP and CFP. However, when no GTS is assigned, the whole active period is allocated for CAP.

adaptation scheme, all nodes remain on the same channel throughout their lifetime. Observing Figures 4.1a and 4.2b, it is noticeable that for λ up to 30%, the GTS scheme has lower energy consumption when compared to CAP. For λ values over 30%, the CAP scheme shows little efficiency in comparison to GTS.

In summary, among all the no-adaptation schemes tested the **non-adaptive CAP** scheme showed the best overall performance, when faced with different values of Δ and λ. Therefore, for the remainder of this thesis only the CAP scheme is used as the representative of non-adaptive schemes. This thesis explores to what extent adaptation schemes could improve the performance as the interference density and intensity increases.

The results given in Section 4.3.2 show that in the presence of interference, the **non-adaptive CAP** scheme shows best performance in terms of both success rate and energy consumption than the other baseline schemes. Therefore, throughout the remainder of this thesis, the results for the CAP mode would be compared with different adaptation schemes. Hereafter, the term **no-adaptation** scheme, will be used in place of the "non-adaptive CAP" scheme.

4.3.3. No-Adaptation and Genie Scheme

This section compares the no-adaptation and the genie scheme to get an impression of the achievable performance gains with frequency adaptation. The genie scheme provides an upper bound on achievable performance, especially for the success rate. The results for varying values of the average number of interferers Δ and varying interferer traffic density λ are shown in Figure 4.3.

Looking at the results presented in Figure 4.3b, it can be clearly seen that the genie scheme achieves a substantially higher success rate than the no-adaptation scheme for increasing interference intensity λ. This difference becomes larger as the interferer node density Δ increases. For instance, for values of $\lambda \leq 20\%$ and $\Delta = 10$, the success rate is nearly 100% – the same for both Genie and for no-adaptation

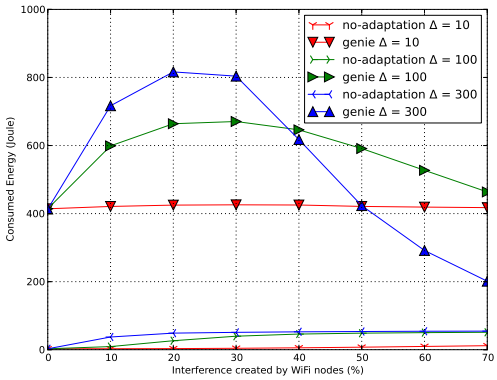

(a) Energy consumed by sensor nodes

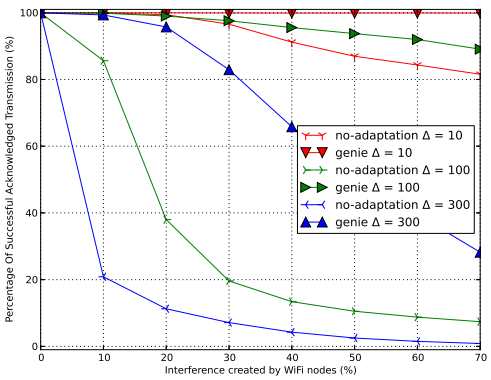

(b) Success rate

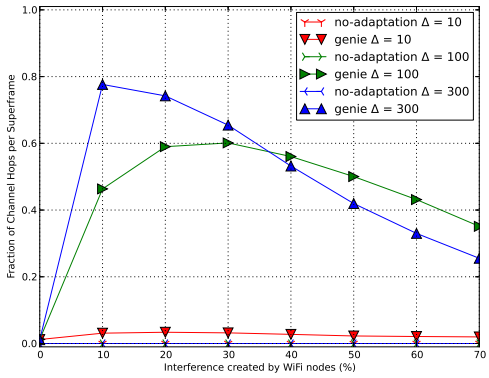

(c) Fraction of channel hops

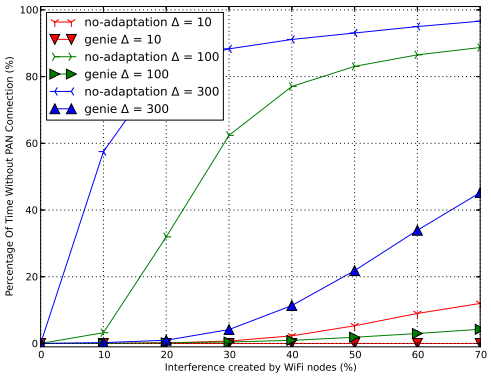

(d) Percentage of time without PAN

Figure 4.3.: Comparison of no-adaptation and genie schemes for $\Delta \in 10, 100, 300$

schemes. However, as the intensity λ is increased – to 70% keeping the density $\Delta = 10$ – the success rate drops to 80% for non-adaptation scheme whereas the Genie scheme still maintains a success rate close to 100%. For Δ values of 100 and 300, and the interference intensity λ at 70%, the Genie scheme still performs well with success rates of more than 80%, while the non-adaptation scheme fares poorly at around 10%. These trends clearly illustrate the severe impact of external interference on schemes with no adaptation. Furthermore, these results show the significant performance gain that frequency adaptation could potentially provide. One of key outcomes of this thesis is that: frequency adaptation alone **can** have substantial advantages in terms of success rate, which for health-related applications is a prime performance measure.

At the same time, the genie scheme requires much more energy at the sensor nodes (Figure 4.3a), which results from the energy expenditure of the (assumed) 16 transceivers on each sensor node, carrying out measurements and potentially switching channels for each new packet. Interestingly, the energy consumed by the sensor nodes increases as the interference traffic intensity λ increases and decreases as the percentage of time without PAN connection increases. This finding can likely be explained by the contribution of the energy to switch channels: as λ increases, sensor nodes incur more channel switching – resulting in higher energy consumption. However as the interference increases it becomes less and less likely that another channel is better than the current one, so no switching is needed. When the external interference reaches the point where no beacon or data packet is successfully transmitted, the nodes become orphaned and the need arises to scan all 16 channels to find a beacon packet. At this stage the sensor nodes only use one transceiver to search through all channels, thus further reducing the energy consumption of the sensor nodes. The usage of all 16 channels in order to reduce the required time to find the coordinator is possible, however due to heavy external interference it did not significantly increase the success rate. This scheme consumed less energy and performed just as well as the scheme where all 16 channels were used for coordinator discovery. In Chapter 5 this phenomenon is described in more detail. The decreasing number of channel hops and percentage of time without PAN is shown in Figures 4.3c and 4.3d.

4.3.4. Periodic Scheme

This section analyses the performance of the periodic schemes for the case where $\Delta = 100$ and 300, shown in Figures 4.4 and 4.5. The trends identified for these values of Δ are similar to the trends for other values of Δ.

The first periodic scheme simulated is the **periodic-random** scheme, which comes in two flavours (period of one and 10 super-frames). The second simu-

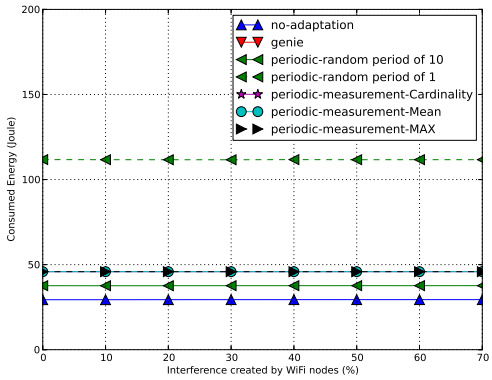

(a) Energy consumed by the coordinator

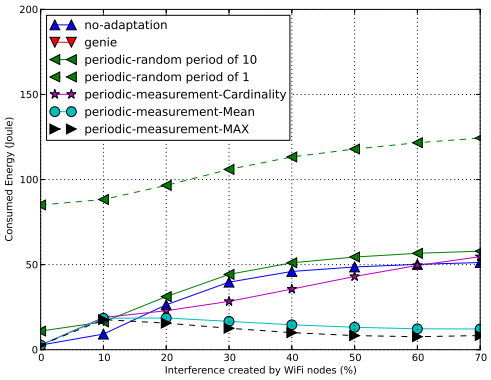

(b) Energy consumed by sensor nodes

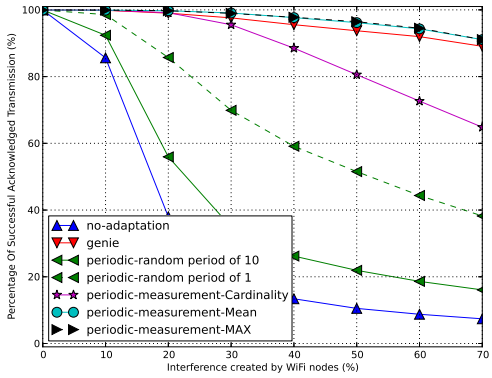

(c) Success rate

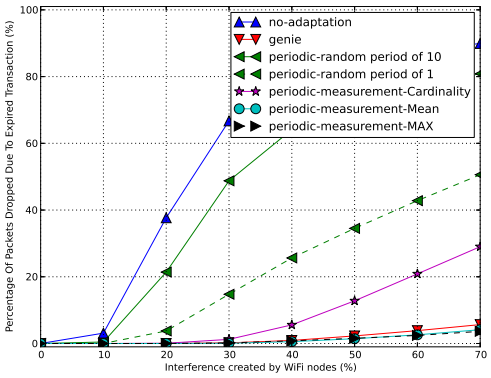

(d) Percentage of expired transaction

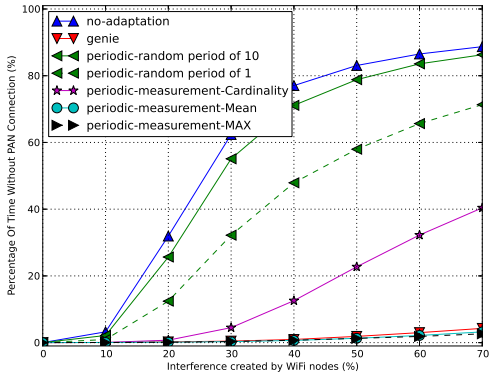

(e) Percentage of time without PAN

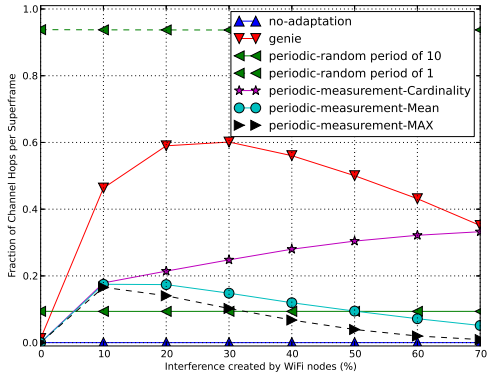

(f) Fraction of channel hops

Figure 4.4.: Comparison of the periodic scheme where $\Delta = 100$

lated periodic scheme is the **periodic-measurement** scheme with a period of ten super-frames. The periodic-measurement scheme comes in three types: periodic-measurement-cardinality, periodic-measurement-mean and periodic-measurement-max (see Section 4.2.1). In Figures 4.4 and 4.5, the periodic schemes are compared

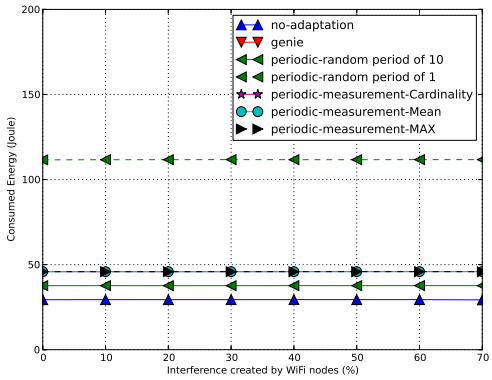

(a) Energy consumed by the coordinator

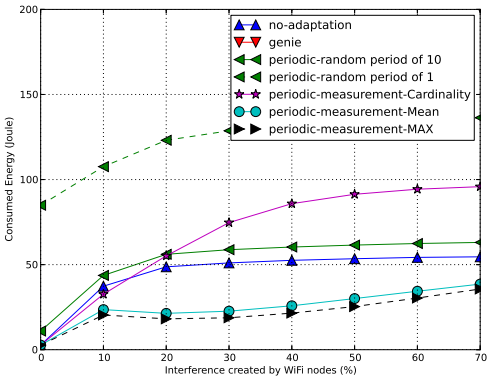

(b) Energy consumed by sensor nodes

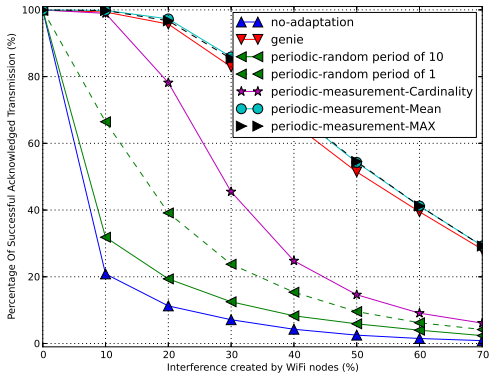

(c) Success rate

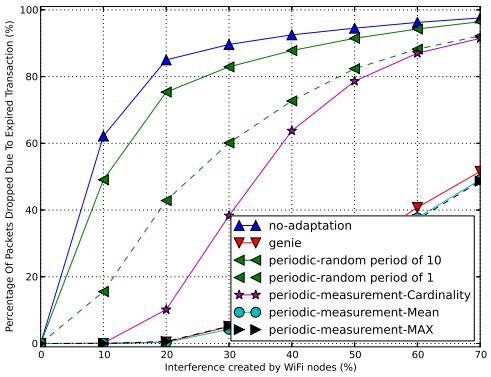

(d) Percentage of expired transaction

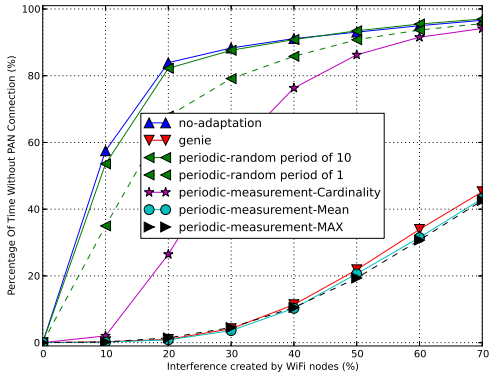

(e) Percentage of time without PAN

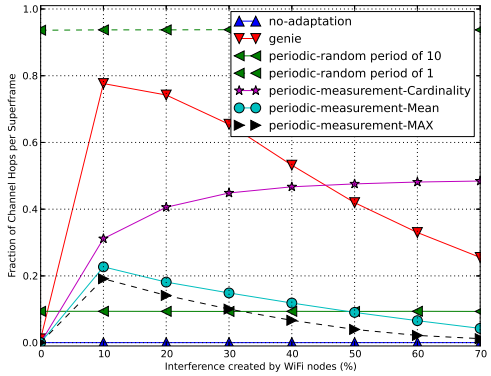

(f) Fraction of channel hops

Figure 4.5.: Comparison of the periodic scheme where $\Delta = 300$

to the no-adaptation scheme and the genie scheme.

There are some surprising findings:

(i) Both periodic-random schemes showed noticeable performance gains in terms

of success rate and time without PAN as compared to the no-adaptation scheme (See Figures 4.4c and 4.5c). However, this improvement came at a cost – the energy consumption of both the sensor nodes and the coordinator node was increased.

(ii) The periodic-random scheme which switched its operating channel every superframe outperformed the periodic-random scheme that switched every hyperframe. One explanation could be that if the current randomly selected frequency channel has high-interference, the WBSN is able to leave the poor channel more quickly when switching happens after each superframe.

(iii) All periodic-measurement schemes achieved higher success rate than the no-adaptation and periodic-random schemes. The energy consumption of the coordinator node (in Figures 4.4a and 4.5a) of periodic-measurement schemes is almost double the energy consumption of the no-adaptation scheme, just under 50 Joule compared with $\approx$ 25 Joule, respectively. On the other hand, the energy consumption of the sensor nodes for periodic-measurement schemes is less than the baseline and periodic-random schemes (see below).

(iv) Amongst the periodic-measurement schemes, the periodic-measurement-MAX and the periodic-measurement-Mean scheme have the highest success rates. Nevertheless, the periodic-measurement-MAX scheme outperforms the periodic-measurement-Mean scheme in terms of energy consumed by the sensor nodes. This is mainly due to less channel hopping (See Figures 4.4f and 4.5f).

(v) The periodic-measurement-MAX scheme has clearly the best performance of all periodic schemes, it even outperforms the genie scheme in terms of success rate. A likely explanation for the advantage of the periodic-measurement-MAX scheme over the genie scheme in terms of success rate is the lack of "history" for the genie scheme: the latter considers only instantaneous channel samples, and it might happen that it samples the channel at a time when a close interferer

has an inter-packet gap. In this case the next WBSN packet would be hit by the next packet of the WiFi interferer. The measurement scheme makes 10 sets of observations for each channel (with a spacing of one super-frame) and has a much better chance to detect interferer activities and to avoid the channel.

(vi) Furthermore, for interferer traffic density of $\lambda > 20\%$, the periodic-measurement-MAX scheme has the lowest sensor energy consumption, even lower than the no-adaptation scheme (while at the same time having more channel hops). The first reason for this finding is that the periodic-measurement-MAX scheme is able to reduce the number of re-transmissions and expired transactions (see Figures 4.4d and 4.5d). The second explanation is the time spent without PAN connection. By detecting interference and switching to a channel with the lowest external interference, this scheme is able to significantly reduce the orphaning duration (see Figures 4.4e and 4.5e).

4.3.5. Lazy Scheme

In the Lazy scheme, the coordinator node does not make a decision to switch to a new channel unless the current channel noise interference level is over a predefined threshold (in this case -90 dBm). In this section the Lazy scheme is compared against the periodic-measurement-MAX scheme and the no-adaptation scheme for average numbers of interferers of $\Delta = 100$ and $\Delta = 300$.

The results are shown in Figures 4.6 and 4.7. For both values of Δ the Lazy scheme achieves almost exactly the same success rate as the periodic-measurement scheme. Furthermore, the percentage of time without PAN connection of the two adaptive schemes is the same. However, the Lazy scheme consumes substantially less energy at the sensor nodes for smaller values of λ and in general. This is mainly due to significantly fewer channel switches needed than for the periodic-measurement-MAX scheme. The Lazy scheme makes the decision to switch channel only if, in the decision phase, the quality of the current operating channel falls below a given

threshold.

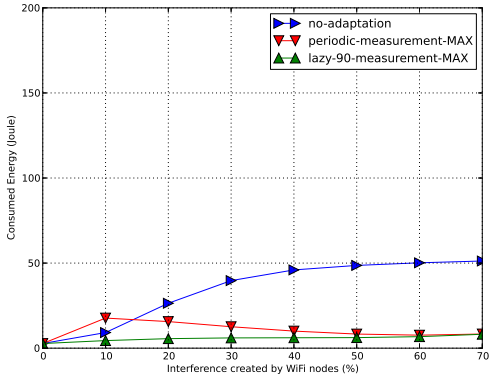

(a) Energy consumed by sensor nodes

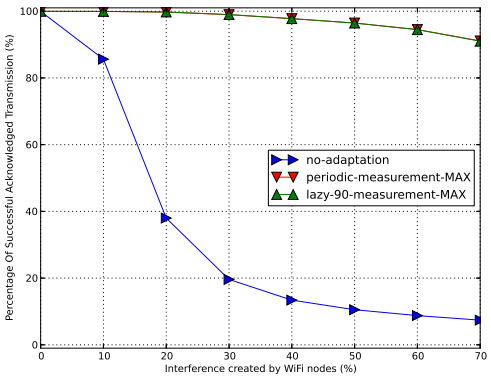

(b) Success rate

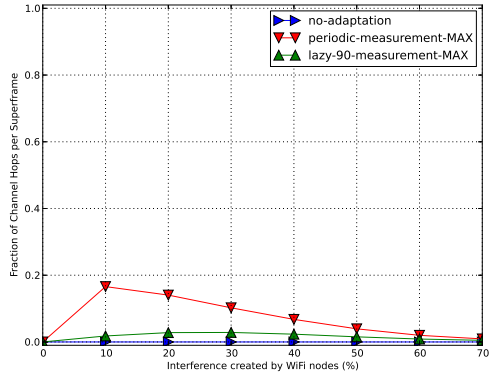

(c) Fraction of channel hops

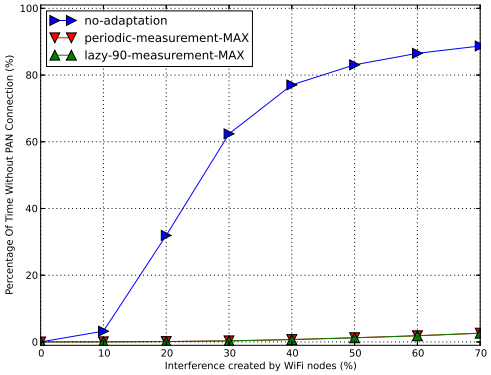

(d) Percentage of time without PAN

Figure 4.6.: Comparison of no-adaptation, periodic-measurement-MAX and Lazy scheme for $\Delta = 100$

4.3.6. Impact of Shadowing by the Human Body

For all results presented, so far the simplifying assumption that there is no additional shadowing between the BSN nodes is made. This assumption allows us to clearly see the effects of interference in isolation (which is the main goal of this thesis). However, it is well-known that the human body can introduce substantial additional path loss in the order of 30 - 35 dB and that, for IEEE 802.15.4 networks, it is often required to use the largest possible transmit power (see [94, 98]).

To study these effects, in this section a new set of simulations is analysed in which

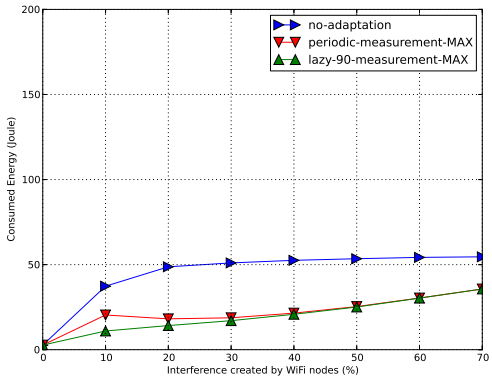

(a) Energy consumed by sensor nodes

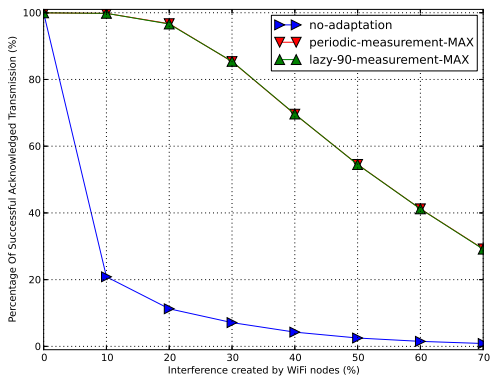

(b) Success rate

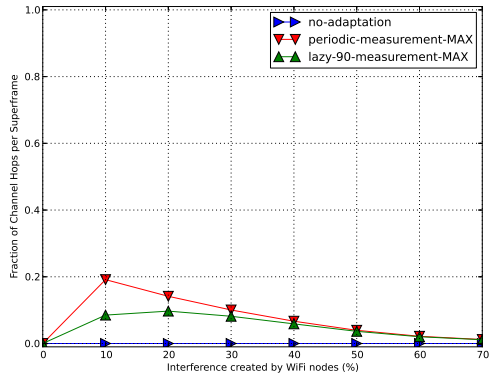

(c) Fraction of channel hops

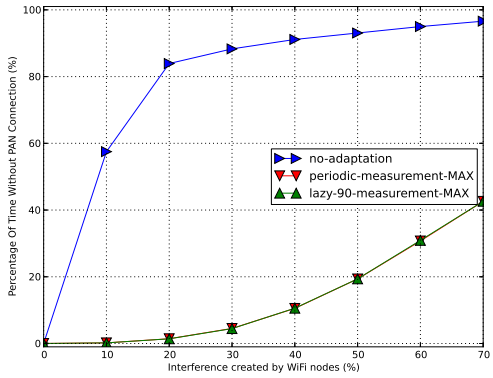

(d) Percentage of time without PAN

Figure 4.7.: Comparison of no-adaptation, periodic-measurement-MAX and Lazy scheme for $\Delta = 300$

additional path loss between the coordinator and the attached nodes is present, and the transmit-power of all nodes is set to 0 dBm. More specifically, there was no additional path loss for the first sensor node (just the 55 dB path loss at the reference distance PL_0), 11 dB additional path loss for the second node, 20 dB for the third node and 30 dB for the fourth node.

For the considered scenarios in this section, the average number of interferers $\Delta \in \{100, 200, 300\}$ and the interference traffic intensity $\lambda \in \{0\%, 10\%, ..., 70\%\}$ are varied. Figures 4.8, 4.9 and 4.10 illustrate the results for the Lazy and the no-adaptation schemes where $\Delta = 100$, $\Delta = 200$ and $\Delta = 300$, respectively. The Lazy and the no-adaptation schemes are compared in the absence and presence of additional path loss (both using 0 dBm transmit-power).

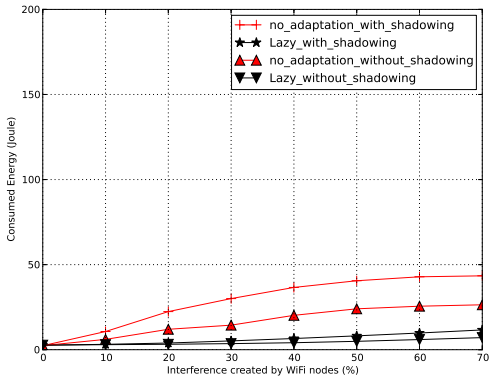

(a) Energy consumed by sensor nodes

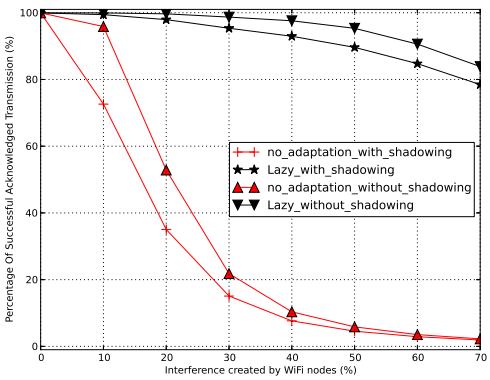

(b) Success rate

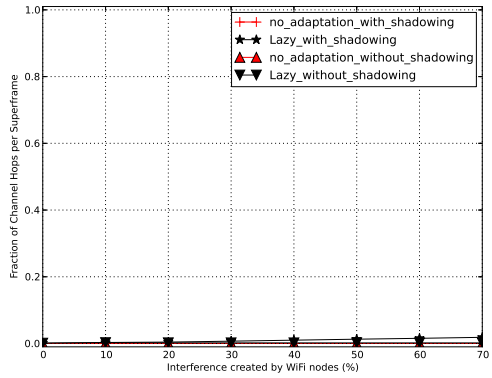

(c) Fraction of channel hops

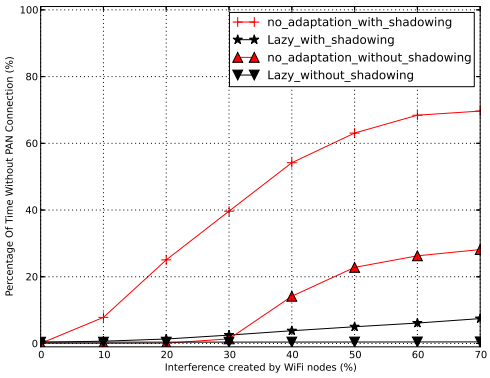

(d) Percentage of time without PAN

Figure 4.8.: Comparison of no-adaptation and Lazy scheme for $\Delta = 100$ and with additional node-dependent path loss

The results show:

(i) The relative performance gains of the Lazy scheme over the no-adaptation scheme in terms of both energy consumed by the sensor node and the success rate remain the same, in the absence and presence of the shadowing effects of the human body. In other words the Lazy scheme still outperforms the no-adaptation scheme.

(ii) When subjecting the schemes to the additional path loss created by the human body, the success rate drops slightly. Furthermore, the orphaning period also increases. This results in an increase in the energy consumption of the sensor node.

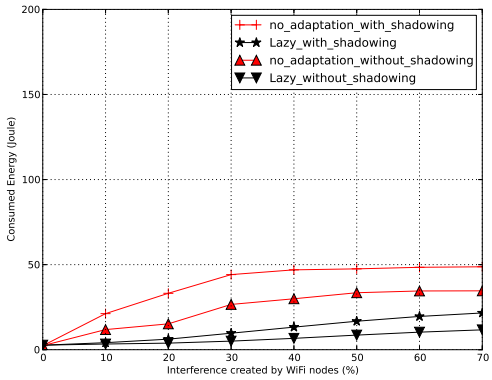

(a) Energy consumed by sensor nodes

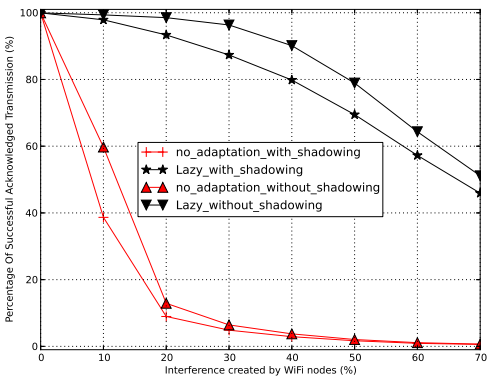

(b) Success rate

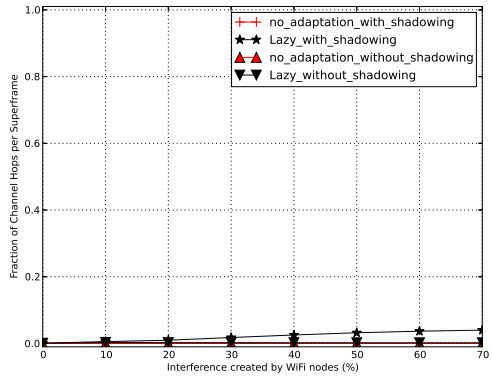

(c) Fraction of channel hops

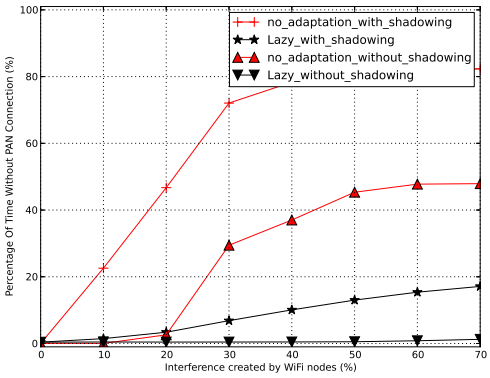

(d) Percentage of time without PAN

Figure 4.9.: Comparison of no-adaptation and Lazy scheme for $\Delta = 200$ and with additional node-dependent path loss

(iii) The performance differences in terms of success rate between the cases with and without additional path loss are modest for all values of Δ.

(iv) The impact of human body shadowing on the performance of the WBSN is better illustrated in the experimental results shown in Chapter 6.

4.4. Discussion

This chapter explored the potential benefits of frequency adaptation. First, the non-adaptive baseline schemes are compared with each other in terms of tolerance and performance in scenarios with harsh interference conditions. The CAP-enabled network proved to be the most tolerable baseline scheme against external interfer-

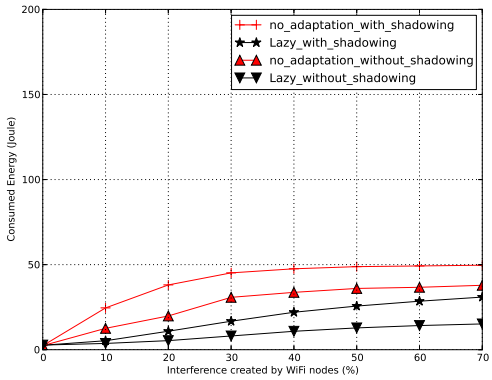

(a) Energy consumed by sensor nodes

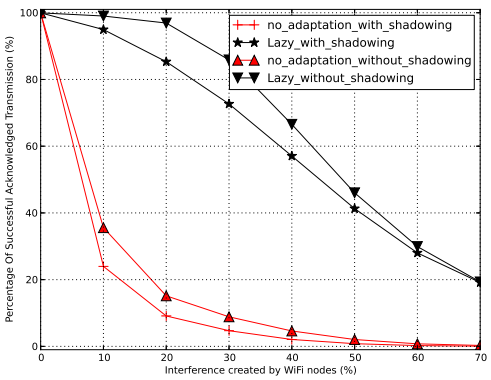

(b) Success rate

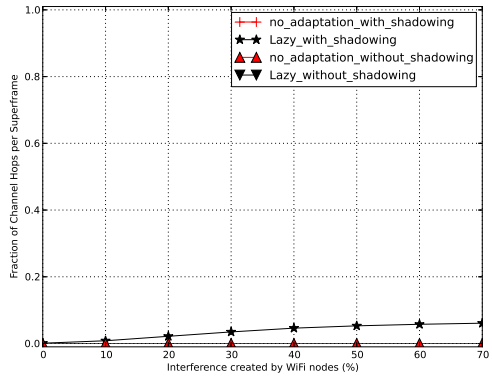

(c) Fraction of channel hops

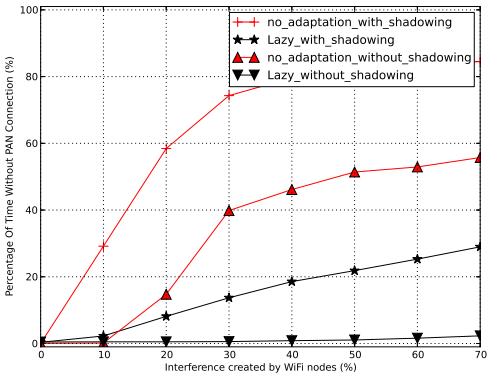

(d) Percentage of time without PAN

Figure 4.10.: Comparison of no-adaptation and Lazy scheme for $\Delta = 300$ and with additional node-dependent path loss

ence. Next, a hypothetical scheme called the Genie scheme has been proposed that illustrated the potential upper bounds of what is achievable if channel adaptation is introduced. These results show that frequency adaptation probability offers a significant performance gain in terms of success rate.

This chapter also looked at more realistic channel adaptation approaches, namely periodic-random, periodic-measurement and the Lazy schemes. The research showed that as the number of channel switches increases in the periodic-random scheme, this scheme becomes more robust against interference. One of the drawbacks of increasing the number of channel switches is the noticeable elevation in consumed energy of all nodes due to the switching costs. The proposed periodic-measurement schemes spend time and energy to measure the available channels to make more intelligent

channel switching decisions. The results for periodic-measurement schemes show first of all that frequency adaptation offers a significant potential for performance improvements over the case of no-adaptation, both in terms of achieved success rate and in terms of energy required at the sensors. Furthermore, the effort required for measurement-based adaptation pays out, presumably by saving sensors from excessive re-transmissions on interference-prone channels. In addition, the enhancement made in the decision process of the Lazy scheme improved the energy consumption while achieving the same success rate as the measurement-based schemes. This decision process improves the performance gains by reducing the number of channel switches. Another key feature of the proposed (periodic-random, periodic-measurement and Lazy) schemes is that they make *no* protocol modification except adding extra information to the beacon payload (in the worst case 8 bytes, see Section 5.1.1).

This chapter further investigated the shadowing effects of the human body on the performance of the proposed schemes. Additional path loss was introduced to the WBSN nodes in order to mimic the shadowing effects of the human carrier. The results showed modest difference in the success rate between the cases with and without additional path loss. Regardless of the shadowing impact caused by the human body, the Lazy scheme still outperforms the no-adaptation scheme for all interference scenarios.

In sum, adding frequency adaptation schemes to the IEEE 802.15.4 standard **can** increase the overall performance and reduce the consumed energy of the network. This chapter has demonstrated a few schemes that are both effective and energy-efficient. In addition, the proposed schemes are easy to implement as would be demonstrated in Chapter 6. However, as the results presented in Figures 4.6 and 4.7 show, the success rate decreases substantially when the interference density λ increases. Analysis of these simulation results has shown that the devices spend more and more time in the orphan state as λ increases. This problem is considered

in more detail in Chapter 5.

5. Orphan Recovery

As already stated in the introduction, the Lazy adaptation scheme, while showing very promising performance, still suffers from the problem of orphan nodes needing to scan through all available channels (because the coordinator might have switched channels), which costs time, energy and leads to losses of data packets during the time a sensor is orphaned. This chapter explores ways of improving the Lazy scheme by reducing the overall time the sensor nodes spend in the orphan state. Specifically, this chapter proposes three different methods to reduce the number of channels that the orphan node has to scan before it re-discovers its coordinator. All schemes are based on providing the sensor nodes with additional information for narrowing down the list of channels on which to search for the coordinator. These three coordinator discovery support schemes are compared against two other schemes in which the channels are either scanned sequentially or in a random order. This chapter first describes the considered schemes and then presents the simulation results followed by a discussion. The results presented in this chapter were published in [173] and [177].

5.1. Considered Schemes

5.1.1. Baseline Schemes

In this chapter three baseline schemes are considered. The first one is the **no-adaptation scheme** described in Section 4.1. Remember that in this scheme the

coordinator picks one frequency channel at the beginning and never changes its frequency channel throughout its lifetime. When a sensor node becomes an orphan, it does not scan any other channels than the one it was operating on previously. To ensure this in our simulation settings sensor nodes are preconfigured with this information.

The other two baseline schemes are based on the Lazy adaptation scheme. In the **Lazy-ordered** scheme, when a sensor has lost synchronisation while operating on channel f, it scans sequentially through all 16 available channels, starting with channel f, then channel $(f + 1) \bmod 16$, then channel $(f + 2) \bmod 16$ and so on. The device listens on each channel for one entire beacon period. To ensure that the sensor devices know their coordinators beacon order, the interference only sets in a few second after the start of every simulation run. This assumption ensures that the sensor nodes have enough time to successfully find and associate with their corresponding coordinator.

In the **Lazy-random** scheme, the orphan node scans all 16 channels using a random permutation of {1, 2, 3, ..., 16}. Please note that in these baseline schemes the orphan does not try to come up with any kind of intelligent guess of the channel on which the coordinator could be. The orphan nodes listen on each channel for one super-frame duration.

5.1.2. Discovery Support Schemes

The following schemes attempt to utilise extra or available information to let sensor nodes to make more intelligent decisions on the order of scanning the available 16 frequency channels.

1. In the **Lazy-energy-scan** scheme the orphan device starts by performing a quick scan on all available channels for their energy level (RSSI). By the term quick scan it is meant that only five RSSI samples are taken from each frequency channel and from these the maximum RSSI value of each channel is

selected to represent the energy level of that frequency channel. The orphan node then sorts the channels according to the RSSI levels in increasing order, and it starts to listen on the channel with the lowest energy level (which is supposedly the "cleanest" channel, to which the coordinator might have moved), then followed by the second-lowest-energy channel and so forth. The additional energy costs involved for RSSI measurements are considered for this scheme. The idea behind this scheme is that if a node becomes orphan, it is most likely to find its coordinator operating on the channel with the lowest noise level. It is assumed that the measurements are noise-free, in order to observe the performance of this scheme under ideal conditions. This scheme would probably suffer from the human body shadowing effects. However, shadowing is not considered for these simulation results.

2. In the **Lazy-sequence-scan** scheme a sensor node does not perform its own measurements. Instead it utilises the measurement results of its corresponding coordinator. The coordinator includes in its beacon packets – as payload[1] – extra information that the sensor nodes could utilise when deciding on the channel order when in orphan state. More specifically, the coordinator includes a ranking of the 16 channels in terms of its own energy measurements, so that the first channel listed in this ranking is the one the coordinator would switch to when it is forced to change channels now – this ranking order may not necessarily be the order in which the coordinator switches, since the channel conditions may drastically change in the future. In the moment a device becomes orphaned, it refers to the last known channel ranking order that the coordinator had and, starting from the first channel, it listens on each channel for a duration of one beacon order in order to find and re-associate with its corresponding coordinator.

3. Finally, the **Lazy-heuristic-sequence-scan** scheme operates by the same

[1]This field is 64 bits and each 4 bits represents the index of a given channel.

principle as the Lazy-sequence-scan scheme. However, the orphan node scans the first two channels in the provided channel ranking sequence from the coordinator twice as long as other channels. The rationale behind this scheme is to increase the probability of finding the coordinator, provided it is indeed on one of the first two channels.

5.2. Performance Metrics

To compare and evaluate the different proposed coordinator discovery schemes with each other and with the other three baseline schemes, this chapter considered the following main performance measures:

i) **Success Rate**: As explained before in Section 1.5.1, the success rate represents the average percentage of data packets reliably transmitted and received from the sensor node to the coordinator node with a successful acknowledgement packet from the coordinator node.

ii) **Consumed Energy**: This performance metric represents the average energy consumption of the sensor nodes. In this chapter the proposed schemes mostly affect the performance of the sensor nodes, therefore the energy consumption of the coordinator node is not presented. For more detail on energy consumption calculation see Section 1.5.1.

iii) **Percentage of time without PAN**: This is the overall percentage of time sensor nodes spent in the orphan state, where sensor nodes need to find their corresponding coordinator by scanning available channels (see Section 1.5.1). The objective of the proposed coordinator discovery schemes in this study is to reduce this performance metric (and consequently improve others as well).

iv) **Average Channel offset**: The average number of channels that the orphan needs to scan before reaching the channel where the corresponding coordinator

has hopped to is represented in this performance metric. This calculation is done right after the node becomes orphan and just before the device starts listening, only in the case of Lazy-energy-scan scheme the offset calculation is made after the sensor has gathered RSSI measurements from all 16 channels. At time t_0 when a device becomes an orphan, it computes a sequence of channels on which it looks for the coordinator. Depending on the enabled discovery scheme, the sensor nodes arrange all available 16 channels to be scanned, so that the first channel in this sequence is considered first, the second channel is considered next and so forth. The average channel offset specifies the position (0-based) of the actual channel of the coordinator at time t_0 on this list – smaller values indicate that the coordinator is potentially found earlier. This value is averaged over the number of orphan states occurred in all simulation runs. This metric illustrates how efficient the proposed schemes are in providing the sensor nodes with information in **ideal** scenarios where no external interference is available.

The considered simulation scenario followed by the simulation results are presented.

5.3. Simulation-Based Performance Evaluation

The results shown here are obtained using the same simulation scenario as in Section 3.2. The schemes described in Section 5.1 are evaluated for varying values of the interference intensity λ and for an average number of WiFi interferers of $\Delta = 300$. The trends observed below are also true for smaller average numbers of interferer densities. However, because in scenarios with lower densities of WiFi interferer nodes the number of occurred orphan states is lower and the percentage of time spent in orphan state is not substantial, therefore the efficiency of the different schemes is hard to measure foe lower values of Δ (see Figure 4.6d). For this study, sufficient replications to reach a relative confidence interval half-width of 5% at a

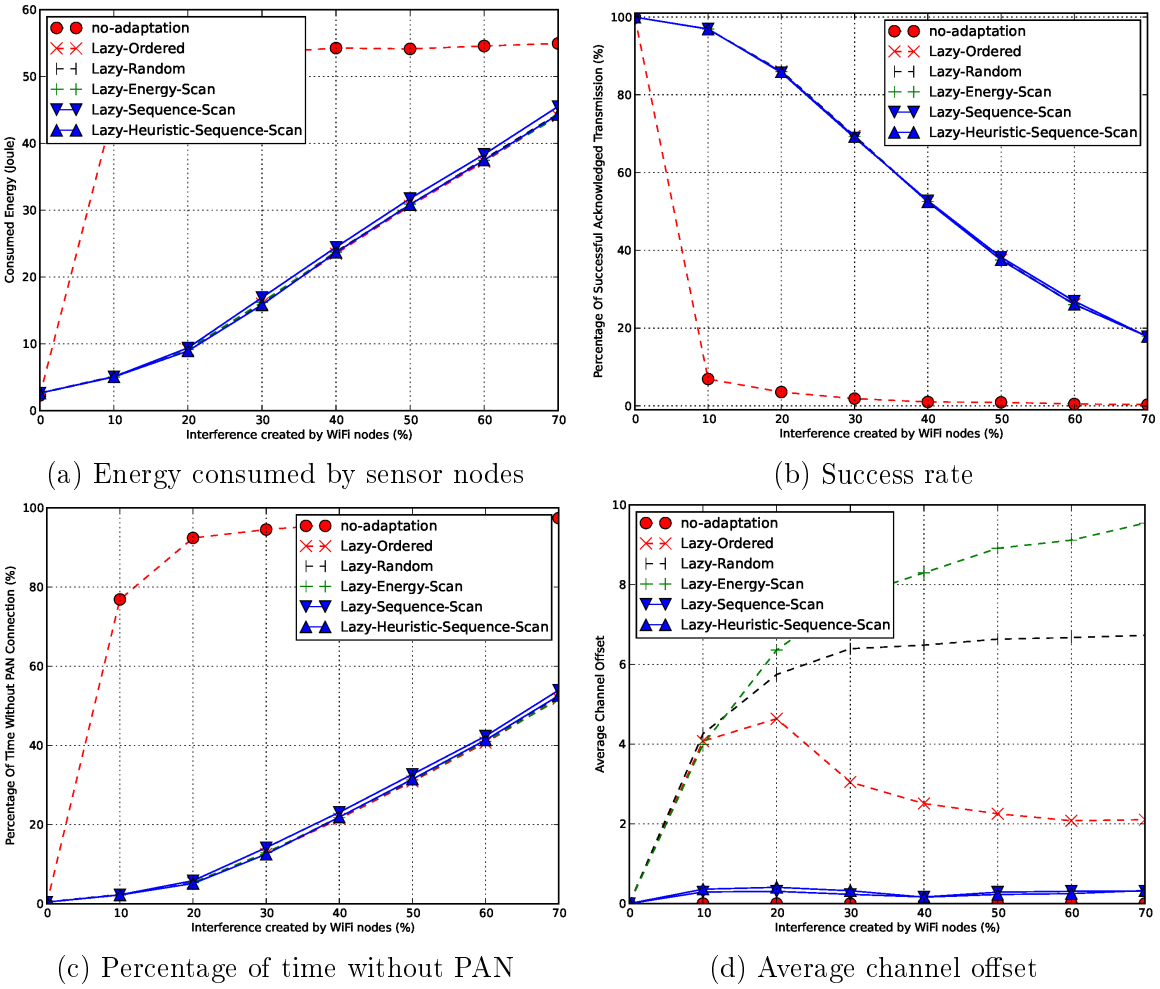

(a) Energy consumed by sensor nodes

(b) Success rate

(c) Percentage of time without PAN

(d) Average channel offset

Figure 5.1.: Comparison of the no-adaptation scheme with the different proposed coordinator discovery schemes added to the Lazy scheme where $\Delta = 300$

95% confidence level for the success rate has been conducted. The results are shown in Figure 5.1.

Looking at Figures 5.1b, 5.1a and 5.1c, the only noticeable difference is between the no-adaptation scheme, which has the lowest performance gains, and all the other schemes which have very similar performance. There are slight variations between the different Lazy schemes, but nothing that is statistically significant.

Nonetheless, Figure 5.1d sets apart these schemes from each other. The no-adaptation scheme does not need to switch channels, therefore this scheme has a constant trend set to zero. In other words, this scheme never needs to switch channels since the coordinator is zero hops away. In scenarios where λ is roughly between 10

and 30%, the Lazy-ordered scheme finds its corresponding coordinator after almost four hops, after which the probability of finding the coordinator decreases to almost 2 hops. One explanation is that usually a WiFi interference source creates interference on four WBSN channels, and the coordinator selects the next best channel with the lowest noise. This is due to an implementation choice: when a coordinator node finds several channels of the same minimal energy level, it selects the channel closest to its current operating channel in ascending order. However, as the interference grows, the options for the next best channel – in terms of noise level – reduces.

In the Lazy-random scheme, the sensor node sorts the sequence of channels to be scanned randomly, therefore it is expected that the average channel offset remains constant at around seven hops (counting from zero). Nevertheless, for scenarios with $\lambda \leq 20\%$ this is not true. This is mainly because for such scenarios, an insufficient number of orphaning states occurs, and the results are not statistically significant[2]. This is the same reason for lower values of Δ no substantial difference was found. Interestingly, the Lazy-energy-scan scheme showed the worst performance in terms of average channel offset. Although it is assumed that channel measurements are not noisy and the coordinator node selects the channel with the minimal energy level, the sensor and the coordinator node measurements are taken at different times and the coordinator selects between channels with minimal energy level the channel numerically closest to its current operating channel. This is the main reason why, as the intensity of the external interference increases, the chance of differentiating between noisy channels reduces.

The Lazy-sequence-scan and the Lazy-heuristic-sequence-scan scheme were able to find the coordinator with in zero to one hop, dramatically reducing the average channel offset. However, due to high-interference conditions the overall performance of these schemes does not change. The Lazy-heuristic-sequence-scan manages to slightly reduce its energy consumption and time without PAN by spending double

[2]As mentioned earlier in this section, sufficient number of replications are considered to reach a relative confidence interval half-width of 5% at a 95% confidence level for the success rate.

the time for scanning on the first two channels in the sequence. However, the performance of Lazy-heuristic-sequence-scan is the same as the Lazy-ordered scheme in terms of the energy consumed by the sensor node, the success rate and the percentage of time without PAN.

5.4. Discussion

The main finding is that, although the proposed Lazy-heuristic-sequence-scan and Lazy-sequence-scan scheme are very effective in predicting the channel where the coordinator could be found (due to the good "average channel offset performance", see Figure 5.1d), the overall time spent in the orphan state is not affected substantially by this, and all the Lazy schemes show approximately the same performance (Figures 5.1c, 5.1b and 5.1a). One likely explanation for this is that the orphan, after switching to the right channel, still fails to receive the beacons because of high-interference levels – after all, the average number $\Delta = 300$ of interferers chosen is relatively high. In other words: these two approaches "do the right thing", but it does not help, at least not in high-interference situations. While this appears to be a negative result, it is nonetheless useful for designers as it might save implementation efforts. The other schemes do much less well in terms of channel offset performance but still spend on average the same time in the orphan state (with exception of the no-adaptation scheme).

6. Experimental Results

This chapter reports on experimental work carried out with implementations of the standard IEEE 802.15.4 MAC (no-adaptation) scheme described in Section 4.1.1, of our Lazy scheme (more precisely, the periodic-random scheme with a period of 1, which hops after each beacon period described in Section 4.2.1 and the Lazy-measurement scheme described in Section 4.2.2. A subset of the results presented in this Chapter has been published in [177].

This chapter gives a brief overview of our implementation, followed by a description of the experimental setups used. Finally, the measurement results obtained using commercially available WSN nodes are presented. These experimental results reveal whether it is possible to qualitatively confirm the performance trends observed in Section 4.3. Furthermore, they allow us to get insights into the behaviour of these schemes under realistic conditions.

6.1. Overview of Implementation

The TKN154 implementation [65] of the IEEE 802.15.4 MAC protocol under the TinyOS operating system in version 2.1.1 [100] is used on MicaZ motes [47]. The code is written in the NesC programming language.

TinyOS is a component-based operating system for embedded platforms. In TinyOS components interact through interfaces. Interfaces have a provider and a user. The user of an interface can call so-called commands implemented by the

provider. In the other direction, the interface provider can signal so-called events to the interface user, which in practical terms means that the interface provider calls a function specified by the interface user.

The TKN154 implementation of the IEEE 802.15.4 protocol is organised as a set of components, interacting with each other and with higher layers through well-defined interfaces. In this study it was decided that the bulk of the implementations of the Lazy and periodic-random schemes shall be placed *outside* the TKN154 components, into the application layer. This decision leaves the TKN154 implementation almost unmodified. The Lazy and periodic-random schemes need no protocol modification except adding extra information (which require in the worst case eight bytes) to the beacon packet payload. Avoiding major modifications to the existing IEEE 802.15.4 standard is a main feature of the schemes proposed in this thesis.

However, in order to obtain the information needed for these schemes to operate, three events are added to the TKN154 implementation. The three events are signalled by the TKN154 MAC to higher layers as follows:

- An event signalling the loss of one individual beacon packet: this event is generated within a sensor node when, after waking up for receiving a beacon from its coordinator, such a beacon is not received. This guard time is referred to as "Beacon Time Out" (see Table 3.1).

- An event signalling the end of the active period: this event is generated for the coordinator node immediately after the active period has ended and before the start of the inactive period. This signal enables the Lazy scheme to start its channel measurements.

- An event immediately before the start of the next beacon: this event is triggered for both coordinator and sensor nodes shortly before the start of the next super-frame and before a beacon packet is transmitted by the coordinator node. This information allows time for both sensor and coordinator node

to initialise their (possibly new) operating channel before the start of the next super-frame.

Besides the extraction of these three events for higher layers, no other changes to the TKN154 MAC have been made. Most importantly, the existing IEEE 802.15.4 protocol implementation of the TKN154 as such has not been modified.

The actual implementations of the Lazy and periodic-random schemes are contained in the application code (but could be placed into a separate component or incorporated to the TKN154 MAC layer). They are driven by receiving the three events from the MAC implementation. For example, on receiving the event signalling the end of the active period, the coordinator in the Lazy scheme starts sampling the energy levels on all available channels. The details of the implementation are discussed in Section 6.2. Moreover, the source code will be made available. Table 6.1 displays the number of code lines required for implementing the Lazy and the periodic-random scheme on the coordinator and devices, respectively. These numbers do not include the number of code lines needed by the TKN154 implementation, but include debugging and logging code. Furthermore, the code includes generic parts that also occur in the implementation of the no-adaptation scheme. Thus, this table also includes the code lines required for the no-adaptation scheme. These numbers show that the implementation of our frequency adaptation schemes requires just a few hundred lines of code, for example about 230 lines of code for the Lazy scheme on the coordinator.

6.2. Implementation in the nesC-TinyOS Environment

The implementation of the no-adaptation, periodic-random and Lazy scheme has been done using the NesC (Network embedded system C) programming language on the TinyOS operating system [65]. This open-source operating system is one

of the most widely used operating systems designed for distributed WSNs. NesC is an event-driven and component-based programming language. In order to build and run an application for the TinyOS platform, a series of components are "wired" together.

6.2.1. Component Diagrams

The component diagram is used to provide an overview of the system structure and how different components in a system are wired together. The component diagram in Figure 6.1, shows the system structure of the proposed no-adaptation, periodic-random and Lazy scheme for both sensor and coordinator node. Our proposed schemes are implemented in the "NoAdaptationCoordinatorC", "NoAdaptationSensorC", "PeriodicRandomCoordinatorC", "PeriodicRandomSensorC", "LazyCoordinatorC", "LazySensorC" and "MainC" components. Furthermore, a subset of system components are used such as "ieee802154BeaconEnabledC", "LedsC", "TimerMillC", "RandomC", "QueueC" and "LocalTime62500hzC".

In all of the proposed schemes, "MainC" is the component triggered at start-up. This component handles all the initialisation of the device. Access to "MainC" is provided with the "boot" interface. "LedsC" provides an interface to control the (Red, Green and Yellow) LEDs available on the MicaZ device, giving a visual indication of current device status, namely sending and receiving beacon packets, sending and

Scheme / Node	**≈ Lines of code**
Lazy / coordinator	420
Lazy / sensor	560
Periodic-random / coordinator	280
Periodic-random / sensor	590
No-adaptation / coordinator	195
No-adaptation / sensor	480

Table 6.1.: Lines of nesC code for implementation of different frequency adaptation schemes

Figure 6.1.: NesC Component diagram for no-adaptation, periodic-random and Lazy schemes.

receiving data packets and whether the node is associated or in orphan mode. The "RandomC" component is only used in the sensor nodes for the generation of random length data packets. The "TimerMillC" and "QueueC" components are used to periodically send debugging and trace information back to the computer through the serial port. Furthermore, to increase the accuracy of our measurements, the "LocalTime62500hzC" component provided more accurate time-stamps for debugging.

The only noticeable difference between the three schemes shown in Figure 6.1 are the extra interfaces used for "LazyCoordinatorC". This scheme utilises the "MLME_SCAN" interface of "ieee802154BeaconEnabledC" to collect RSSI measurements of the 16 channels, and the "MLME_SYNC_LOSS" interface to receive a signal before the start of next super-frame. Moreover, this scheme also utilises a "QueueC" to store channel in a window of measurement values.

6.3. Experimental Setup

An experimental setup is created in which a WBSN with one coordinator and one sensor node moves through an outdoor field with varying numbers of WiFi access points. To eliminate unwanted WiFi interference – other than the WiFi interference that is introduced for this experimental study – the location where these results have been taken has been carefully selected far away from other buildings[1].

6.3.1. Experimental Scenarios

In this experimental study, two different scenarios for the placement of the WiFi interferers has been considered:

Scenario 1: In this scenario (see Figure 6.2), WiFi APs are placed very close to each other in the middle of the field, with a few centimetres distance between them. The WBSN was carried by a person and the person moved along a straight

[1]The Groynes park in Christchurch, New Zealand

line of length 140 meter, in the middle of which the APs were placed. The path taken by the WBSN goes directly over the APs, so that in the middle of the path the BSN experiences maximum interference. The person has moved at constant pedestrian speed of approximately 5 km/h – The movement speed in the field was controlled with a stop watch timer. The number of APs in this scenario is varied from zero to five, creating external interference on channels 1, 3, 6, 9, and 11, respectively. In this scenario, the WBSN was allowed to work on all 16 available channels, and even with all WiFi interferers present there was always one IEEE 802.15.4 channel available without interference (channel 26).

Scenario 2: In this scenario the APs were not placed on the same spot. Instead, three APs were placed on a straight line with a spacing of 30 m between them (see Figure 6.3). The person carrying the WBSN again moves at a constant speed of approximately 5 km/h along a 140 m long line which coincides with the line where the APs are placed. In this scenario all three WiFi APs are turned on and configured to create interference on channels 1, 4, and 7, respectively. Furthermore, the WBSN were only allowed to operate on channels 11 to 20. This limitation ensures that all WBSN channels are faced with external WiFi interference at some point in the experimentation round. The goal of this experimental setup is to illustrate how each scheme performs in an environment where interference is on all channels but interferers are spread over distance. Moreover, a secondary goal was to see how the adaptation process behaves over time.

6.3.2. Experimental Components

The BSN uses a transmit power of -25 dBm and the sensor generates data packets with a period of one second. The beacon order has been chosen as 6 and the super-

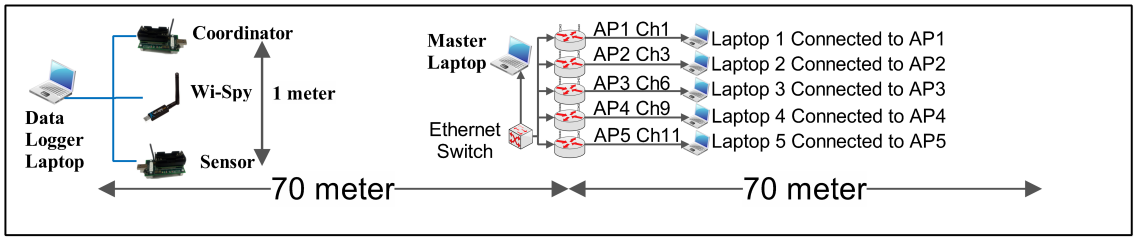

Figure 6.2.: Scenario one.

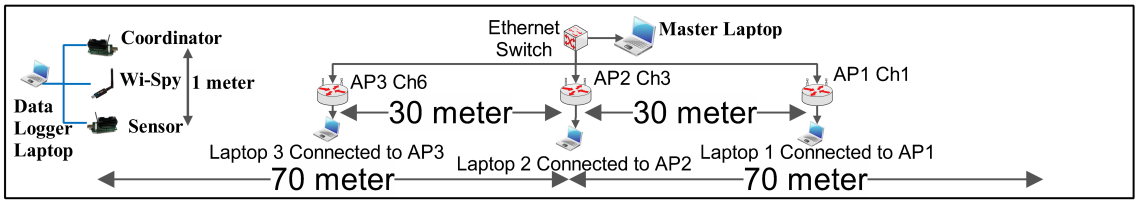

Figure 6.3.: Scenario two.

frame order as 4. The distance between the coordinator and the sensor is fixed to be one metre apart. The channel for the no-adaptation scheme is fixed to channel 22. This is selected so that in the presence of interference the WBSN would always be operating on the channel with external interference. Both motes were placed in front of the person carrying out the experiments so that the WBSN devices had a direct line-of-sight to each other. When the person passes the interference source their body provides partial shielding for the WBSN. This explains the somewhat asymmetric appearance of the spectrum utilisation over time seen in Figures 6.4 and 6.5.

These figures show the spectrum utilisation (maximum RSSI measurements) recorded during one experimental run (moving along the 140 m path), using the WiSpy spectrum analyser. These USB-based Wi-Spy 2.4 GHz spectrum analysers are able to track all radio activities from WiFi, Cordless Phones, Microwaves, ZigBee, Bluetooth, and other devices operating in the 2.4 GHz frequency band. It takes 419 samples between frequencies 2400 MHz and 2483 MHz at a spacing of 199 kHz. The sample rate of this device is 2 Hz.

For the WiFi interferers, the Cisco Aironet 1130AG Series WiFi access points are used. Each AP operated at maximum transmit power of 20 dBm using the 802.11b

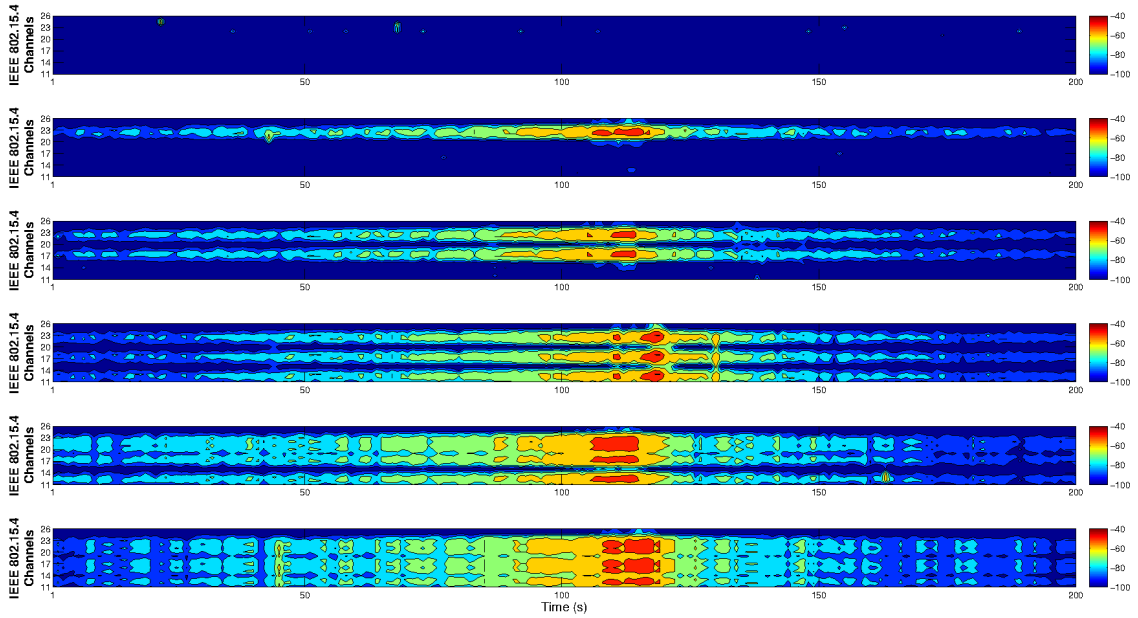

Figure 6.4.: Spectrum utilisation over time for scenario one and for varying numbers of access points, from zero (top figure) to five (bottom figure).

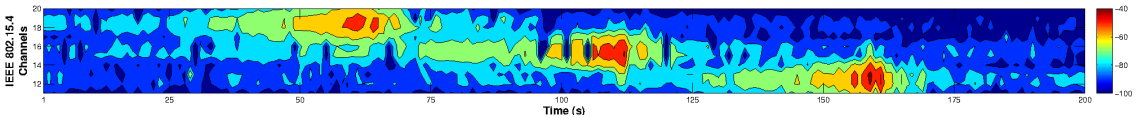

Figure 6.5.: Spectrum utilisation over time for scenario two.

modulation and the lowest data rate of 1 Mbit/s, with the default carrier-sensing capability of WiFi APs. The open-source packet traffic generator and analyser called "Ostinato"[2] is used to generate a continuous stream of UDP packets. The packet length has been set to 1518 bytes.

For this experimental study a number of laptops were used for different purposes.

- One laptop was used as the master laptop, running a DHCP server and a NTP server to synchronise the clock between the laptops. Furthermore, the master laptop is responsible for initial configuration of all WiFi access points (disabling and enabling, setting transmit power, operating channel, etc.), and for running the Ostinato load generator. The master laptop was connected to the APs through Ethernet.

[2]http://code.google.com/p/ostinato/

- Next, for each AP there was a separate laptop configured as a wireless client – without this, the intelligent Cisco APs would not have forwarded the UDP packets generated by the master laptop.

- Finally, the data logger laptop connected to the Wi-Spy spectrum analyser and the two MicaZ motes making up the BSN. It logs the information being generated by them and sent via USB.

6.3.3. Performance Metrics

To evaluate and compare the different proposed schemes with each other, the following main performance measures are considered:

i) **Success Rate**: The percentage of data packets sent by the sensor node which were successfully acknowledged by the coordinator node (see Section 1.5.1).

ii) **Percentage of time without PAN**: Similar to Section 1.5.1, the overall percentage of time that the sensor node spends in the orphan state is the "Percentage of time without PAN".

iii) **Number of Channel Hops**: This is the average number of channel hops needed before a coordinator discovery occurs. This number has a direct relationship with the overall energy consumption. In other words, the longer the coordinator discovery takes, the more energy the orphan nodes need to consume for scanning channel(s) in order to re-associate to their corresponding coordinate node.

iv) **Number of Channel Switches**: This is the average number of channel switches sensor nodes make to maintain synchronisation with their corresponding coordinator node. Depending on the scheme used, the number of channel switches differs.

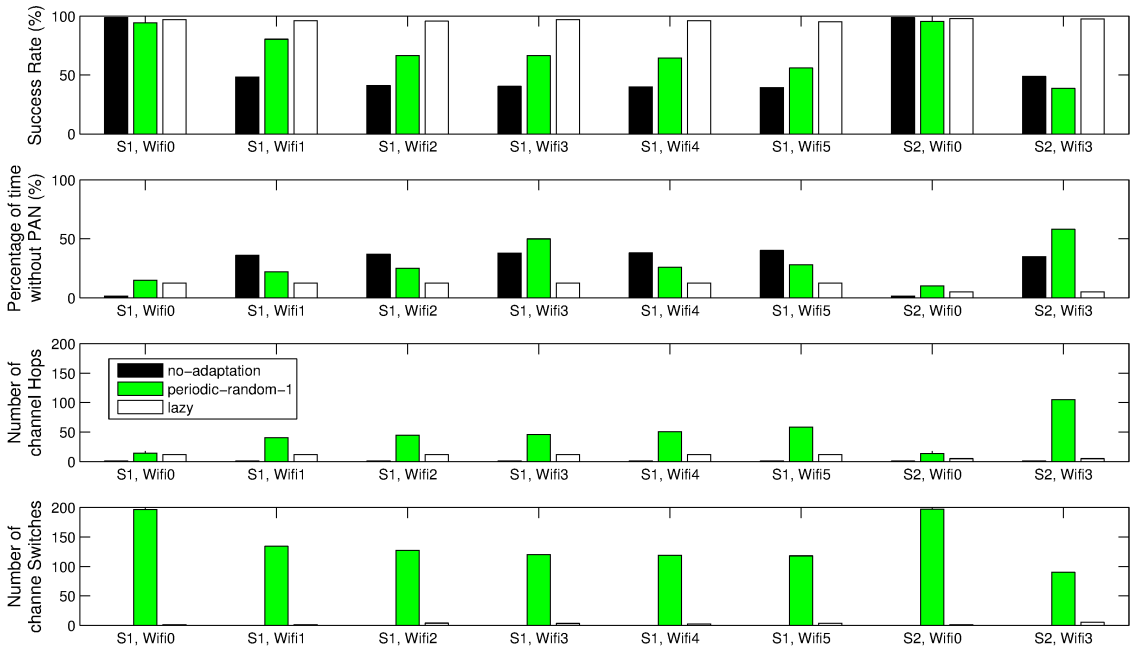

Figure 6.6.: Summary experimental results for both scenarios.

6.4. Results

This section presents our experimental results. For each scheme and scenario the experiment is repeated 10 times. Figure 6.6 shows the packet success rate, the percentage of time spent in the orphan state, the number of channel hops made by the sensor while searching for beacons, and the number of channel switching decisions executed by the sensor for varying numbers of WiFi access points in the first scenario (marked "S1" in the figure). This figure also includes the corresponding results for the second scenario (marked "S2"). Each bar in this figure is averaged over all 10 repetitions of the corresponding experiment, and the outcome of each repetition is averaged over the entire time it takes to move along the path.

While not directly comparable, the results for the packet success rate confirm the relative performance trends observed in our simulation results (see Section 4.3.5). The Lazy scheme has an almost perfect packet success rate and outperforms both the periodic-random-1 scheme and the no-adaptation scheme significantly in both scenarios. In the first scenario, this is due to the ability of the Lazy scheme to find

the free channel and to leverage it. In the second scenario, the Lazy scheme uses its ability to pick the instantaneously best channel to "move around" the interferers. Furthermore, in the first scenario the periodic-random-1 scheme outperforms the no-adaptation scheme, whereas in the second scenario the latter scheme has a slight advantage. This is mainly due to the location of the WiFi APs which spread the interference over a larger portion of the field in the second scenario, rather than having all APs at the same spot. The fact that the no-adaptation scheme still has an overall success rate of $\geq 40\%$ is because a substantial part of the path taken by the WBSN is outside the interference range.

The percentage of time spent in the orphan state is almost constant and very low for the Lazy scheme (See Figure 6.6). This is mainly due to the initialisation phase of the system where the sensor node tries to find its coordinator for the first time. However, the fact that this trend is not changed for increasing number of access points in scenario one can again be explained by the Lazy scheme's ability to find the free channel and to avoid the orphan state. Even in the second scenario this scheme's time spent in the orphan state is very small. The two other schemes show generally declining performance as the number of access points is increased. The performance of the no-adaptation scheme remains constant for varying number of interferers in both scenarios. This is mainly due to having one fixed channel. Nevertheless, the performance of the periodic-random-1 scheme appears to vary inconsistently with the number of interferers. This is probably due to having only ten repetitions.

The number of channel hops required for sensor nodes to re-discover their corresponding coordinator node is constant and very small for the Lazy and the no-adaptation scheme in both scenarios. However, the no-adaptation scheme is able to find its coordinator with fewer channel hops, since both coordinator and the sensor nodes remain on their pre-configured frequency channel. The worst performance is seen by the periodic-random-1 scheme. This is mainly due to random channel

hopping.

Although the Lazy scheme has less than five channel switches during the course of one experimentation round, as compared to the periodic-random-1 scheme, the former has a higher success rate and lower percentage of time without PAN. This is mainly due to its intelligent channel selection ability. Randomly selecting channels and utilising more of the available spectrum improves the success rate performance of the network over the no-adaptation scheme to some extent. Nevertheless, spending a small duration of time to estimate the available channel and making intelligent decisions is still beneficial in comparison with the cost involved with the no-adaptation and the periodic-random-1 schemes.

In order to get a more detailed insight into the behaviour of our schemes, Figures 6.7, 6.8, 6.9,6.10, 6.11, and 6.12 show for the first scenario and the three implemented schemes how various important performance figures evolve over time. Similar graphs are created for the second scenario, shown in Figures 6.13, 6.14 and 6.15, respectively. These figures show results for one representative repetition. The parameters shown in the figures are:

i) **Beacon RX**: This parameter shows the number of beacon packets received by the sensor node (the time axis is partitioned into windows of 10 second).

ii) **Data RX First Time**: This parameter displays how many data packets are successfully transmitted in the first attempt (again in windows of ten second size).

iii) **Data RX With Retry**: This parameter shows the number of data packets that are successfully transmitted after at least one re-transmission (in windows of ten second size).

iv) **Beacon Sequence**: This parameter illustrates the sequence in which the beacon packets are received by the sensor node. A successful received beacon packet

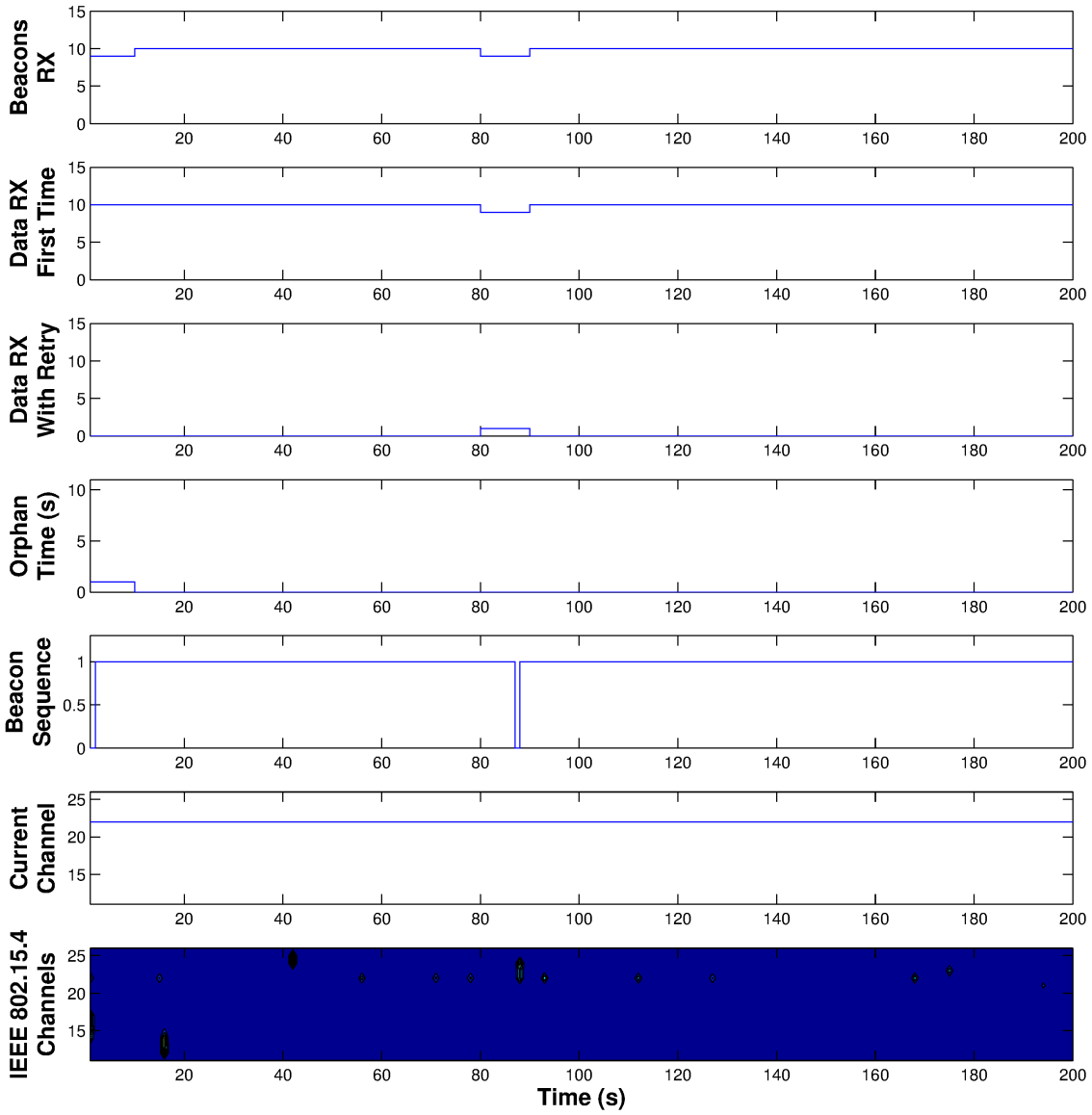

Figure 6.7.: Behaviour of the no-adaptation scheme for zero interferers, first scenario.

is represented by a value of one, a missed or dropped beacon packet (due to external interference) is indicated by a value of zero.

v) **Orphan Time**: Orphan Time shows for each ten-second-window the duration of time that the sensor node has lost its synchronisation with the coordinator node and is scanning the channel(s) in order to find and re-associate with the coordinator node.

vi) **Current Channel**: This shows the current operating channel of the coordi-

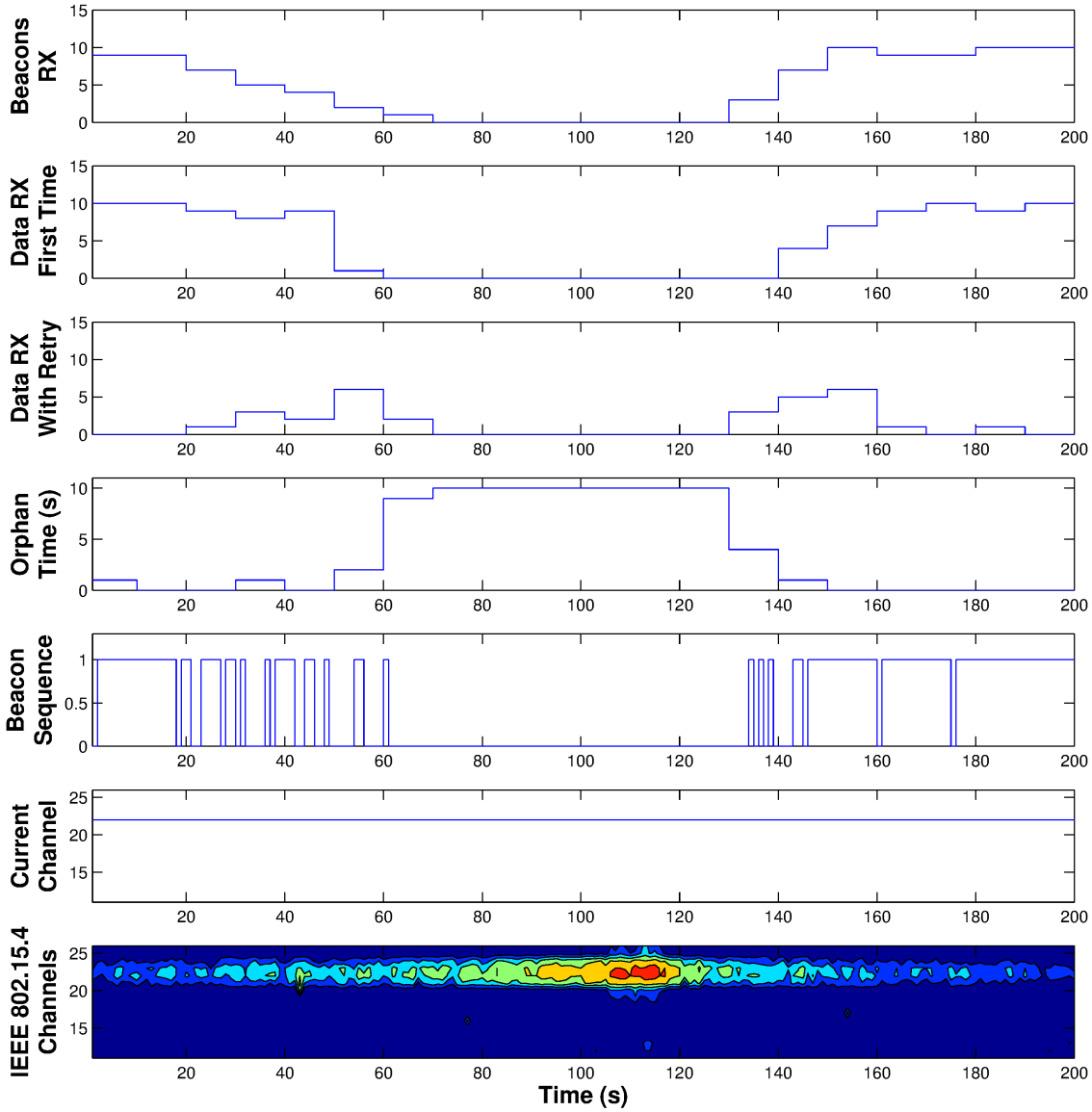

Figure 6.8.: Behaviour of the no-adaptation scheme for one interferer, first scenario.

nator. An associated sensor node must operate on the same frequency channel as its coordinator node, otherwise it would not be able to receive beacon packets. Not being able to receive four consecutive beacon packets results in node orphaning.

vii) **Channel Hops**: This shows the sequence in which the sensor node scans the channel(s) to discover its corresponding coordinator node after being orphaned.

viii) **Channel Switches**: This shows channels that the sensor node switches in

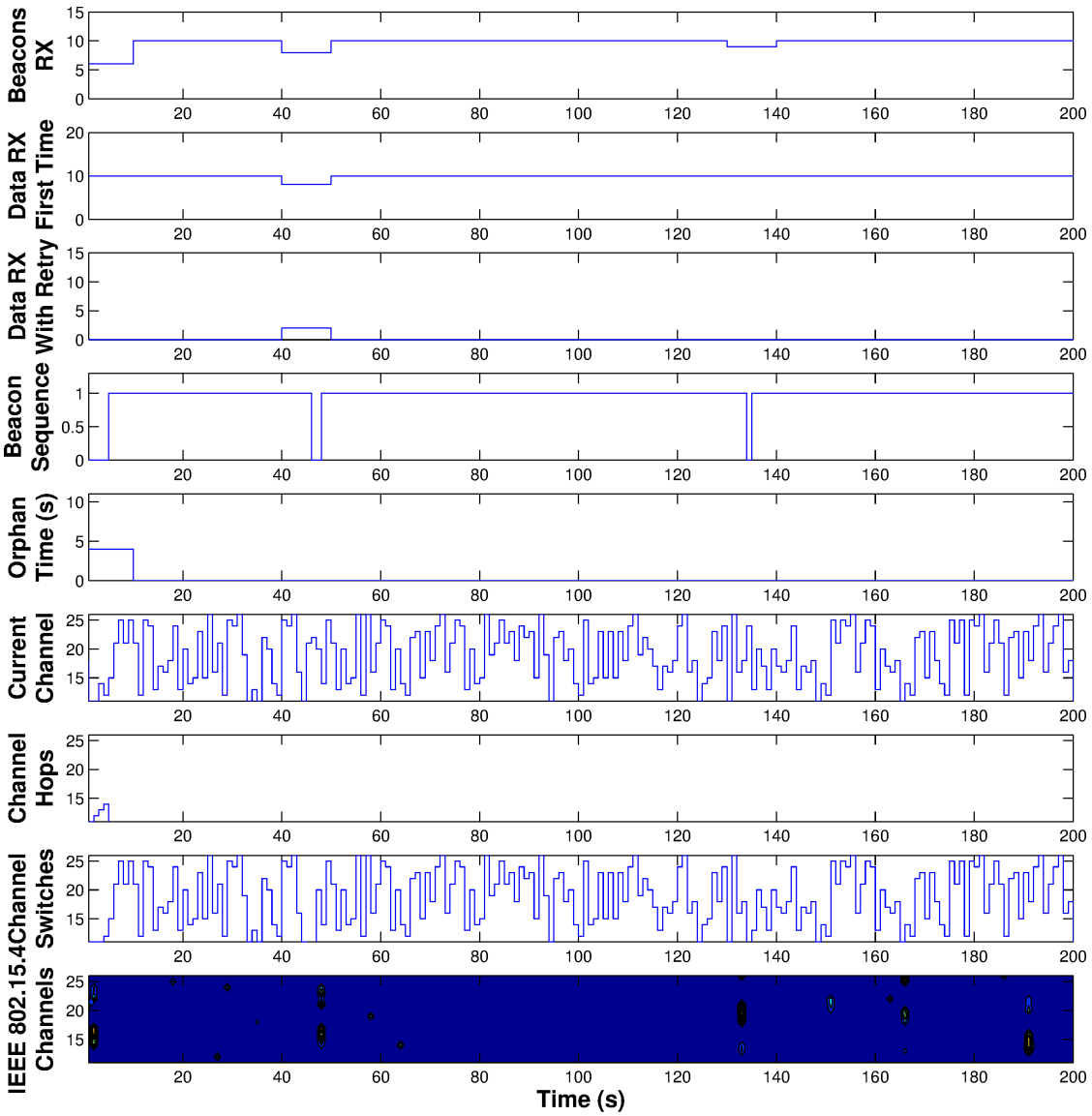

Figure 6.9.: Behaviour of the periodic-random-1 scheme for zero interferers, first scenario.

order to maintain synchronisation with its coordinator node.

ix) **IEEE 802.15.4 Channels**: Displays the spectrum utilisation (RSSI level) measured by the Wi-Spy spectrum analyser, over time.

Considering the no-adaptation scheme illustrated in Figures 6.7 and 6.8, it could be seen that adding one interferer already impacts many performance parameters significantly. As the WBSN approaches the interferer, fewer beacons are received, more data packets are lost or need re-transmissions. Furthermore, the time that is

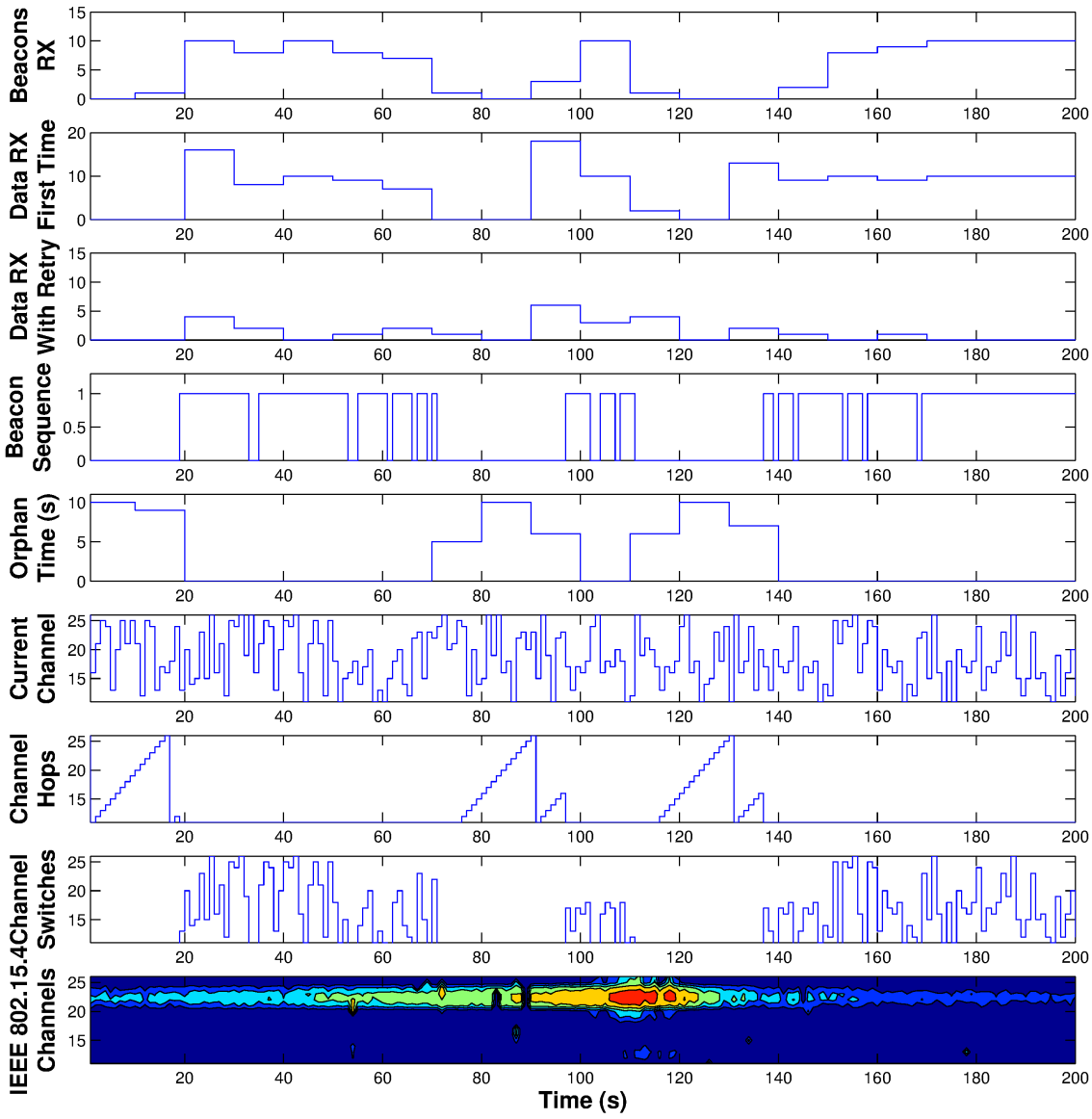

Figure 6.10.: Behaviour of the periodic-random-1 scheme for one interferer, first scenario.

spent in the orphan state is significantly increased as the WBSN passes the interference source. This behaviour is predictable since the coordinator node remains on the same predefined channel (Channel 22) and the WiFi AP is configured to operate in an overlapping channel (Channel 11).

For the periodic-random-1 scheme displayed in Figures 6.9 and 6.10, the coordinator randomly jumps over all 16 channels. After the sensor node becomes orphaned (and at start-up), it scans through all available channels to find the coordinator

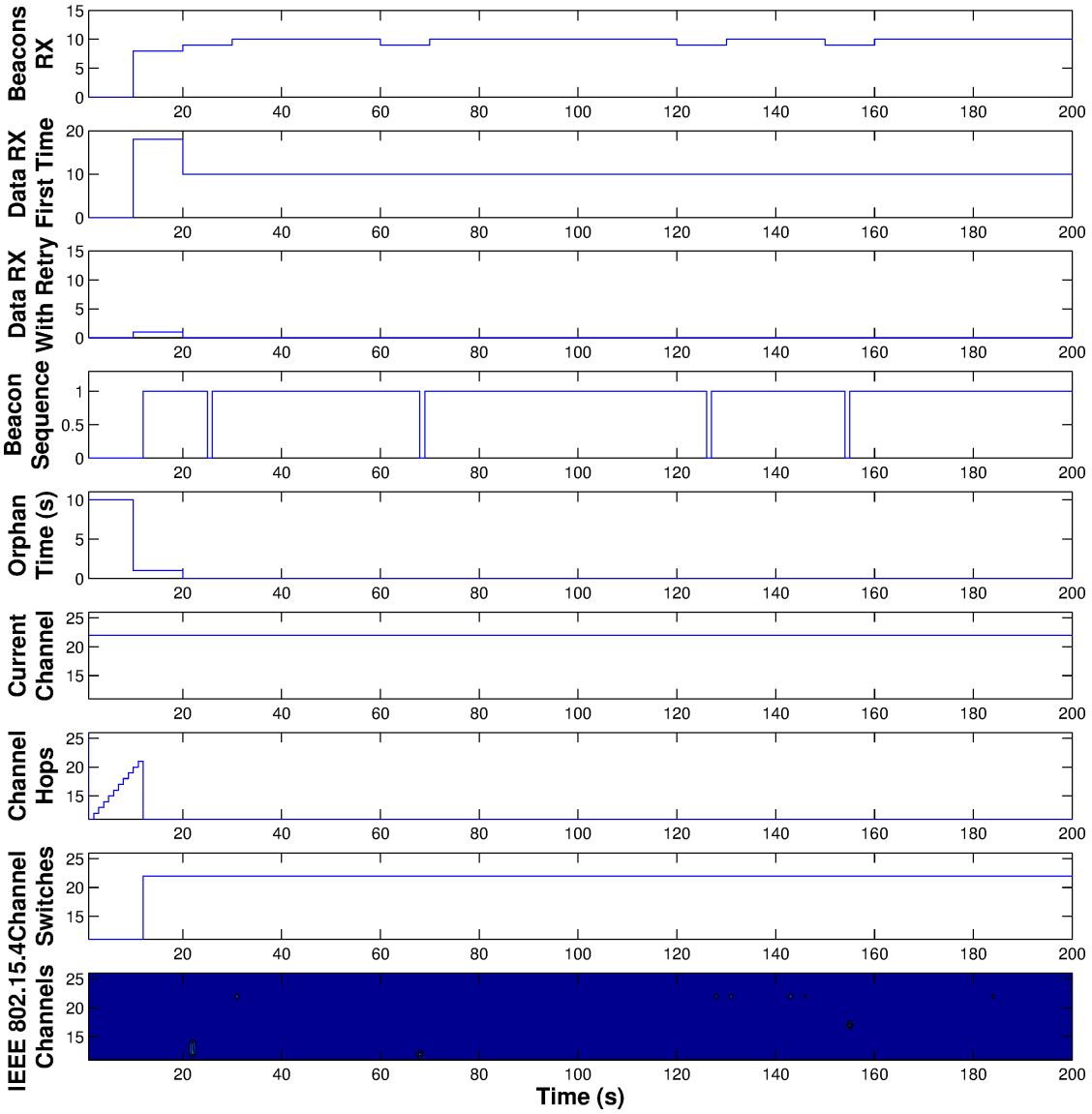

Figure 6.11.: Behaviour of the Lazy scheme for one interferer, first scenario.

(see curve for channel hops). The main disadvantage of periodic-random-1 scheme in comparison with the no-adaptation scheme is the long duration needed for the sensor nodes to discover their corresponding coordinator node. This is mainly due to the unpredictable randomness of this scheme. The no-adaptation scheme does not have this problem, however for the whole duration that the sensor is in close proximity to the interference source it is unable to re-establish its connection to its coordinator node. On the other hand, the periodic-random-1 scheme may resume its communication on other channels with low-interference.

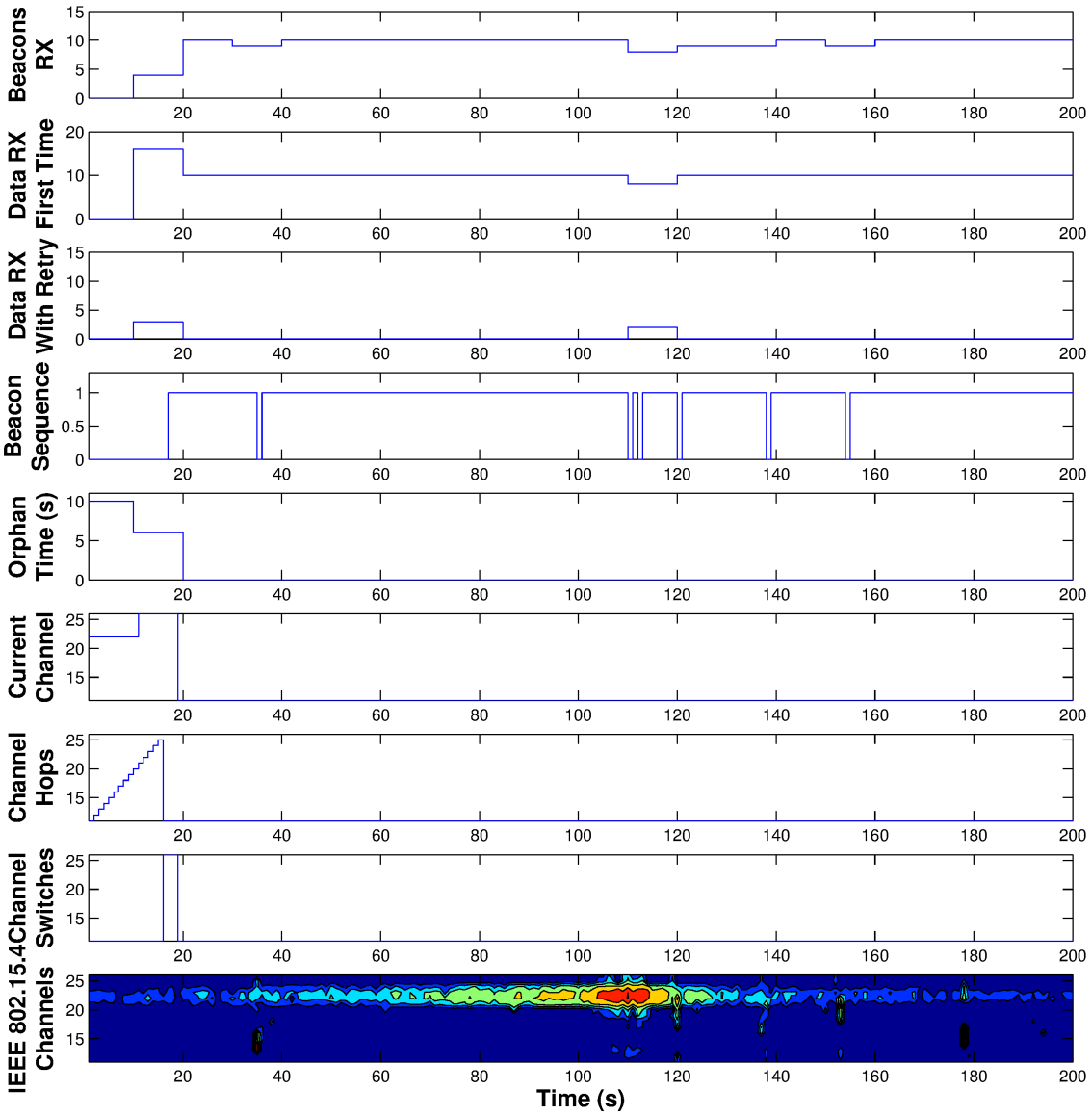

Figure 6.12.: Behaviour of the Lazy scheme for one interferer, first scenario.

Finally, in the Lazy scheme, shown in Figures 6.11 and 6.12, channel search occurs only once (at start-up) and, aside from this initial search, no time is spent in the orphan state. This is for both cases where there is zero and one interferer active. The main reason is that the Lazy scheme detects the noise level of the current channel and, if the measured RSSI value of the current channel exceeds the predefined threshold (of -90 dBm), it selects a channel with the lowest noise and switches to that channel. The coordinator discovery time for the case with one active interferer, is slightly longer, as compared to the case of zero interferers. This is due to the

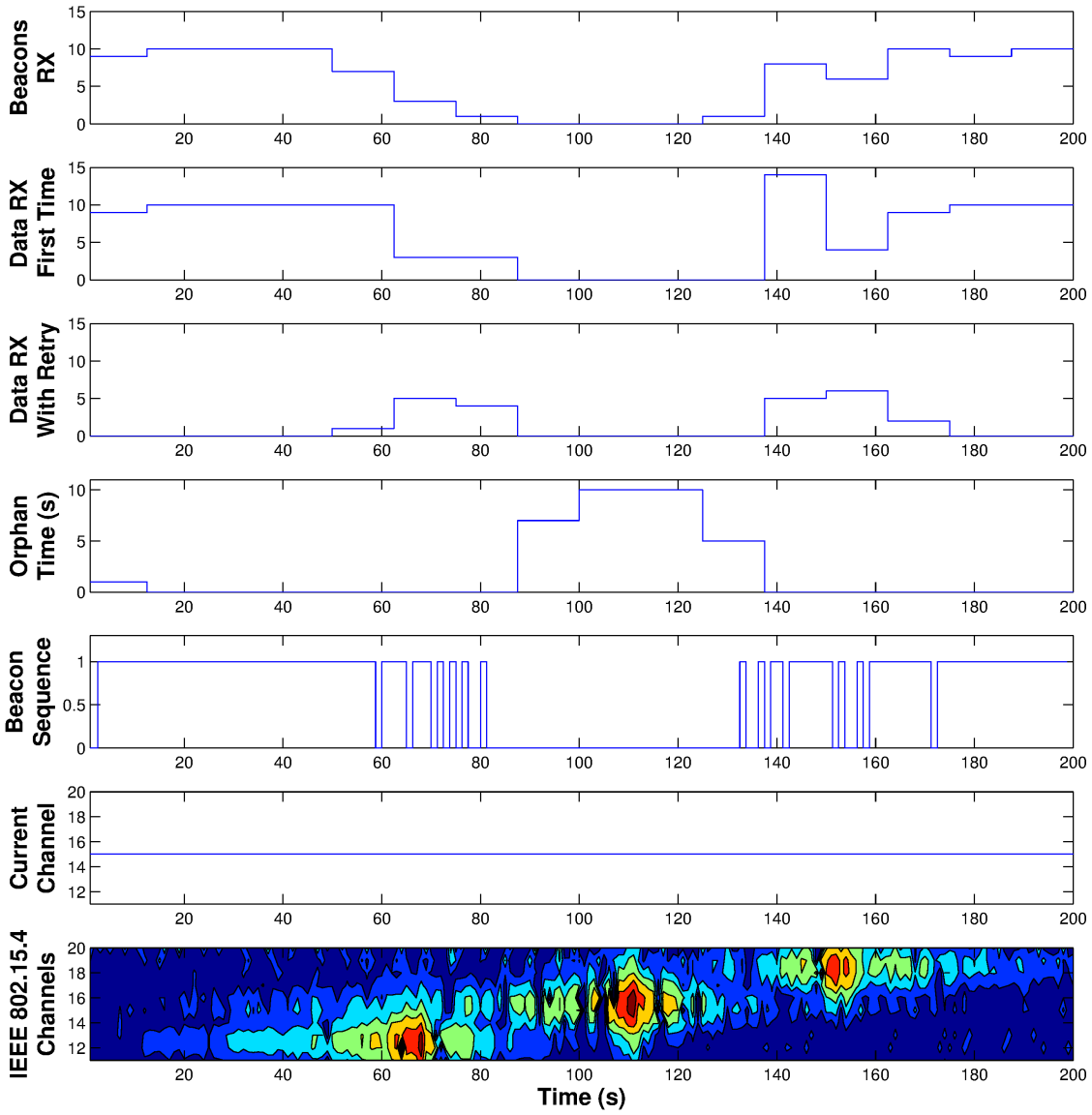

Figure 6.13.: Behaviour of the no-adaptation scheme with three interferers, second scenario.

coordinator's start-up phase.

In the second scenario, the no-adaptation scheme is mainly affected by one of the interferers (the middle one operating on channel 3). Figure 6.13 looks similar to the one for the first scenario (see Figure 6.8). However, looking closer, it could be seen that as the WBSN passes the other two interferers, at 60 and 150 second the number of data packets transmitted successfully after the first try drops significantly. One explanation could be the adjacent interference caused by the WiFi side-bands.

In the second scenario, the periodic-random-1 scheme is much more badly affected

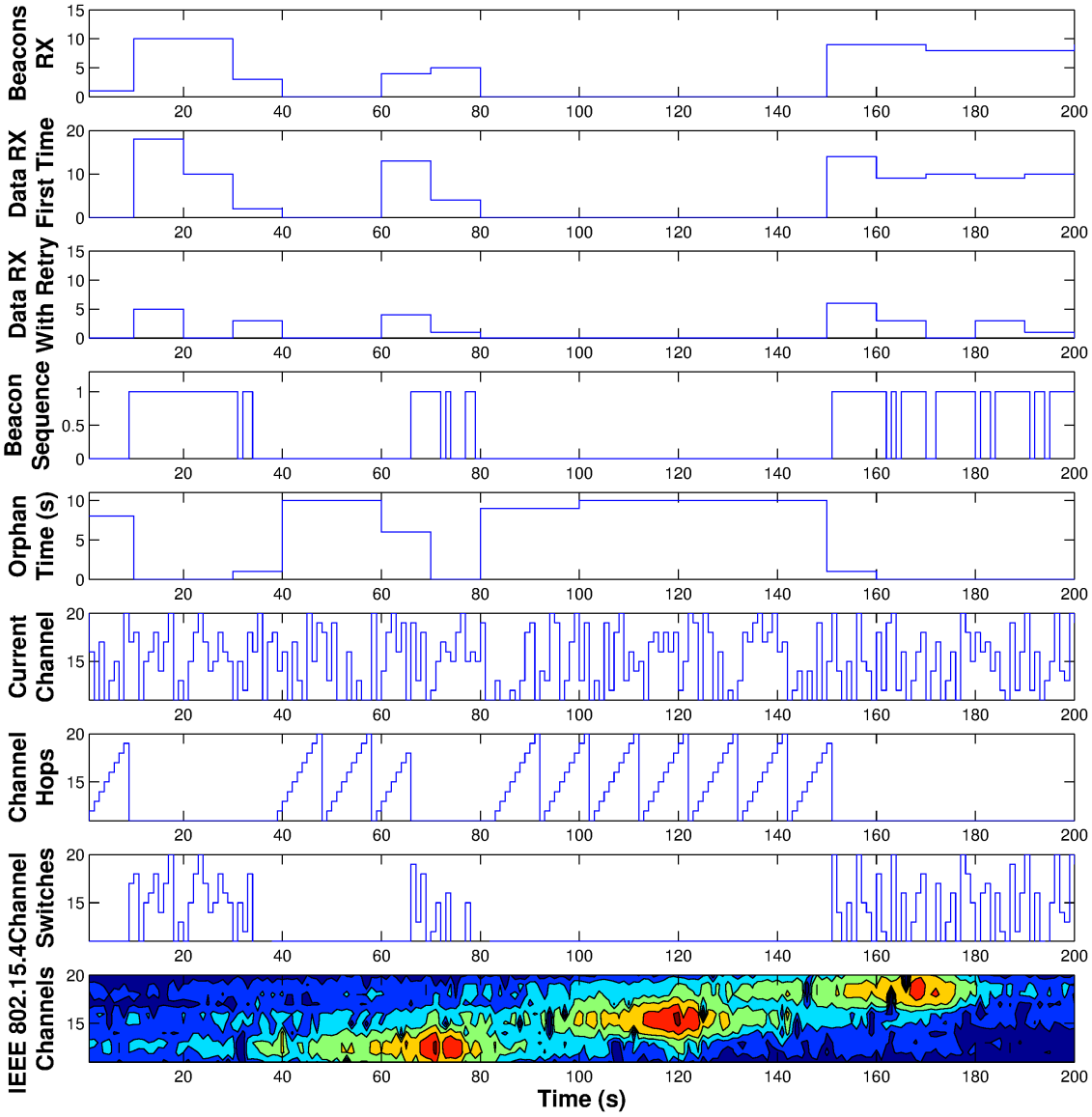

Figure 6.14.: Behaviour of the periodic-random-1 scheme with three interferers, second scenario.

than in the first scenario, especially when looking at the time spent in the orphan state (see Figures 6.10 and 6.14). This is mainly because it effectively suffers from interference for a much larger proportion of its path. After losing synchronisation, sensor nodes start performing their normal[3] scanning routine[97, Sec. 7.5.2.1.3]. Therefore, due to the coordinators unpredictable behaviour, the sensor node has

[3]To further improve this scheme, information related to the seed number and next channel hop can be used. Although, in scenarios with low to medium interference improving the coordinator discovery process might improve both success rate and energy consumption of the sensor nodes, in scenarios with high interference this improvement is negligible (see Chapter 5).

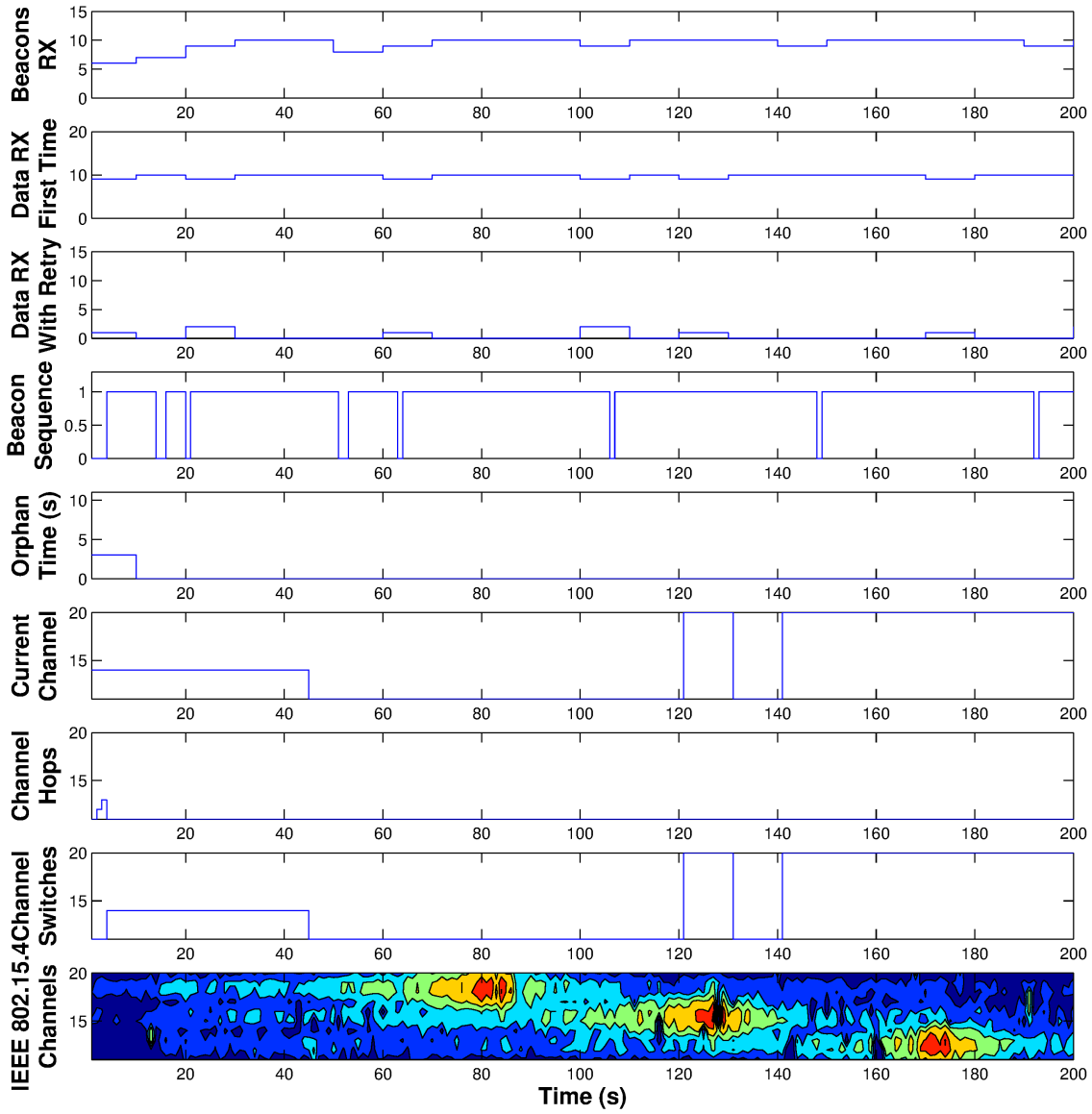

Figure 6.15.: Behaviour of the Lazy scheme with three interferers, second scenario.

difficulties finding and re-associating with its corresponding coordinator. One possible solution could be for the sensor node to measure the energy level of all available channels and remain on the channel with the lowest interference, waiting for its coordinator to randomly switch to that channel, instead of sequentially scanning all available channels.

Finally, when looking at the behaviour of the Lazy scheme in the second scenario shown in Figure 6.15, it can be seen that it manages to change its channel according to its relative position with respect to the interferers. At 45 meter distance the coor-

dinator chooses a channel that avoids the first and second interferer well (switching from channel 14 to 11). However, when the WBSN comes at close proximity to the second interferer, the adjacent channel interference triggers the coordinator to switch channel (jumping to channel 20). The side bands of the second interferer also trigger the coordinator at channel 20. However, the process of detecting interference and informing the sensor nodes about the next best channel takes time, reducing the amount of channel switching. After switching back to channel 11, the WBSN collides with the third interferer on this channel and changes again. Overall, the Lazy scheme manages to maintain a very good packet success rate. Unlike the first scenario (see Figure 6.12), in this scenario the interference free channel was eliminated and the Lazy scheme needed to make more channel switches. The false positive trigger that created the ping-pong effect at 120 and 130 second could be further limited by increasing the threshold value of -90 dBm.

6.5. Discussion

The behaviour of the two frequency adaptation schemes (Lazy and periodic-random-1 scheme) compared with the no-adaptation scheme is demonstrated in this chapter. This study was carried out under two real-life experimental scenarios. The results reveal that the Lazy scheme outperforms both the periodic-random-1 and the no-adaptation schemes in terms of success rate and percentage of time without PAN. As mentioned earlier in Section 4.3.2, the percentage of time without PAN has a direct relationship with energy consumption of the sensor node. Therefore, as illustrated in Figure 6.6, the Lazy scheme has the lowest percentage of time without PAN[4] when faced with interference. However, it is observed that in scenarios with no interference the no-adaptation scheme outperforms the two frequency adaptation schemes in terms of both success rate and energy consumption. This is mainly

[4]Percentage of time without PAN has a direct relationship with the energy consumed by the sensor node. Therefore, the lower the percentage of time without PAN the less energy consumed by the sensor nodes.

due to the extra initial scanning phase that is required at the start-up. This small advantage would be negligible for longer experimental runs.

In summary, the results assert the feasibility of implementing the proposed schemes on commercially available WSN nodes and reassure the validity of our simulation results by observing the same qualitative trends under real WiFi interference. The next chapter explores the impact of transmit-power on the performance of WBSNs in varying interference scenarios.

7. The Influence of Transmit-Power on Performance

Previous chapters explored the performance benefits of frequency adaptation in isolation – by keeping the transmit-power fixed to the minimum – in densely populated urban environments where WBSNs are faced with an ever changing WiFi "interference landscape". In this chapter the influence of transmit-power on performance is explored. This exploration is subdivided into three main parts. The potential benefits of varying transmit-power settings with the no-adaptation scheme are explored first in varying interference conditions. Next, frequency adaptation under different transmit-power settings is explored. Finally, a joint transmit-power and frequency adaptation scheme is considered. A subset of the results presented in this chapter has been published in [175, 176].

7.1. Considered Schemes

7.1.1. Baseline Schemes

Two baseline schemes are considered in this chapter, namely the **no-adaptation_Low** scheme and the **Lazy_Low** scheme.

The **no-adaptation_Low** scheme is the same no-adaptation scheme as intro-

duced and used in Section 4.1.1. The suffix "Low" indicates that the lowest transmit-power level (-25 dBm) is being used for all sensors and the coordinator node. This scheme represents the default IEEE 802.15.4 standard – previously described – without any modification. This baseline scheme represents the lower bound of what is achievable in the absence of both transmit-power and frequency adaptation.

The **Lazy_Low** scheme is the second baseline scheme that represents the lower bound of what is achievable if frequency adaptation is enabled. However, in order to see the performance gain of frequency adaptation in isolation, the lowest transmit-power level is used for this scheme, hence the addition of the "Low" suffix – all devices (sensor and coordinator) are configured to transmit packets at -25 dBm transmit-power level. For a more detailed description of the Lazy scheme see Section 4.2.2.

7.1.2. Transmit-Power Variation Schemes

A set of schemes are proposed with both uniform and non-uniform transmit-power allocation in the absence and the presence of frequency adaptation.

no-adaptation_High This scheme represents the upper bounds of what is achievable in terms of success rate if an ideal transmit-power adaptation scheme is proposed. Similar to the genie scheme proposed in Section 4.1.2, this scheme is included to show the possible performance gains of transmit-power adaptation in varying interference scenarios. In this scheme the transmit-power of all sensor and coordinator nodes is fixed to the maximum transmit-power level of the CC2420 transceiver (0 dBm).

Lazy_High This scheme is proposed to represent the upper bound of coupling transmit-power with frequency adaptation. The transmit-power of all sensor nodes including the coordinator is fixed to 0 dBm. This has been included to illustrate the potential performance gains of these two schemes in terms of success rate.

no-adaptation_Sensor_High and Lazy_Sensor_High In these schemes the sensor nodes are configured to transmit packets at their maximum transmit-power level (0 dBm), while the coordinator is fixed to its lowest transmit-power level of -25 dBm. For applications where sensor nodes periodically generate critical human vital signs, data reliability and timely transfer of information is of utmost importance. These scheme are proposed in order to increase the successful transfer of data from the sensor node to its corresponding coordinator node and at the same time reduce the overall energy consumption of the network. It is expected that by increasing the transmit-power level to maximum, data packets have a higher chance of successfully being received by the coordinator. Although the calculation of success rate also involves a successful reception of acknowledgement packets, since these packets are small (only 5 bytes[1]), they still have a higher success rate than data packets with medium to large payload size. For more information regarding the claim that packets with small payload have higher chance of being successfully received in scenarios with varying interference density and intensity see Appendix C.

no-adaptation_Coordinator_High and Lazy_Coordinator_High Opposite to the two previously mentioned schemes, these schemes maintain the default low transmit-power (of -25 dBm) for the sensor nodes and only increase the transmit-power level of their coordinator node to the maximum (0 dBm). The idea behind proposing these schemes is to increase the chance of beacon reception for both the no-adaptation and Lazy schemes. In Chapters 4 and 5, it has been mentioned that one of the main causes of increased energy consumption in sensor nodes is that the sensor nodes lose their synchronisation with the corresponding coordinator node and become orphaned. By increasing the chance of beacon reception these schemes are expected to increase the sensor

[1]An acknowledgement packet consists of a MAC header (Frame Control and Sequence number fields) and the CRC checksum field (not including the synchronisation and physical headers).

node lifetime, while maintaining an acceptable success rate.

7.1.3. A Joint Transmit-Power and Frequency Adaptation Scheme

The **Adaptive-Lazy** scheme enhances the lazy scheme by enabling transmit-power adaptation. In the absence of interference this scheme uses the low transmit-power level and switches to the highest transmit-power when interference emerges. The decision is made by the coordinator and communicated to the sensor nodes as part of the beacon payload. The restriction to only two considered power levels (lowest and highest) simplifies implementation and requires the addition of only one bit in the beacon payload. Currently the lazy scheme uses a noise-level threshold of $n_l = -90$ dBm as the threshold point – for noise levels below this value, the coordinator stays on the same operating channel. A second threshold $n_h \geq n_l$ is proposed which changes the decision rule as follows:

i) When the noise level n on the current channel is below the low threshold (i.e. $n \leq n_l$), the network remains on the current operating channel and uses the lowest transmit-power level (this will be signalled in the beacon packet by setting a flag to FALSE);

ii) when the noise level n is between the lower and the higher threshold (i.e. $n_l < n \leq n_h$) the network still remains on the same operating channel; however, it uses the highest transmit-power (this will be signalled in the beacon packet by setting a flag to TRUE);

iii) and when the noise level n is larger than the higher threshold (i.e. $n > n_h$), the network uses the highest transmit-power level, but also it would prepare to switch to a better channel, if there is one (this will be signalled in the beacon packet by keeping the flag to TRUE and adding information regarding the next channel index and the offset before the channel hop).

The choice of transmit-power on the new channel follows the same decision rule. The results shown in this chapter use a simplified version of this scheme, where $n_l = n_h = -90$ dBm. With this assumption the network remains on the current operating channel and operates with the lowest transmit-power level as long as the noise level n is below the threshold. When the noise level n is larger than the threshold, the network operates at its highest transmit-power level and spontaneously starts the channel switching process. During the four[2] super-frames that are required to inform the sensor nodes before switching the operating channel, both sensors and the coordinator node continue their transmissions with maximum transmit-power level. After the channel switch is made, depending on the noise level of the new operating channel the coordinator decides whether to allow the network to operate at its lowest or highest transmit-power level.

7.2. Simulation-Based Performance Evaluation

The same simulation scenario as used in Chapters 4 and 5 is considered in this chapter. The schemes described in Section 7.1 are evaluated for an average number of WiFi interferers of $\Delta = 10, 50, 100, 200$ and 300, and traffic intensities of $\lambda = 0\%, 10\%, 20\%, ..., 70\%$. Furthermore, since for a given transmit-power level the energy consumption of the sensor node(s) depends directly on the data generation rate, the performance benefits of transmit-power variation for different data generation rates are also considered, namely when data packets are generated with periods of 1, 0.5, 0.25 and 0.125 second, respectively. The data packet generation period of 0.125 second is used to clearly show the impact of load on the energy consumption. For this data generation period only one sensor node is used. This choice allows us to see the changes in the energy consumption as the interference varies, whereas with more sensors and a data generation period of 0.125 second, the energy consumption would also be influenced by increased levels of MAC contention (time spent in the

[2]see *initialSwitchCount* parameter in Section 3.5

back-off periods).

For each parameter set (Δ, λ and data generation rate), sufficient replications have been performed to reach a maximum relative confidence interval half-width of 5% or less at a 95% confidence level for the success rate. In each replication a new WiFi deployment is generated and the WBSN moves exactly once from its starting position in the playground to its end position. The performance results obtained from each replication are averaged over all replications and those averages are reported.

7.2.1. Performance Metrics

To compare and evaluate the different proposed schemes with each other two main performance measures are considered. These performance measures have been previously explained in Section 1.5.1. The **Success Rate** is defined as the average (taken over all sensors) percentage of uplink packets that the coordinator has successfully received (possibly after some retransmissions) and for which the sending device has received an acknowledgement. The **Consumed Energy** is the average energy consumed by the transceiver as the carrier walks once from the left to the right side of the field.

7.3. Performance Benefits of Transmit-Power Variation in Isolation

Our first set of results illustrates the performance benefits of transmit-power variation compared with the baseline schemes. Figure 7.1b shows the success rate of the sensor nodes for varying interferer density ($\Delta = 10, 50$ and 100), and traffic intensity λ when sensor nodes generate data packets every second. It can be seen that overall the Lazy_Low scheme has a substantial advantage over the no-adaptation_High and no-adaptation_Low scheme. Observing the no-adaptation scheme, the advan-

tage of using a high transmit-power in terms of success rate vanishes quickly as λ is increased. This trend further increases as the average number of interferers grow. Furthermore, as our results in Figure 7.1b indicate, frequency adaptation overall has much more impact on success rate performance than using the highest transmit-power, maintaining an approximate 99% success rate at $\lambda = 70\%$ for $\Delta = 10$, and over 80% success rate when Δ is increased to 100 at $\lambda = 70\%$.

Figure 7.1a compares the no-adaptation_High scheme with the baseline schemes in terms of consumed energy of the sensor nodes. The energy consumption for the coordinator does not offer any surprises. The coordinator node using the no-adaptation_Low scheme consumes roughly 15 Joule for varying values of λ and Δ. For similar conditions the no-adaptation_High scheme consumes 0.1 Joule more than the no-adaptation_Low scheme and the Lazy_Low scheme consumes just over 24.5 Joule. However, on the sensor side it is actually better to use the frequency adaptation scheme than both variations of the no-adaptation scheme. Looking closer at Figures 7.1a and 7.1b suggests that if the overall network lifetime is considered (the consumed energy of the sensor nodes and the coordinator node), the additional investment in transmit-power level pays off for only scenarios with very low-interference. The 0.03 joule difference observed between the two baseline schemes (Lazy_Low and no-adaptation_Low) is likely caused by the additional coordinator discovery process that the Lazy scheme sensor nodes need to complete in order to find and associate with their corresponding coordinator node. The extra energy costs for start-up are negligible and could be ignored.

Figures 7.2, 7.3 and 7.4, illustrate the performance difference when sensor nodes generate two and four times more data packets per second. Increasing the data generation rate has a direct relationship with the energy consumption of the sensor nodes and reciprocal impact on the success rate. This difference becomes more pronounced as the interferer density grows. One reason is, as the interference increases the probability of packet loss due to external interference increases. This leads to

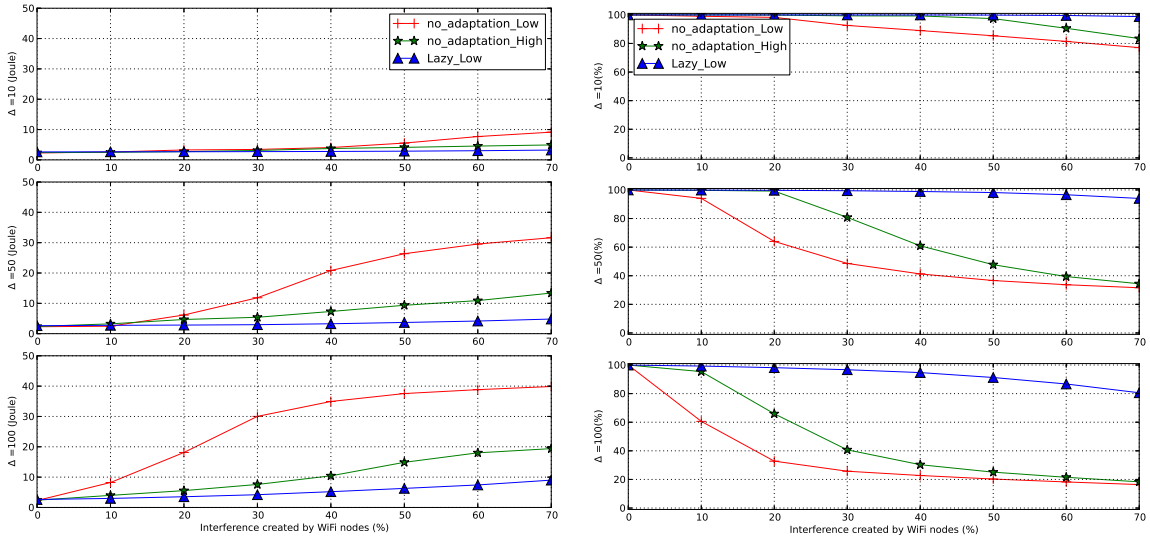

(a) Energy consumed by sensor nodes (b) Success rate

Figure 7.1.: Transmit-power variation scheme where data is generated every 1 s

increases in the number of re-transmission, which in turn leads to higher energy consumption and drop in success rate.

In the scenario where only one sensor node is introduced and a new data packet is generated every 0.125 second (see Figure 7.4), the average energy consumed by the sensor node is much lower than in scenarios with four sensor nodes and lower data generation rates. This is mainly due to the additional time the nodes spend in contention period. In order for the sensor nodes to transmit their data in the CAP period they first needed to compete for channel access with three other sensor nodes. Every time the sensor node performs a CS and the channel is busy it needs to back-off. These additional delays increase the time sensor nodes need to stay awake in the CAP period before being able to transmit their data, elevates the overall consumed energy of the sensor nodes and increases the percentage of packets dropped due to expired transactions. On the other hand, in the scenario where only one sensor node is introduced, after sending all its data packets the sensor node is allowed to go to sleep mode till the start of the next super-frame, thus saving more energy. Regardless of the data packet generation period, the frequency adaptation scheme still outperforms both no-adaptation schemes.

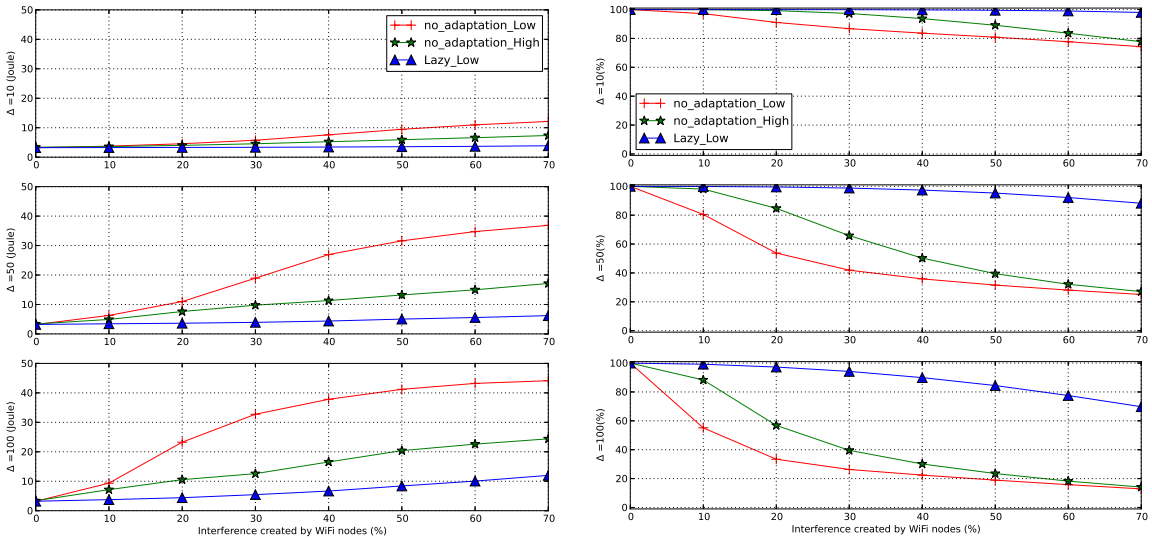

(a) Energy consumed by sensor nodes

(b) Success rate

Figure 7.2.: Transmit-power variation scheme where data is generated every 0.5s

7.4. Performance Benefits of Coupling Transmit-Power with The Lazy Scheme

In our second set of results presented in Figure 7.5, the Lazy_Low scheme is compared with Lazy_High for varying interferer traffic intensity λ and interferer density Δ. The first column illustrates the consumed energy of the sensor node, while the second column shows the success rate for the respective interferer density. The last two columns present a close-up of the consumed energy and success rate, respectively. Each of the rows in this figure represents the results for $\Delta = 10, 50, 100, 200$ and 300 starting from top to bottom.

Looking at the results it can be observed that for low interferer traffic intensity and interferer density of $\Delta = 10$, the Lazy_Low scheme outperforms the Lazy_High scheme in terms of consumed energy of the sensor node. Furthermore, no significant difference is seen in the success rate. In the scenario with $\Delta = 10$ and $\lambda = 70\%$, the success rate drops down to approximately 99.5% for both schemes, and the Lazy_High scheme on average consumes 2.92 Joule, around 0.05 Joule more energy than the Lazy_Low scheme. The energy consumption of the coordinator for the

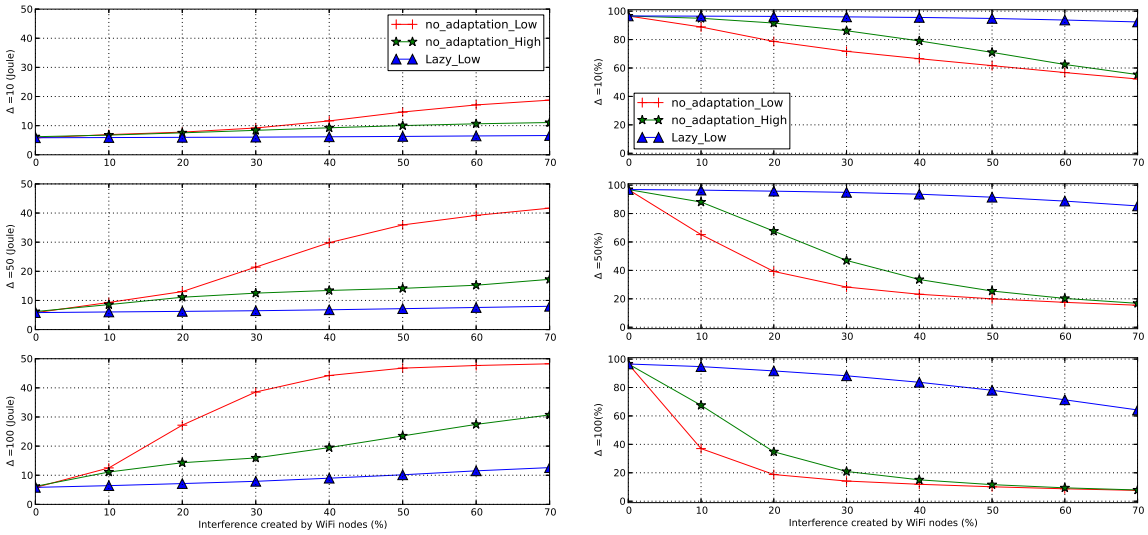

(a) Energy consumed by sensor nodes (b) Success rate

Figure 7.3.: Transmit-power variation scheme where data is generated every 0.25s

Lazy_High scheme remains roughly the same for all λ values at 24.7 Joule, about 0.07 Joule higher than for the Lazy_Low scheme.

Assuming that a typical AA battery used to power a sensor node contains approximately 10 kJ, and knowing the time duration that is needed for the WBSN to move from one side of the field to the other (864 s), the network lifetime[3] for the two proposed schemes in Figure 7.5 is calculated and shown in Table 7.1. In the scenarios with zero interference the lifetime of the sensor nodes using the Lazy_Low scheme is just under 43 days. In the same scenario, the Lazy_High scheme's sensor lifetime is more than one and half day shorter than for the Lazy_Low scheme. Nevertheless, as the interferer density and intensity increases, the lifetime of the sensor

[3]The energy consumption of other components apart from its radio transceiver is not considered in these calculations.

Δ	10	10	50	100	200	300	
λ	0	70	70	70	70	70	
Lazy_Low	1031.814	835.654	557.620	257.566	101.359	53.626	hours
Lazy_High	989.282	819.392	588.235	356.718	219.018	158.405	hours
Difference	-1.77	-0.67	1.27	4.13	4.9	4.36	days

Table 7.1.: Node lifetime

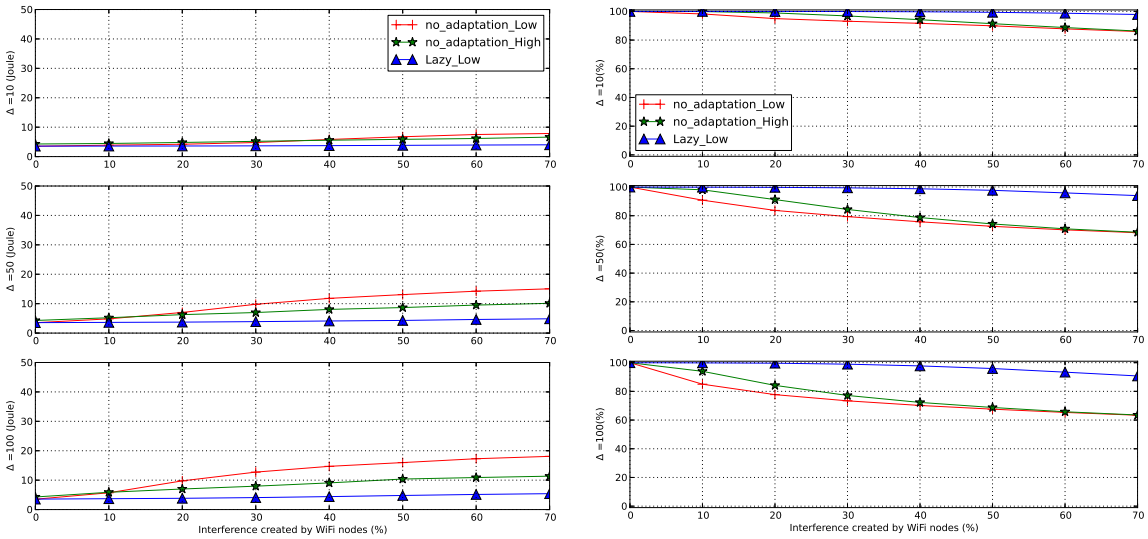

(a) Energy consumed by sensor nodes

(b) Success rate

Figure 7.4.: Transmit-power variation scheme where data is generated every 0.125s

nodes using the Lazy_High scheme is extended to just under 5 days in comparison with the Lazy_Low scheme.

Comparing the energy costs of each scheme with the maximum performance gain observed for different interference density levels in terms of success rate (see Figure 7.5) – the maximum success rate difference between the two schemes for $\Delta = 10, 50, 100, 200$ and 300 is approximately 0%, 0.2%, 3%, 8% and 17%, respectively – it is clear that partial performance gains could be achieved by coupling transmit-power adaptation with frequency adaptation, when sensor nodes are generating and sending data packets every second.

Looking at Figures 7.6, 7.7, and 7.8, where the data packet generation rate is increased to two, four and eight times per second, the success rate difference between Lazy_High and Lazy_Low gets smaller and smaller. In addition, the performance gap between the two schemes in terms of consumed energy becomes larger, to the extent that Lazy_Low has a maximum performance drop of less than 2% in terms of success rate and consumes on average around one Joule less than the Lazy_High scheme for the scenario where sensor nodes generate data packets every 0.125 second (see Figure 7.8).

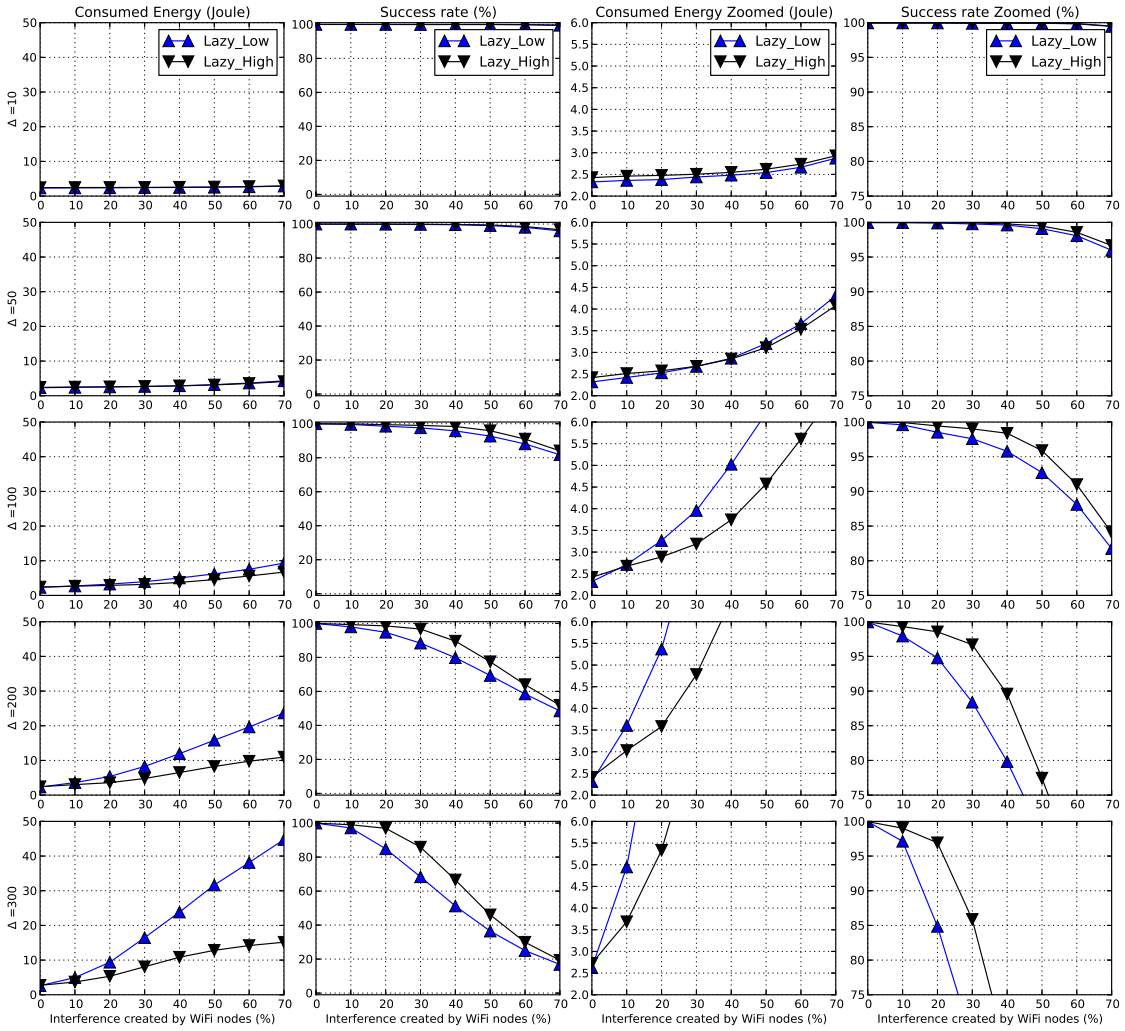

Figure 7.5.: Comparison of Lazy_High with Lazy_Low where $\Delta = 10, 50, 100, 200$ and 300

Considering the consumed energy difference between the two Lazy schemes for different interference scenarios and data generation rates, it is recommended to use the Lazy scheme coupled with transmit-power variation.

7.5. Transmit-Power Variation Schemes

The results obtained with schemes where sensors and coordinators are configured with non-uniform allocation of transmit-power are presented in this section. Figure 7.9 shows four versions of the Lazy scheme and four versions of the no-adaptation scheme for scenarios with varying interference traffic intensity and interferer density

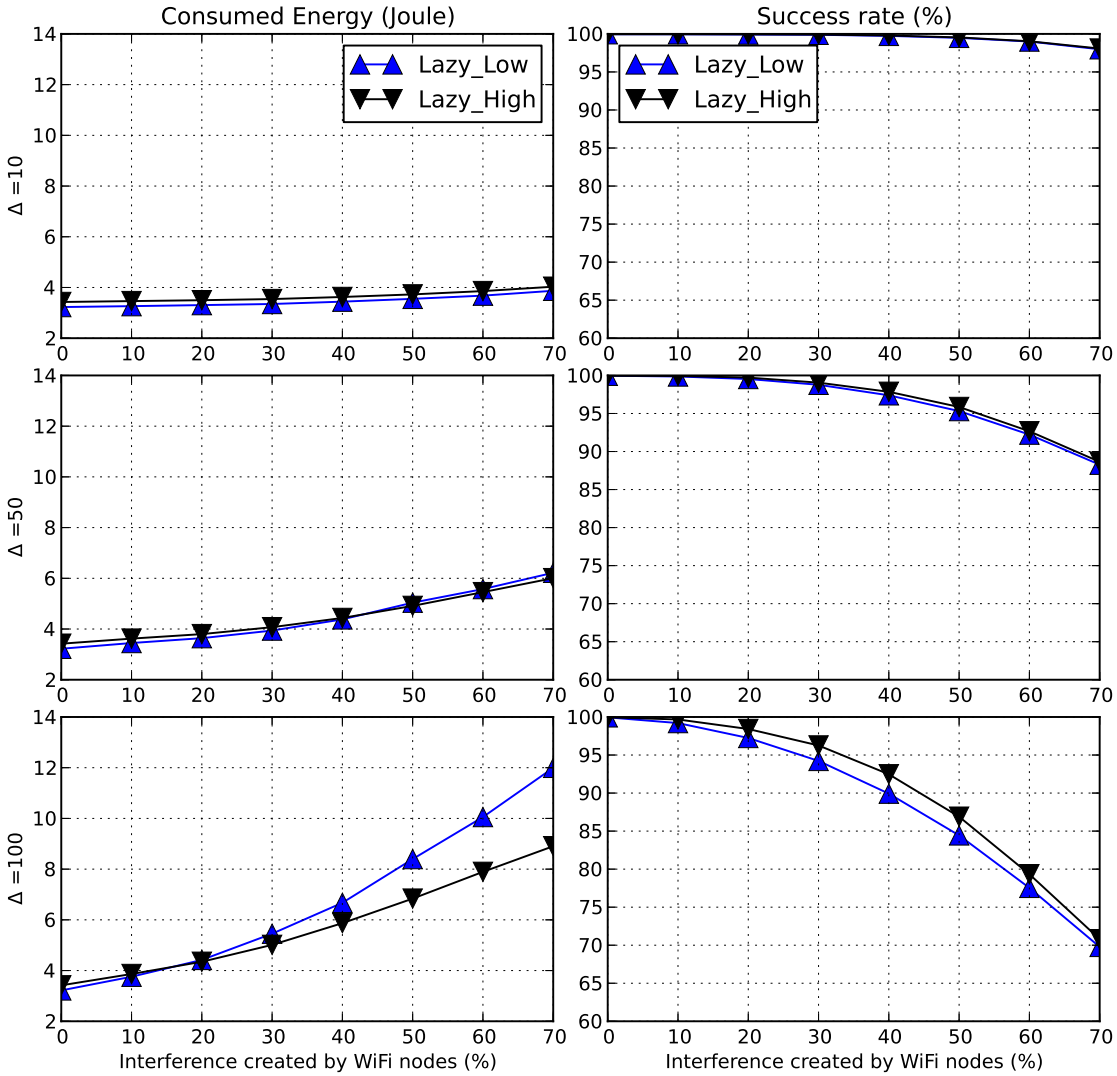

Figure 7.6.: Comparison of Lazy_High with Lazy_Low where data packets are generated every 0.5 second and $\Delta = 10, 50$ and 100

of $\Delta = 300$. For both the no-adaptation and frequency adaptation schemes it can be seen that the trends for the two non-uniform power allocation schemes stay much closer to the results obtained for the all-low power allocation than to the all-high allocation. This suggests that in order to reap most of the effects of using a high transmit-power, indeed all nodes need to use it.

Furthermore, schemes where the coordinator uses high transmit-power (for example the Lazy-high and the Lazy-coordinator-high schemes) achieve roughly the same performance in terms of consumed energy (see Figure 7.9a). The ability of the sensor nodes to maintain synchronisation with their corresponding coordinator

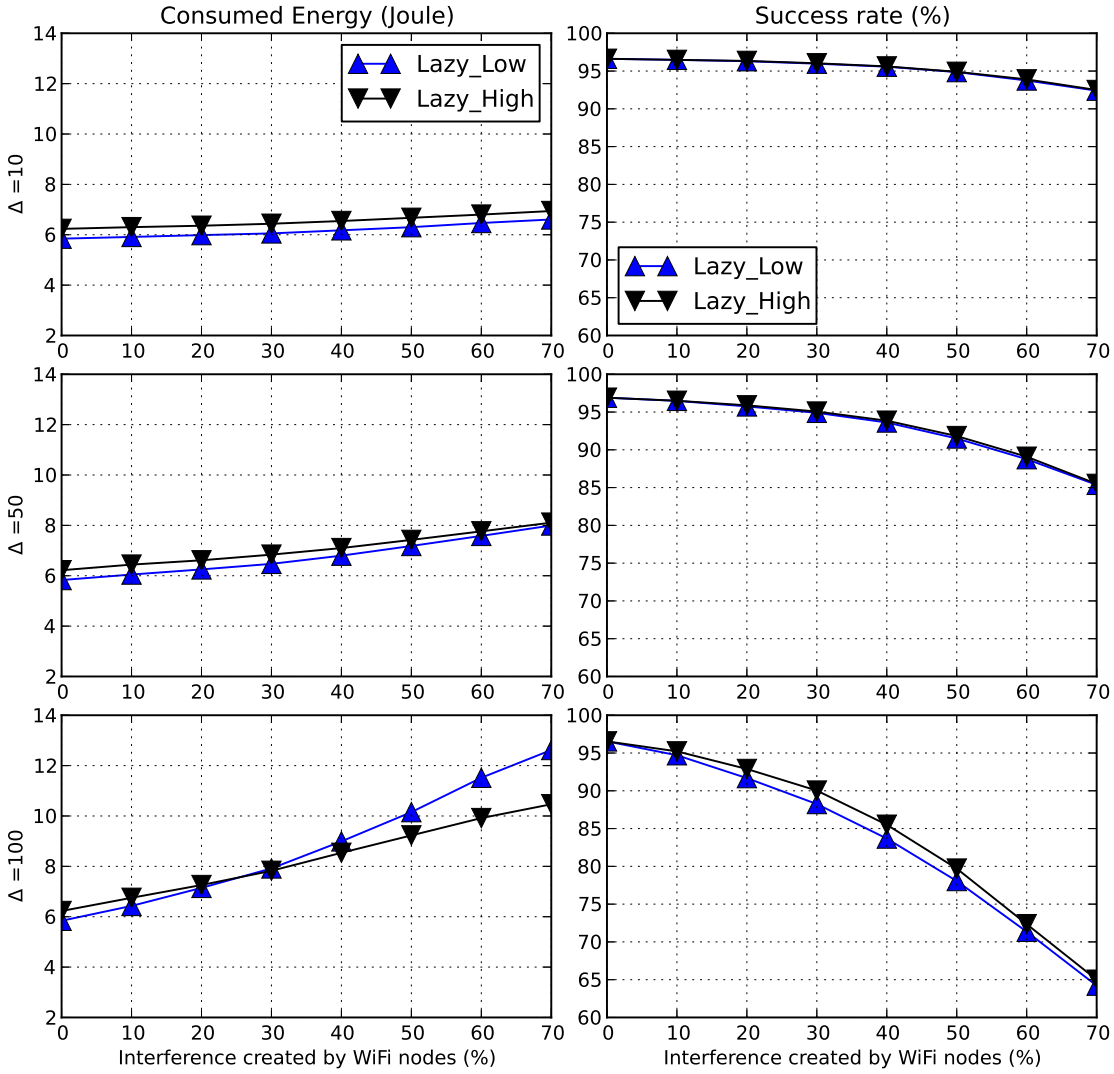

Figure 7.7.: Comparison of Lazy_High with Lazy_Low where data packets are generated every 0.25 second and $\Delta = 10, 50$ and 100

node, due to an increased probability of successful reception of beacon packets, is one explanation for the low consumed energy of these schemes.

7.6. A Joint Transmit-Power and Frequency Adaptation Scheme

In this section, the Adaptive_Lazy scheme is compared against the Lazy_Low and Lazy_High schemes shown in Figure 7.10.

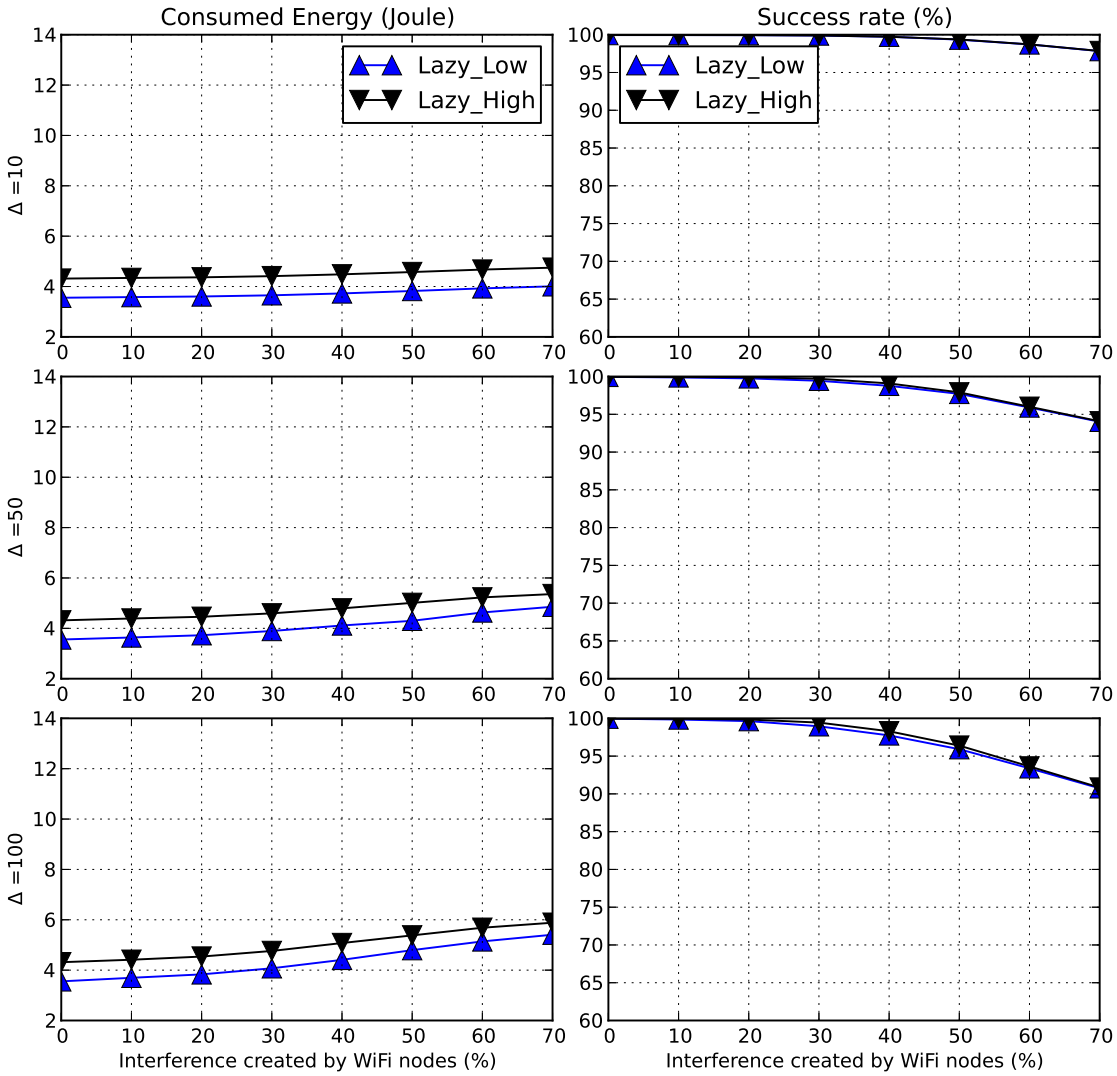

Figure 7.8.: Comparison of Lazy_High with Lazy_Low where data packets are generated every 0.125 second and $\Delta = 10, 50$ and 100

Our results indicate that clearly using the highest transmit-power level (Lazy_High) has a visible positive effect on the overall success rate of the network and that this difference grows as the data generation rate increases (see Figures 7.5, 7.6, 7.7, and 7.8). Furthermore, it has been shown that the lazy schemes have a much better success probability than the no-adaptation schemes (and the relative advantage becomes even larger when larger values of Δ are considered). Therefore, to better illustrate the advantage of the combination of transmit-power adaptation with frequency adaptation, the Adaptive_Lazy scheme is compared against the Lazy_Low and Lazy_High schemes in scenarios where data packets are generated every 0.125

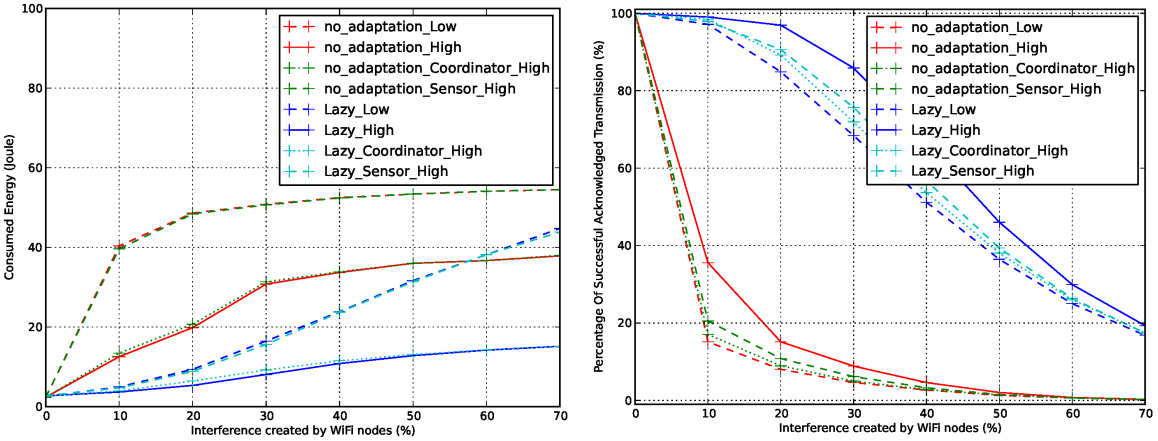

(a) Energy consumed by sensor nodes

(b) Success rate

Figure 7.9.: Percentage of energy consumed with respect to the Lazy_High scheme

second and the interferer density and traffic intensity is varied.

Figure 7.10 shows that under low to medium interference, it is better to use the Lazy-Low scheme with minimum transmit-power level rather than the maximum. On the other hand, in scenarios with high interference it is always beneficial to deploy the Lazy-High scheme. This finding is one of the motivations of proposing the Adaptive-Lazy scheme. Furthermore, for the Lazy scheme the relative influence of transmit-power is comparably small. This small difference is only distinguishable for Δ values equal to 200 and 300. The Lazy-High scheme and the Adaptive-Lazy scheme, which for these interference levels switches to the highest transmit-power, achieve a higher success rate than the Lazy-Low scheme.

The most important result though is the behaviour of the Adaptive-Lazy scheme: the results in Figure 7.10 confirm that it has virtually the same packet success rate as the Lazy-High scheme for all considered values of Δ and λ, but it has a consistently lower energy consumption than both Lazy-High and Lazy-Low. This advantage (over the lazy-Low scheme) can again be explained by savings in the number of re-transmissions in the presence of interference, whereas the savings compared to the Lazy-High scheme can be attributed to those periods of time where the WBSN experiences no interference and the Adaptive-Lazy scheme uses the lowest transmit-power. In the absence of interference the Adaptive-Lazy scheme has the same (low)

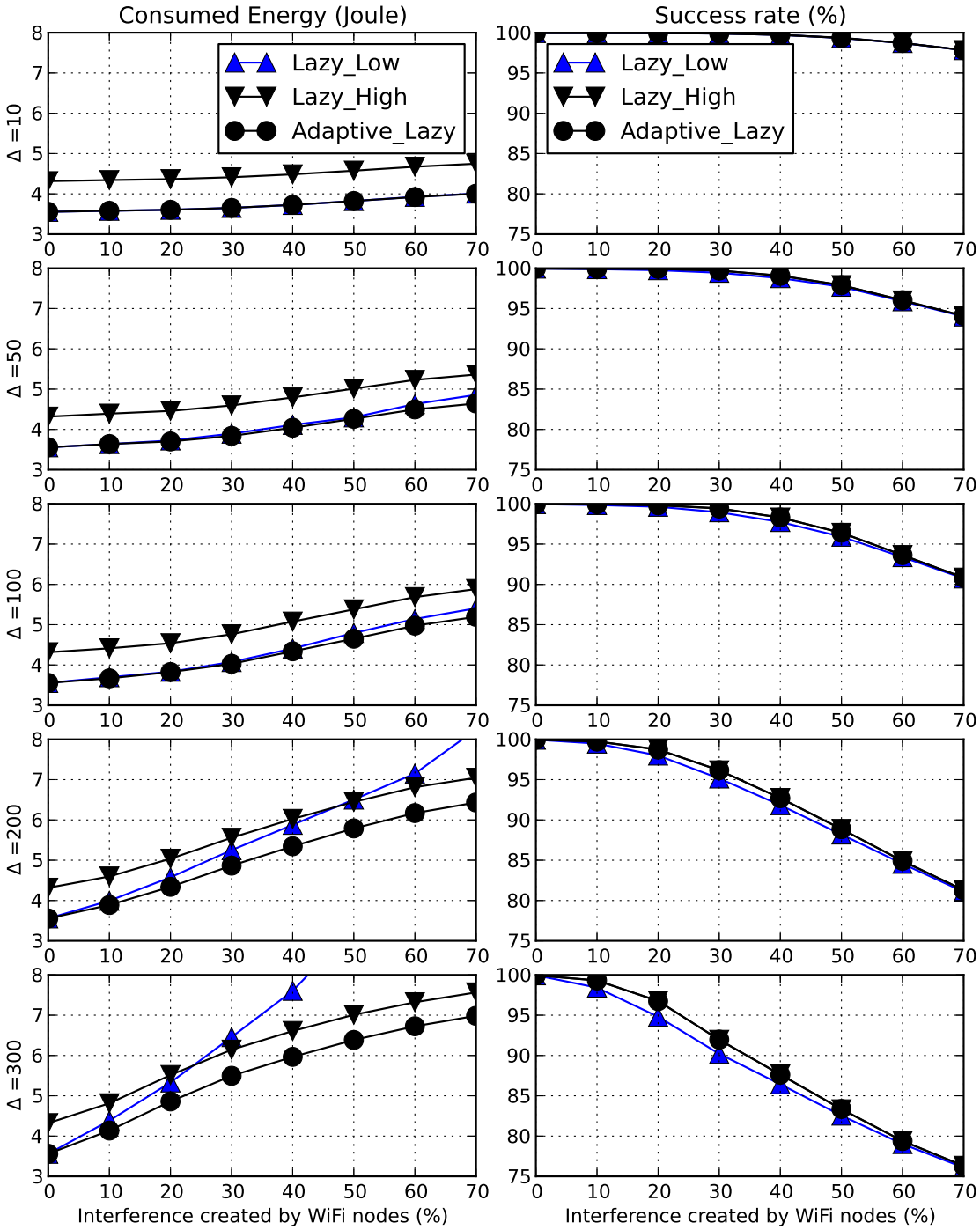

Figure 7.10.: Comparison of the Adaptive_Lazy scheme when data rate is 0.125 s

energy consumption as the Lazy-Low scheme ($\approx$ 3.5 Joule), whereas the Lazy-High scheme uses $\approx$ 4.3 Joule.

7.7. Discussion

In summary, the effects of varying transmit-power in IEEE 802.15.4 WBSNs in the absence and presence of frequency adaptation has been considered in this chapter. The transmit-power variation has been evaluated for scenarios with very light to heavy interference and for varying data generation rates. Our results indicate clearly that using a high transmit-power has a visible positive effect on the packet success rate, but overall the impact of frequency adaptation is much larger than anything that an ideal transmit-power adaptation could possibly achieve. This advantage becomes more pronounced as the interference increases. Interestingly, the same statement could not be claimed for transmit-power variation coupled with frequency adaptation. It is observed that for scenarios with low data generation rates and low-interference levels, the frequency adaptation scheme with the lowest transmit-power level consumes less energy while achieving the same success rate as the frequency adaptation scheme coupled with the highest transmit-power level. Nevertheless, the Adaptive-Lazy scheme achieves the best possible network performance in terms of both success rate and energy consumption by combining characteristics of both Lazy-Low and Lazy-High schemes for all interference scenarios. Interestingly, the Adaptive-Lazy scheme achieves this performance gain while utilising the same available information that is previously used by the Lazy scheme.

8. Conclusions

It has been shown throughout the thesis that it is possible to reach the primary goal of **maintaining a reliable data connection** between the sensor nodes and their corresponding coordinator node and **to increase the overall lifetime of the network** (by reducing the energy consumed by the WBSN nodes) by using **adaptive resource allocation** techniques in scenarios with an ever-changing interference landscape. Furthermore, practical implementation of these schemes ensured the feasibility of embedding such approaches on commercially available WBSN devices. This chapter summarises the results presented in this thesis followed by future possible research.

8.1. Results and Findings

Adaptive resource allocation for wireless body sensor networks was explored in this thesis. Since most WBSN devices are battery-powered, reducing the energy consumption has been one of the main objectives of WBSN protocol design. However, there is a trade-off between network performance in terms of data reliability and timely data transfer on the one hand and energy-efficiency on the other hand, which both are of great importance in health related applications.

This thesis examined two main resource allocation mechanisms for WBSNs in varying interference deployments, namely frequency and transmit-power adaptation. Following is a summary of some of these results and findings:

- Comparison of the three no-adaptation schemes in scenarios with interferer density of $\Delta = 10$ and 100 and for varying traffic intensity of λ, showed that networks that only use the CAP period (without assigning GTS) achieve higher success rate, while consuming marginally lower energy by the sensor nodes.

- To explore the benefits of frequency adaptation, a hypothetical scheme called the Genie scheme was proposed. By enabling all nodes in the network with oracle knowledge about the channel quality, the network with Genie scheme functionality was able to mitigate the external interference by switching the operation channel to a channel with lower noise floor. The comparison of the Genie scheme with the no-adaptation scheme in scenarios where Δ =10, 100 and 300, showed a significant improvement in terms of success rate.

- Having established the performance benefits of frequency adaptation, our first attempt to reach this goal was to propose the periodic-random scheme, which periodically switched to a random channel every hyper-frame. The results showed noticeable improvements over the no-adaptation schemes. However, this performance gain in terms of success rate was nowhere near the desired achievable performance gain of the Genie scheme. Furthermore, due to excessive channel switching of the periodic-random scheme the energy consumption of both sensor and coordinator were increased.

- In order to reduce the number of channel switches and make more intelligent decisions, a number of periodic-measurement schemes were proposed. Out of these, the periodic-measurement-MAX scheme achieved the highest success rate and outperformed the Genie scheme in both success rate (slightly) and energy consumption.

- To further improve the periodic-measurement-MAX scheme a more intelligent switching rule was proposed, which prevented the network from switching channels until the conditions of the current channel dropped below a

predefined threshold. This new scheme was named the Lazy scheme. The Lazy scheme, when compared to periodic-measurement-MAX scheme, not only achieved the same performance in terms of success rate, but also reduced the energy consumed by the sensor node via reducing the number of required channel switches.

- The proposed Lazy scheme and the no-adaptation scheme were compared in scenarios where the additional path loss created by the human body was taken into consideration. The relative performance gains of both these schemes remained the same. Although the shadowing effects had a negative effect on both success rate and energy consumption of the sensor nodes, the Lazy scheme outperformed the no-adaptation scheme in both scenarios (with and without path loss).

- Since in scenarios with high interference sensor nodes spend the most of their time in the orphan state, trying to find and re-associate with their corresponding coordinator node, a number of discovery support schemes were proposed. Our proposed Lazy-Sequence-Scan and Lazy-Heuristic-Sequence-Scan schemes were able to predict the frequency channel that the coordinator node had switched to very well. Nonetheless, due to extreme interference conditions, the proposed schemes were not able to significantly reduce the energy consumed by the sensor nodes or to increase the overall success rate.

- The behaviour of the proposed periodic-random and lazy schemes were implemented in commercially available WBSN nodes and compared with the no-adaptation scheme under real WiFi traffic. This experimental study not only verified our simulation results, but also reassures the feasibility of our proposed approaches on commercially available sensor devices.

- To explore the benefits of transmit-power adaptation in isolation from frequency adaptation and in scenarios with varying interferer density and data

generation rate, the no-adaptation scheme with minimum and maximum transmit-power levels was compared with the Lazy scheme with minimum transmit-power. These comparisons revealed that frequency adaptation schemes in isolation can outperform transmit-power adaptation schemes.

- When frequency adaptation is coupled with transmit-power variation, our results showed that for scenarios with medium to high interference the Lazy scheme coupled with maximum transmit power achieves higher success rate and consumes lower energy at the sensor side when compared with the Lazy scheme coupled with minimum transmit power. However, for scenarios with zero to low interference the Lazy_Low scheme out performed the the Lazy scheme coupled with maximum transmit-power.

- The previous findings motivated us to experiment with other combinations of transmit-power allocation schemes. Schemes which allocated maximum transmit-power for their sensor nodes achieved higher success rate at the cost of higher energy consumption at the sensor side, while schemes which allocated maximum transmit-power for the coordinator nodes were able to maintain a reasonably high success rate while reducing the energy consumed by the sensor nodes.

- Finally, a joint transmit-power and frequency adaptation scheme was proposed, called the Adaptive_Lazy scheme. This scheme utilised the existing information gathered for channel switching in order to adapt the transmit-power of the network between maximum and minimum transmit-power levels. The results showed noticeable improvement in terms of energy consumed by the sensor nodes, while maintaining the best success rate compared with Lazy_High and lazy_Low.

8.2. Evaluation of The Hypotheses

By using simulation and experimentation, this thesis answers the following hypotheses stated in Section 1.5.2:

- **Hypothesis 1**: By adaptively changing the current operating frequency of the WBSN to a channel with lower interference in environments with rapidly changing interference background, despite the energy costs of adaptation and the increasing risk of node orphaning, the performance measures **can** be improved significantly.

- **Hypothesis 2**: By introducing channel adaptation schemes the risk of node orphaning increases. Shortening this period would enhance the network performance. However, in high-interference environments, utilising more complex coordinator-discovery techniques **do not** result in a shorter average node-orphaning duration.

- **Hypothesis 3**: Frequency adaptation schemes **can** outperform any ideal transmit-power adaptation schemes in isolation when faced with external interference.

- **Hypothesis 4**: Joint transmit-power and frequency adaptation schemes in environments with varying WiFi interference **can** significant improve the network performance when compared with either of them individually.

8.3. Future Works

The groundwork described in this thesis will pave the way for a multitude of future explorations; some of these are suggested as follows:

- One of the important aspects in designing a robust protocol is when energy-heterogeneity in the network is not managed evenly. This would result in

shorter lifetime for a subset of devices and longer lifetime for others. In our case, the coordinator takes the responsibility of scanning all available channels, while this task could potentially be assigned to the sensor nodes, increasing both the speed of channel estimation and increasing the overall network lifetime.

- It is also interesting to see how the proposed schemes could be added to the IEEE 802.15.6 standard. Furthermore, would similar outcomes be achieved as illustrated in this thesis?

- Currently, the assumption of this thesis is that the WBSN is configured in a one-hop star topology. It would be interesting to see how the proposed schemes could be improved to address multi-hop networks.

- The current Adaptive_Lazy scheme is a simplified version of the proposed scheme, where both thresholds n_h and n_l are equal to each other. Furthermore, the transmit-power switches between the minimum and maximum transmit-power levels. It would be interesting to see how gradual increase or decrease in transmit-power level can be incorporated into the Adaptive_Lazy scheme and whether having different n_h and n_l values would improve the WBSN's performance.

- It is clearly interesting to look into a wider range of interference scenarios, for example, how these schemes would perform in scenarios with bursty interference patterns.

- In this thesis, RSSI measurements were used to evaluate and estimate the current channel quality. In scenarios where shadowing caused by the human body adds additional path loss, other channel estimators (e.g. PER) might be explored.

- One could also address scenarios where multiple WBSNs get in close proximity

to each other (for example in shopping malls or hospitals). In such scenarios where all WBSNs are using the same frequency adaptive scheme, all WBSNs might switch to the same operating channel as the other WBSNs. In such conditions, it is interesting to see how these schemes could be further improved to efficiently utilise the current operating channel and avoid the interference caused by homogeneous WBSNs.

REFERENCES

[1] *MiXiM simulator for wireless and mobile networks using OMNeT++*. URL `http://mixim.sourceforge.net (Last accessed July 2014)`.

[2] Supplement to IEEE Standard for Information Technology - Telecommunications and Information Exchange Between Systems - Local and Metropolitan Area Networks - Specific Requirements - Part 11: Wireless LAN Medium Access Control (MAC) and Physical Layer (PHY) Specifications: Higher-Speed Physical Layer Extension in the 2.4 GHz Band. *IEEE Std. 802.11b-1999*, pages i–90, 2000.

[3] IEEE Standard for Telecommunications and Information Exchange Between Systems - LAN/MAN - Specific Requirements - Part 15: Wireless Medium Access Control (MAC) and Physical Layer (PHY) Specifications for Wireless Personal Area Networks (WPANs). *IEEE Std 802.15.1-2002*, pages 1–473, June 2002.

[4] IEEE Standard for Information Technology - Telecommunications and Information Exchange Between Systems - Local and Metropolitan Area Networks - Specific Requirements Part II: Wireless LAN Medium Access Control (MAC) and Physical Layer (PHY) Specifications. *IEEE Std 802.11g-2003 (Amendment to IEEE Std 802.11, 1999 Edn. (Reaff 2003) as amended by IEEE Stds 802.11a-1999, 802.11b-1999, 802.11b-1999/Cor 1-2001, and 802.11d-2001)*, pages i–67, 2003.

[5] IEEE Standard for Information Technology - Telecommunications and Information Exchange Between Systems - Local and Metropolitan Area Networks - Specific Requirements. - Part 15.1: Wireless Medium Access Control (MAC) and Physical Layer (PHY) Specifications for Wireless Personal Area Networks (WPANs). *IEEE Std 802.15.1-2005 (Revision of IEEE Std 802.15.1-2002)*, pages 1–580, 2005.

[6] IEEE Standard for Information technology - Local and metropolitan area networks - Specific requirements - Part 22: Cognitive Wireless RAN Medium Access Control (MAC) and Physical Layer (PHY) specifications: Policies and procedures for operation in the TV Bands. *IEEE Std 802.22-2011*, pages 1–680, July 2011.

[7] IEEE Standard for Local and metropolitan area networks - Part 15.6: Wireless Body Area Networks. *IEEE Std 802.15.6-2012*, pages 1–271, February 2012.

[8] *INET Framework for OMNeT++ Manual*, June 2012. URL `http://inet.omnetpp.org/doc/INET/inet-manual-draft.pdf (Last accessed July 2014)`.

[9] IEEE Standard for Local and metropolitan area networks Part 15.4: Low-Rate Wireless Personal Area Networks (LR-WPANs) Amendment 5: Physical Layer Specifications for Low Energy, Critical Infrastructure Monitoring Networks. *IEEE Std 802.15.4k-2013 (Amendment to IEEE Std 802.15.4-2011 as amended by IEEE Std 802.15.4e-2012, IEEE Std 802.15.4f-2012, IEEE Std 802.15.4g-2012, and IEEE Std 802.15.4j-2013)*, pages 1–149, August 2013.

[10] O.G. Adewumi, K. Djouani, and A.M. Kurien. RSSI based indoor and outdoor distance estimation for localization in WSN. In *IEEE International Conference on Industrial Technology (ICIT)*, pages 1534–1539, February 2013.

[11] O.B. Akan, O. Karli, and O. Ergul. Cognitive radio sensor networks. *IEEE Network*, 23(4):34–40, July 2009.

[12] I.F. Akyildiz, Weilian Su, Y. Sankarasubramaniam, and E. Cayirci. Wireless Sensor Networks: A Survey. *Computer Networks*, 38(4):393–422, 2002.

[13] I.F. Akyildiz, Weilian Su, Y. Sankarasubramaniam, and E. Cayirci. A survey on sensor networks. *IEEE Communications Magazine*, 40(8):102–114, August 2002.

[14] Hande Alemdar and Cem Ersoy. Wireless Sensor Networks for Healthcare: A Survey. *Computer Networks*, 54(15):2688–2710, 2010.

[15] Saima Ali, Ehsan Tabatabaei Yazdi, and Andreas Willig. Investigations on passive discovery schemes for IEEE 802.15.4 based Body Sensor Networks. In *Australasian Telecommunication Networks and Applications Conference (ATNAC)*, pages 89–94, November 2013.

[16] ZigBee Alliance. *IEEE 802.15. 4, ZigBee standard*, 2009. URL `http://www.zigbee.org (Last accessed July 2014)`.

[17] P. Amaro, R. Cortesao, J. Landeck, and P. Santos. Implementing an Advanced Meter Reading infrastructure using a Z-Wave compliant Wireless Sensor Network. In *Proceedings of the 3rd International Youth Conference on Energetics (IYCE)*, pages 1–6, July 2011.

[18] L. Angrisani, M. Bertocco, D. Fortin, and A. Sona. Assessing coexistence problems of IEEE 802.11b and IEEE 802.15.4 wireless networks through cross-layer measurements. In *IEEE Instrumentation and Measurement Technology Conference Proceedings*, pages 1–6, May 2007.

[19] L. Angrisani, M. Bertocco, D. Fortin, and A. Sona. Experimental Study of Coexistence Issues Between IEEE 802.11b and IEEE 802.15.4 Wireless Networks.

IEEE Transactions on Instrumentation and Measurement, 57(8):1514–1523, August 2008.

[20] J. Ansari, T. Ang, and P. Mahonen. Spectrum Agile Medium Access Control Protocol for Wireless Sensor Networks. In *7th Annual IEEE Communications Society Conference on Sensor Mesh and Ad Hoc Communications and Networks (SECON)*, pages 1–9, June 2010.

[21] Junaid Ansari and Petri Mähönen. Channel Selection in Spectrum Agile and Cognitive MAC Protocols for Wireless Sensor Networks. In *Proceedings of the 8th ACM International Workshop on Mobility Management and Wireless Access*, MobiWac '10, pages 83–90, New York, NY, USA, 2010.

[22] Junaid Ansari, Xi Zhang, and Petri Mahonen. Multi-radio Medium Access Control Protocol for Wireless Sensor Networks. *International Journal of Sensor Networks*, 8(1):47–61, 2010.

[23] Junaid Ansari, Tobias Ang, and Petri Mähönen. WiSpot: fast and reliable detection of Wi-Fi networks using IEEE 802.15.4 radios. In *Proceedings of the 9th ACM international symposium on Mobility management and wireless access*, MobiWac '11, pages 35–44, New York, NY, USA, 2011.

[24] Kenneth Bannister, Gianni Giorgetti, and Sandeep KS Gupta. Wireless sensor networking for hot applications: Effects of temperature on signal strength, data collection and localization. In *Proceedings of the 5th Workshop on Embedded Networked Sensors (HotEmNets' 08)*. Citeseer, 2008.

[25] Hemant M. Baradkar and Sudhir G. Akojwar. Implementation of Energy Detection Method for Spectrum Sensing in Cognitive Radio Based Embedded Wireless Sensor Network Node. In *International Conference on Electronic Systems, Signal Processing and Computing Technologies (ICESC)*, pages 490–495, January 2014.

[26] F. Bashir, Woon-Sung Baek, P. Sthapit, D. Pandey, and Jae-Young Pyun. Coordinator assisted passive discovery for mobile end devices in IEEE 802.15.4. In *IEEE Consumer Communications and Networking Conference (CCNC)*, pages 601–604, January 2013.

[27] R. Bellazreg, N. Boudriga, and Sunshin An. Border surveillance using sensor based thick-lines. In *International Conference on Information Networking (ICOIN)*, pages 221–226, January 2013.

[28] Kaigui Bian, Jung-Min Park, and Ruiliang Chen. A quorum-based framework for establishing control channels in dynamic spectrum access networks. In *Proceedings of the 15th ACM Annual International Conference on Mobile Computing and Networking*, MobiCom '09, pages 25–36, New York, NY, USA, 2009.

[29] Douglas M. Blough, Mauro Leoncini, Giovanni Resta, and Paolo Santi. The K-Neigh Protocol for Symmetric Topology Control in Ad Hoc Networks. In *Proceedings of the 4th ACM International Symposium on Mobile Ad Hoc Networking & Computing*, MobiHoc '03, pages 141–152, New York, NY, USA, 2003.

[30] Steven A. Borbash, Anthony Ephremides, and Michael J. McGlynn. An Asynchronous Neighbor Discovery Algorithm for Wireless Sensor Networks. *Ad Hoc Networks*, 5(7):998–1016, September 2007.

[31] A. Boulis, D. Smith, D. Miniutti, L. Libman, and Y. Tselishchev. Challenges in body area networks for healthcare: the MAC. *IEEE Communications Magazine*, 50(5):100–106, May 2012.

[32] Athanassios Boulis. *Castalia A simulator for Wireless Sensor Networks and Body Area Networks User's Manual*, 2010.

URL `https://forge.nicta.com.au/docman/view.php/301/592/Castalia+-+User+Manual.pdf` (Last accessed July 2014).

[33] G. Bravos and A.G. Kanatas. Energy consumption and trade-offs on wireless sensor networks. In *IEEE 16th International Symposium on Personal, Indoor and Mobile Radio Communications (PIMRC)*, volume 2, pages 1279–1283, September 2005.

[34] J.M.L.P. Caldeira, J.J.P.C. Rodrigues, and P. Lorenz. Toward ubiquitous mobility solutions for body sensor networks on healthcare. *IEEE Communications Magazine*, 50(5):108–115, May 2012.

[35] E. Callaway, P. Gorday, L. Hester, J.A. Gutierrez, M. Naeve, B. Heile, and V. Bahl. Home networking with IEEE 802.15.4: a developing standard for low-rate wireless personal area networks. *IEEE Communications Magazine*, 40(8):70–77, August 2002.

[36] A.M. Canthadai, S. Radhakrishnan, and V. Sarangan. Multi-Radio Wireless Sensor Networks: Energy Efficient Solutions for Radio Activation. In *IEEE Global Telecommunications Conference (GLOBECOM)*, pages 1–5, December 2010.

[37] Liting Cao, Jingwen Tian, and Yanxia Liu. Remote Real Time Automatic Meter Reading System Based on Wireless Sensor Networks. In *3rd International Conference on Innovative Computing Information and Control (ICICIC '08)*, pages 591–591, June 2008.

[38] Liting Cao, Jingwen Tian, and Yanxia Liu. Remote Wireless Automatic Meter Reading System Based on Wireless Mesh Networks and Embedded Technology. In *5th IEEE International Symposium on Embedded Computing (SEC '08)*, pages 192–197, October 2008.

[39] Min Chen, Sergio Gonzalez, Athanasios Vasilakos, Huasong Cao, and Victor C. Leung. Body Area Networks: A Survey. *Mobile Networks and Applications*, 16(2):171–193, April 2011.

[40] Kaushik R. Chowdhury, Nagesh Nandiraju, Pritam Chanda, Dharma P. Agrawal, and Qing-An Zeng. Channel allocation and medium access control for wireless sensor networks. *Ad Hoc Networks*, 7(2):307–321, 2009.

[41] K.R. Chowdhury and I.F. Akyildiz. Interferer Classification, Channel Selection and Transmission Adaptation for Wireless Sensor Networks. In *IEEE International Conference on Communications (ICC '09)*, pages 1–5, June 2009.

[42] Scott L Collins, Luís MA Bettencourt, Aric Hagberg, Renee F Brown, Douglas I Moore, Greg Bonito, Kevin A Delin, Shannon P Jackson, David W Johnson, Scott C Burleigh, et al. New opportunities in ecological sensing using wireless sensor networks. *Frontiers in Ecology and the Environment*, 4(8): 402–407, 2006.

[43] Moteiv Corporation. Tmote Sky Datasheet, 2006. URL `http://www.eecs.harvard.edu/konrad/projects/shimmer/references/tmote-sky-datasheet.pdf (Last accessed July 2014)`.

[44] P. Corral, B. Coronado, A.C. De Castro Lima, and O. Ludwig. Design of Automatic Meter Reading based on ZigBee. *IEEE Latin America Transactions (Revista IEEE America Latina)*, 10(1):1150–1155, January 2012.

[45] F.M. Costa and H. Ochiai. A Comparison of Modulations for Energy Optimization in Wireless Sensor Network Links. In *IEEE Global Telecommunications Conference (GLOBECOM)*, pages 1–5, December 2010.

[46] P. Costa, M. Cesana, S. Brambilla, L. Casartelli, and L. Pizziniaco. A cooperative approach for topology control in Wireless Sensor Networks: Experimental

and simulation analysis. In *International Symposium on a World of Wireless, Mobile and Multimedia Networks (WoWMoM)*, pages 1–10, June 2008.

[47] *MICAz Wireless Measurement System*. Crossbow Technology, San Jose, California, 2004. URL `http://www.openautomation.net/uploadsproductos/micaz_datasheet.pdf (Last accessed July 2014)`.

[48] Xuewu Dai, J.E. Mitchell, Yang Yang, I. Glover, K. Sasloglou, R. Atkinson, I. Panella, J. Strong, W. Schiffers, and P. Dutta. Development and validation of a simulator for wireless data acquisition in gas turbine engine testing. *IET Wireless Sensor Systems*, 3(3):183–192, September 2013.

[49] F. De Stefani, P. Gamba, E. Goldoni, A. Savioli, D. Silvestri, and F. Toffalini. REnvDB, a RESTful Database for Pervasive Environmental Wireless Sensor Networks. In *IEEE 30th International Conference on Distributed Computing Systems Workshops (ICDCSW)*, pages 206–212, June 2010.

[50] I. Demirkol, C. Ersoy, and F. Alagoz. MAC protocols for wireless sensor networks: a survey. *IEEE Communications Magazine*, 44(4):115–121, April 2006.

[51] C. Diallo, M. Marot, and M. Becker. Link Quality and Local Load Balancing Routing Mechanisms in Wireless Sensor Networks. In *6th Advanced International Conference on Telecommunications (AICT)*, pages 306–315, May 2010.

[52] C. Diallo, M. Marot, and M. Becker. A distributed link quality based d-clustering protocol for dense ZigBee sensor networks. In *IFIP Wireless Days (WD)*, pages 1–6, October 2010.

[53] A.L. Diedrichs, M.I. Robles, F. Bromberg, G. Mercado, and D. Dujovne. Characterization of LQI behavior in WSN for glacier area in Patagonia Argentina. In *4th Argentine Symposium and Conference on Embedded Systems (SASE/CASE)*, pages 1–6, August 2013.

[54] L.E. Doyle, P.D. Sutton, K.E. Nolan, J. Lotze, B. Ozgul, T.W. Rondeau, S.A. Fahmy, H. Lahlou, and L.A. DaSilva. Experiences from the IRIS Testbed in Dynamic Spectrum Access and Cognitive Radio Experimentation. In *IEEE Symposium on New Frontiers in Dynamic Spectrum*, pages 1–8, April 2010.

[55] Prabal Dutta and David Culler. Practical Asynchronous Neighbor Discovery and Rendezvous for Mobile Sensing Applications. In *Proceedings of the 6th ACM Conference on Embedded Network Sensor Systems*, SenSys '08, pages 71–84, New York, NY, USA, 2008.

[56] Jae-Young Pyun Faisal Bashir Hussain. Coordinator Discovery and Association in Beacon-Enabled IEEE 802.15.4 Network. *International Journal of Distributed Sensor Networks*, pages 1–11, 2013.

[57] K. Fitzpatrick, M.A. Brewer, and S. Turner. Another look at pedestrian walking speed. *Transportation Research Record: Journal of the Transportation Research Board*, 1982(1):21–29, 2006.

[58] Yong Fu, Mo Sha, G. Hackmann, and Chenyang Lu. Practical control of transmission power for Wireless Sensor Networks. In *20th IEEE International Conference on Network Protocols (ICNP)*, pages 1–10, October 2012.

[59] S. Ganesh and R. Amutha. Efficient and secure routing protocol for wireless sensor networks through SNR based dynamic clustering mechanisms. *Journal of Communications and Networks*, 15(4):422–429, August 2013.

[60] R. Gomaa, I. Adly, K. Sharshar, A. Safwat, and H. Ragai. ZigBee wireless sensor network for radiation monitoring at nuclear facilities. In *6th Joint IFIP Wireless and Mobile Networking Conference (WMNC)*, pages 1–4, April 2013.

[61] Dawei Gong and Yuanyuan Yang. Low-latency SINR-based data gathering in wireless sensor networks. In *Proceedings of IEEE INFOCOM*, pages 1941–1949, April 2013.

[62] Ramakrishna Gummadi, David Wetherall, Ben Greenstein, and Srinivasan Seshan. Understanding and mitigating the impact of RF interference on 802.11 networks. In *Proceedings of the ACM conference on Applications, technologies, architectures, and protocols for computer communications*, SIGCOMM '07, pages 385–396, New York, NY, USA, 2007.

[63] V.C. Gungor, Bin Lu, and G.P. Hancke. Opportunities and Challenges of Wireless Sensor Networks in Smart Grid. *IEEE Transactions on Industrial Electronics*, 57(10):3557–3564, October 2010.

[64] Gregory Hackmann, Octav Chipara, and Chenyang Lu. Robust Topology Control for Indoor Wireless Sensor Networks. In *Proceedings of the 6th ACM Conference on Embedded Network Sensor Systems*, SenSys '08, pages 57–70, New York, NY, USA, 2008.

[65] Jan Hauer. TKN15.4: An IEEE 802.15.4 MAC Implementation for TinyOS 2. TKN Technical Report Series TKN-08-003, Telecommunication Networks Group, Technical University of Berlin, March 2009. URL `http://www.tkn.tu-berlin.de/fileadmin/fg112/Papers/TKN154.pdf` `(Last accessed July 2014)`.

[66] Jan-Hinrich Hauer, Vlado Handziski, and Adam Wolisz. Experimental Study of the Impact of WLAN Interference on IEEE 802.15.4 Body Area Networks. 5432:17–32, 2009.

[67] Jason Hill, Robert Szewczyk, Alec Woo, Seth Hollar, David Culler, and Kristofer Pister. System Architecture Directions for Networked Sensors. *ACM SIGARCH Computer Architecture News*, 28(5):93–104, November 2000.

[68] P. Honeine, F. Mourad, M. Kallas, H. Snoussi, H. Amoud, and C. Francis. Wireless sensor networks in biomedical: Body area networks. In *7th In-*

ternational Workshop on Systems, Signal Processing and their Applications (WOSSPA), pages 388–391, May 2011.

[69] James Hou, Benjamin Chang, Dae-Ki Cho, and Mario Gerla. Minimizing 802.11 interference on ZigBee medical sensors. In *Proceedings of the Fourth International Conference on Body Area Networks*, BodyNets '09, pages 5:1–5:8, ICST, Brussels, Belgium, Belgium, 2009.

[70] I. Howitt. WLAN and WPAN coexistence in UL band. *IEEE Transactions on Vehicular Technology*, 50(4):1114–1124, July 2001.

[71] I. Howitt and J.A. Gutierrez. IEEE 802.15.4 low rate - wireless personal area network coexistence issues. In *IEEE Wireless Communications and Networking (WCNC)*, volume 3, pages 1481–1486, March 2003.

[72] Qian Hu and Zhenzhou Tang. An adaptive transmit power scheme for wireless sensor networks. In *3rd IEEE International Conference on Ubi-media Computing (U-Media)*, pages 12–16, July 2010.

[73] Tingpei Huang, Haiming Chen, Li Cui, and Yuqing Zhang. EasiND: Neighbor Discovery in Duty-Cycled Asynchronous Multichannel Mobile WSNs. *International Journal of Distributed Sensor Networks*, 2013.

[74] M.N. Jambli, H. Lenando, K. Zen, S.M. Suhaili, and A. Tully. Simulation Tools for Mobile Ad-hoc Sensor Networks: A State-of-the-Art Survey. In *International Conference on Advanced Computer Science Applications and Technologies (ACSAT)*, pages 1–6, November 2012.

[75] Jaein Jeong, D. Culler, and Jae-Hyuk Oh. Empirical Analysis of Transmission Power Control Algorithms for Wireless Sensor Networks. In *4th International Conference on Networked Sensing Systems (INSS '07)*, pages 27–34, June 2007.

[76] A. Jimenez, S. Jimenez, P. Lozada, and C. Jimenez. Wireless Sensors Network in the Efficient Management of Greenhouse Crops. In *9th International Conference on Information Technology: New Generations (ITNG)*, pages 680–685, April 2012.

[77] Arvind Kandhalu, Karthik Lakshmanan, and Ragunathan (Raj) Rajkumar. U-connect: A Low-latency Energy-efficient Asynchronous Neighbor Discovery Protocol. In *Proceedings of the 9th ACM/IEEE International Conference on Information Processing in Sensor Networks*, IPSN '10, pages 350–361, New York, USA, 2010.

[78] M.B. Kannamma, B. Chanthini, and D. Manivannan. Controlling and monitoring process in industrial automation using ZigBee. In *International Conference on Advances in Computing, Communications and Informatics (ICACCI)*, pages 806–810, August 2013.

[79] V. Kapnadak and E.J. Coyle. Optimal non-uniform deployment of sensors for detection in single-hop Wireless Sensor Networks. In *8th Annual IEEE Communications Society Conference on Sensor, Mesh and Ad Hoc Communications and Networks (SECON)*, pages 89–97, June 2011.

[80] Holger Karl and Andreas Willig. *Protocols and architectures for wireless sensor networks*. John Wiley & Sons, 2007.

[81] Samuel Karlin and Howard M. Taylor. *A First Course in Stochastic Processes*. Academic Press, San Diego, California, second edition, 1975.

[82] Samuel Karlin and Howard M. Taylor. *A Second Course in Stochastic Processes*. Academic Press, San Diego, California, 1981.

[83] N. Karowski, A.C. Viana, and A. Wolisz. Optimized asynchronous multi-channel neighbor discovery. In *Proceedings of IEEE INFOCOM*, pages 536–540, April 2011.

[84] N. Karowski, A.C. Viana, and A. Wolisz. Optimized Asynchronous Multi-channel Discovery of IEEE 802.15.4-Based Wireless Personal Area Networks. *IEEE Transactions on Mobile Computing*, 12(10):1972–1985, October 2013.

[85] Arpit Kasture, Akshay Raut, and Swaroop Thool. Visualization of Wireless Sensor Network by a Java Framework for Security in Defense Surveillance. In *International Conference on Electronic Systems, Signal Processing and Computing Technologies (ICESC)*, pages 256–261, January 2014.

[86] R. Khalili, D.L. Goeckel, D. Towsley, and A. Swami. Neighbor Discovery with Reception Status Feedback to Transmitters. In *Proceedings of IEEE INFOCOM*, pages 1–9, March 2010.

[87] Hyunchul Kim and Jungsuk Kim. Energy-efficient resource management in Wireless Sensor Network. In *IEEE Topical Conference on Wireless Sensors and Sensor Networks (WiSNet)*, pages 69–72, January 2011.

[88] Youngmin Kim, Hyojeong Shin, and Hojung Cha. Y-MAC: An Energy-Efficient Multi-channel MAC Protocol for Dense Wireless Sensor Networks. In *Proceedings of the 7th IEEE Computer Society International Conference on Information Processing in Sensor Networks*, IPSN '08, pages 53–63, Washington, DC, USA, 2008.

[89] A.V. Kini, N. Singhal, and S. Weber. Performance of a WSN in the Presence of Channel Variations and Interference. In *IEEE Wireless Communications and Networking Conference (WCNC)*, pages 2899–2904, March 2008.

[90] JeongGil Ko, Tia Gao, and Andreas Terzis. Empirical study of a medical sensor application in an urban emergency department. In *Proceedings of the 4th International Conference on Body Area Networks*, BodyNets '09, pages 10:1–10:8, ICST, Brussels, Belgium, 2009.

[91] M. Kubisch, H. Karl, A. Wolisz, L.C. Zhong, and J. Rabaey. Distributed algorithms for transmission power control in wireless sensor networks. In *IEEE Wireless Communications and Networking (WCNC)*, volume 1, pages 558–563, March 2003.

[92] S Kumar, K Ovsthus, et al. An Industrial Perspective on Wireless Sensor Networks - A Survey of Requirements, Protocols, and Challenges. *IEEE Communications Surveys Tutorials*, PP(99):1–22, 2014.

[93] N Kushalnagar, G Montenegro, C Schumacher, et al. IPv6 over low-power wireless personal area networks (6LoWPANs): overview, assumptions, problem statement, and goals. *RFC4919*, 10, August 2007.

[94] Kyung-Sup Kwak, S. Ullah, and N. Ullah. An overview of IEEE 802.15.6 standard. In *the 3rd International Symposium on Applied Sciences in Biomedical and Communication Technologies (ISABEL)*, pages 1–6, November 2010.

[95] M. Lagana, I. Glaropoulos, V. Fodor, and C. Petrioli. Modeling and estimation of partially observed WLAN activity for cognitive WSNs. In *IEEE Wireless Communications and Networking Conference (WCNC)*, pages 1526–1531, April 2012.

[96] LAN/MAN Standards Committee of the IEEE Computer Society. *802.15.4-2003 - IEEE Standard for Telecommunications and Information Exchange Between Systems - LAN/MAN Specific Requirements - Part 15: Wireless Medium Access Control (MAC) and Physical Layer (PHY) Specifications for Low Rate Wireless Personal Area Networks (WPAN)*, October 2003.

[97] LAN/MAN Standards Committee of the IEEE Computer Society. *IEEE Standard for Information technology - Telecommunications and information exchange between systems - Local and metropolitan area networks - Specific*

requirements - Part 15.4: Wireless Medium Access Control (MAC) and Physical Layer (PHY) Specifications for Low Rate Wireless Personal Area Networks (LR-WPANs), September 2006. Revision of 2006.

[98] Benoît Latré, Bart Braem, Ingrid Moerman, Chris Blondia, and Piet Demeester. A Survey on Wireless Body Area Networks. *Wireless Networks*, 17 (1):1–18, January 2011.

[99] Jungwook Lee and Kwangsue Chung. An Efficient Transmission Power Control Scheme for Temperature Variation in Wireless Sensor Networks. *Sensors*, 11 (3):3078–3093, 2011.

[100] Philip Levis and David Gay. *TinyOS programming*. Cambridge University Press, Cambridge, UK, 2009.

[101] Zhenyu Liao, Sheng Dai, and Chong Shen. Precision agriculture monitoring system based on wireless sensor networks. In *IET International Conference on Wireless Communications and Applications (ICWCA)*, pages 1–5, October 2012.

[102] Shan Lin, Jingbin Zhang, Gang Zhou, Lin Gu, John A. Stankovic, and Tian He. ATPC: Adaptive Transmission Power Control for Wireless Sensor Networks. In *Proceedings of the 4th ACM International Conference on Embedded Networked Sensor Systems*, SenSys '06, pages 223–236, New York, NY, USA, 2006.

[103] Shan Lin, Gang Zhou, K. Whitehouse, Yafeng Wu, J.A. Stankovic, and Tian He. Towards Stable Network Performance in Wireless Sensor Networks. In *30th IEEE Real-Time Systems Symposium (RTSS)*, pages 227–237, December 2009.

[104] Wei Lin. Real time monitoring of electrocardiogram through IEEE 802.15.4

network. In *8th International Conference Expo on Emerging Technologies for a Smarter World (CEWIT)*, pages 1–6, November 2011.

[105] Chen Liu, Dingyi Fang, Zhe Yang, Xiaojiang Chen, Wei Wang, Tianzhang Xing, Na An, and Lin Cai. RDL: A novel approach for passive object localization in WSN based on RSSI. In *IEEE International Conference on Communications (ICC)*, pages 586–590, June 2012.

[106] Zhiwu Liu and Wei Wu. A Dynamic Multi-radio Multi-channel MAC Protocol for Wireless Sensor Networks. In *2nd International Conference on Communication Software and Networks (ICCSN)*, pages 105–109, February 2010.

[107] Hanjiang Luo, Kaishun Wu, Zhongwen Guo, Lin Gu, and L.M. Ni. Ship Detection with Wireless Sensor Networks. *IEEE Transactions on Parallel and Distributed Systems*, 23(7):1336–1343, July 2012.

[108] J. Markkula and J. Haapola. Impact of smart grid traffic peak loads on shared LTE network performance. In *IEEE International Conference on Communications (ICC)*, pages 4046–4051, June 2013.

[109] S. McCanne, S. Floyd, K. Fall, K. Varadhan, et al. *The Network Simulator NS-2*. URL `http://www.isi.edu/nsnam/ns (Last accessed July 2014)`.

[110] S. Mirshahi, S. Uysal, and A. Akbari. Integration of RFID and WSN for supply chain intelligence system. In *International Conference on Electronics, Computers and Artificial Intelligence (ECAI)*, pages 1–6, June 2013.

[111] U. Mitra, B.A. Emken, Sangwon Lee, Ming Li, V. Rozgic, G. Thatte, H. Vathsangam, D. Zois, M. Annavaram, S. Narayanan, M. Levorato, D. Spruijt-Metz, and G. Sukhatme. KNOWME: a case study in wireless body area sensor network design. *IEEE Communications Magazine*, 50(5):116–125, May 2012.

[112] O. Modeler. *OPNET Technologies, Inc.* URL `http://www.opnet.com (Last accessed July 2014)`.

[113] Amirhossein Moravejosharieh and Ehsan Tabatabaei Yazdi. Study of Resource Utilization in IEEE 802.15.4 Wireless Body Sensor Network, Part I: The Need for Enhancement. In *IEEE 16th International Conference on Computational Science and Engineering (CSE)*, pages 1226–1231, December 2013.

[114] Amirhossein Moravejosharieh, Ehsan Tabatabaei Yazdi, and Andreas Willig. Study of resource utilization in IEEE 802.15.4 Wireless Body Sensor Network, Part II: Greedy Channel Utilization. In *19th IEEE International Conference on Networks (ICON)*, pages 1–6, December 2013.

[115] Amirhossein Moravejosharieh, Ehsan Tabatabaei Yazdi, Andreas Willig, and Krzysztof Pawlikowski. Coupling Power and Frequency Adaptation for Interference Mitigation in IEEE 802.15.4-Based Mobile Body Sensor Networks: Part II. In *Australasian Telecommunication Networks and Applications Conference (ATNAC)*, 2014. (Accepted).

[116] R.N. Murty, G. Mainland, I. Rose, A.R. Chowdhury, A. Gosain, J. Bers, and M. Welsh. CitySense: An Urban-Scale Wireless Sensor Network and Testbed. In *IEEE Conference on Technologies for Homeland Security*, pages 583–588, May 2008.

[117] R. Musaloiu-E and A. Terzis. Minimising the effect of WiFi interference in 802.15. 4 wireless sensor networks. *International Journal of Sensor Networks*, 3(1):43–54, 2008.

[118] Arnab Nandi and Sumit Kundu. On Energy Level Performance of Adaptive Power Based WSN in Presence of Fading. *International Journal of Energy, Information & Communications*, 3(2), 2012.

[119] Swetha Narayanaswamy, Vikas Kawadia, R. S. Sreenivas, and P. R. Kumar. Power Control in Ad-Hoc Networks: Theory, Architecture, Algorithm and Implementation of the COMPOW Protocol. In *in European Wireless Conference*, pages 156–162, 2002.

[120] Nhat-Quang Nhan, Minh-Thanh Vo, Tuan-Duc Nguyen, and Huu-Tue Huynh. Improving the performance of mobile data collecting systems for electricity meter reading using Wireless Sensor Network. In *International Conference on Advanced Technologies for Communications (ATC)*, pages 241–246, October 2012.

[121] S. Niranchana and E. Dinesh. Optimized tracking and detection of target nodes in wireless sensor networks. In *International Conference on Information Communication and Embedded Systems (ICICES)*, pages 695–700, February 2013.

[122] Minsu Park, Hyunsung Kim, and Sung-Woon Lee. User Authentication for Hiererchical Wireless Sensor Networks. In *14th ACIS International Conference on Software Engineering, Artificial Intelligence, Networking and Parallel/Distributed Computing (SNPD)*, pages 203–208, July 2013.

[123] A. Paventhan, Sai Krishna, Hari Krishna, R. Kesavan, and N.Mohan Ram. WSN Monitoring for Agriculture: Comparing SNMP and Emerging CoAP Approaches. In *Texas Instruments India Educators' Conference (TIIEC)*, pages 353–358, April 2013.

[124] P. Pelegris and K. Banitsas. Investigating the efficiency of IEEE 802.15.4 for medical monitoring applications. In *Annual International Conference of the IEEE Engineering in Medicine and Biology Society (EMBC)*, pages 8215–8218, August 2011.

[125] M. Petrova, Lili Wu, P. Mahonen, and J. Riihijarvi. Interference Measurements

on Performance Degradation between Colocated IEEE 802.11g/n and IEEE 802.15.4 Networks. In *6th International Conference on Networking (ICN)*, pages 93–93, April 2007.

[126] Wint Yi Poe and Jens B. Schmitt. Node deployment in large wireless sensor networks: coverage, energy consumption, and worst-case delay. In *ACM Asian Internet Engineering Conference*, AINTEC '09, pages 77–84, New York, NY, USA, 2009.

[127] Joseph Polastre, Jason Hill, and David Culler. Versatile low power media access for wireless sensor networks. In *Proceedings of the 2nd ACM International Conference on Embedded networked sensor systems*, SenSys '04, pages 95–107, New York, NY, USA, 2004.

[128] S. Pollin, I. Tan, B. Hodge, C. Chun, and A. Bahai. Harmful Coexistence Between 802.15.4 and 802.11: A Measurement-based Study. In *3rd International Conference on Cognitive Radio Oriented Wireless Networks and Communications (CrownCom)*, pages 1–6, May 2008.

[129] Sofie Pollin, Mustafa Ergen, Michael Timmers, Antoine Dejonghe, Liesbet van der Perre, Francky Catthoor, Ingrid Moerman, and Ahmad Bahai. Distributed cognitive coexistence of 802.15.4 with 802.11. pages 1–5, June 2006.

[130] N. Pustchi and T. Korkmaz. Improving packet reception rate for mobile sinks in wireless sensor networks. In *IEEE International Symposium on a World of Wireless, Mobile and Multimedia Networks (WoWMoM)*, pages 1–9, June 2012.

[131] QualNet. URL `http://www.scalable-networks.com/products/qualnet (Last accessed July 2014)`.

[132] T. S. Rappaport. *Wireless Communications: Principles And Practice, Second Edition*. Pearson Education, 2010.

[133] I. Rasool, N. Salman, and A.H. Kemp. RSSI-based positioning in unknown path-loss model for WSN. In *Sensor Signal Processing for Defence (SSPD)*, pages 1–5, September 2012.

[134] M. Rihan, M. El-Khamy, and M. El-Sharkawy. On ZigBee coexistence in the ISM band: Measurements and simulations. In *International Conference on Wireless Communications in Unusual and Confined Areas (ICWCUCA)*, pages 1–6, August 2012.

[135] Michele Rossi, Nicola Bui, Giovanni Zanca, Luca Stabellini, Riccardo Crepaldi, and Michele Zorzi. SYNAPSE++: Code Dissemination in Wireless Sensor Networks Using Fountain Codes. *IEEE Transactions on Mobile Computing*, 9 (12):1749–1765, December 2010.

[136] L.B. Ruiz, J.M. Nogueira, and A. A F Loureiro. MANNA: a management architecture for wireless sensor networks. *IEEE Communications Magazine*, 41(2):116–125, February 2003.

[137] W. Rukpakavong, I. Phillips, and Lin Guan. Neighbour Discovery for Transmit Power Adjustment in IEEE 802.15.4 Using RSSI. In *4th IFIP International Conference on New Technologies, Mobility and Security (NTMS)*, pages 1–4, February 2011.

[138] P. Santi. The critical transmitting range for connectivity in mobile Ad Hoc networks. *IEEE Transactions on Mobile Computing*, 4(3):310–317, May 2005.

[139] H. Shariatmadari, A. Mahmood, and R. Jantti. Channel ranking based on packet delivery ratio estimation in wireless sensor networks. In *IEEE Wireless Communications and Networking Conference (WCNC)*, pages 59–64, April 2013.

[140] Sai Shen and Dong Wang. Research on Warehouses Management Based on

RFID and WSN Technology. In *2nd International Workshop on Database Technology and Applications (DBTA)*, pages 1–4, November 2010.

[141] R. Sheyibani, E. Sharififar, M. Khosronejad, M.R. Mazaheri, and B. Homayounfar. A Reliable and QoS Aware Multi-path Routing Algorithm in WSNs. In *3rd International Conference on Emerging Intelligent Data and Web Technologies (EIDWT)*, pages 125–132, September 2012.

[142] SooYoung Shin, Sunghyun Choi, HongSeong Park, and WookHyun Kwon. Lecture Notes in Computer Science: Packet Error Rate Analysis of IEEE 802.15.4 Under IEEE 802.11b Interference. 3510:279–288, 2005.

[143] S.Y. Shin, H.S. Park, and W.H. Kwon. Mutual interference analysis of IEEE 802.15.4 and IEEE 802.11b. *Elsevier Computer Networks*, 51(12):3338–3353, 2007.

[144] G.N. Shirazi, Peijie Wang, Xiangxu Dong, Zhi Ang Eu, and Chen-Khong Tham. A QoS network architecture for multi-hop, multi-sink target tracking WSNs. In *11th IEEE Singapore International Conference on Communication Systems (ICCS)*, pages 17–21, November 2008.

[145] K. Sohraby, D. Minoli, and T.F. Znati. *Wireless sensor networks: technology, protocols, and applications*. John Wiley and Sons, 2007.

[146] K. Srinivasan and P. Levis. RSSI is under appreciated. In *Proceedings of the 3rd ACM Workshop on Embedded Networked Sensors (EmNets)*, May 2006.

[147] Carl R. Stevenson, Gerald Chouinard, Zhongding Lei, Wendong Hu, Stephen J. Shellhammer, and Winston Caldwell. IEEE 802.22: The First Cognitive Radio Wireless Regional Area Network Standard. *IEEE Communications Magazine*, 47(1):130–138, January 2009.

[148] Yong Tang, Zhipeng Wang, Tianyu Du, D. Makrakis, and H.T. Mouftah. Study of clear channel assessment mechanism for ZigBee packet transmission under Wi-Fi interference. In *IEEE Consumer Communications and Networking Conference (CCNC)*, pages 765–768, January 2013.

[149] Texas Instruments. *CC2420: Single-Chip 2.4 GHz IEEE 802.15.4 Compliant and ZigBee Ready RF Transceiver*. URL `http://www.ti.com/product/cc2420 (Last accessed July 2014)`.

[150] M. Timmers, S. Pollin, A. Dejonghe, L. Van der Perre, and F. Catthoor. Exploring vs exploiting: Enhanced distributed cognitive coexistence of 802.15.4 with 802.11. In *IEEE Sensors*, pages 613–616, October 2008.

[151] N.F. Timmons and W.G. Scanlon. Analysis of the performance of IEEE 802.15.4 for medical sensor body area networking. In *1st Annual IEEE Communications Society Conference on Sensor and Ad Hoc Communications and Networks (SECON)*, pages 16–24, October 2004.

[152] Emanuele Toscano and Lucia Lo Bello. Cross-Channel Interference in IEEE 802.15.4 Networks. In *Proceedings of the 7th IEEE International Workshop on Factory Communication Systems (WFCS)*, Dresden, Germany, May 2008.

[153] S. Trigui, A. Koubaa, M. Ben Jamaa, I. Chaari, and K. Al-Shalfan. Coordination in a multi-robot surveillance application using Wireless Sensor Networks. In *16th IEEE Mediterranean Electrotechnical Conference (MELECON)*, pages 989–992, March 2012.

[154] Lieven Tytgat, Opher Yaron, Sofie Pollin, Ingrid Moerman, and Piet Demeester. Avoiding collisions between IEEE 802.11 and IEEE 802.15.4 through coexistence aware clear channel assessment. *EURASIP Journal on Wireless Communications and Networking*, 2012(1):1–15, 2012.

[155] A. Vagas. *OMNet++ Discrete Event Simulation System.* URL `http://www.omnetpp.org (Last accessed July 2014)`.

[156] S. Vellingiri, A. Ray, and M. Kande. Wireless infrastructure for oil and gas inventory management. In *39th Annual Conference of the IEEE Industrial Electronics Society (IECON)*, pages 5461–5466, November 2013.

[157] Federico Viani, Paolo Rocca, Manuel Benedetti, Giacomo Oliveri, and Andrea Massa. Electromagnetic passive localization and tracking of moving targets in a WSN-infrastructured environment. *Inverse Problems*, 26(7), 2010.

[158] H. Viswanathan, Baozhi Chen, and D. Pompili. Research challenges in computation, communication, and context awareness for ubiquitous healthcare. *IEEE Communications Magazine*, 50(5):92–99, May 2012.

[159] Minh-Thanh Vo, Truong-Tien Vo, T.T. Thanh Nghi, Tuan-Duc Nguyen, and Chi-Thong Le. Real time Wireless Sensor Network for building automation applications: A simulation study and practical implementation. In *International Conference on Control, Automation and Information Sciences (ICCAIS)*, pages 305–310, November 2013.

[160] R.S. Wagner and R.J. Barton. Performance Comparison of Wireless Sensor Network Standard Protocols in an Aerospace Environment: ISA100.11a and ZigBee Pro. 2011.

[161] Tong Wang, R.C. De Lamare, and P.D. Mitchell. BEACON channel estimation for cooperative wireless sensor networks based on data selection. In *7th International Symposium on Wireless Communication Systems (ISWCS)*, pages 140–144, September 2010.

[162] Christopher JCH Watkins and Peter Dayan. Q-learning. *Machine learning*, 8 (3-4):279–292, 1992.

[163] Andreas Willig, Niels Karowski, and Jan-Hinrich Hauer. Passive discovery of IEEE 802.15.4-based body sensor networks. *Ad Hoc Networks*, 8(7):742–754, 2010.

[164] Kritchai Witheephanich and Martin J. Hayes. On the applicability of model predictive power control to an IEEE 802.15.4 wireless sensor network. In *IET Irish Signals and Systems Conference (ISSC)*, pages 1–8, June 2009.

[165] Yafeng Wu, Matthew Keally, Gang Zhou, and Weizhen Mao. Traffic-Aware Channel Assignment in Wireless Sensor Networks. 5682:479–488, 2009.

[166] T.F. Wykret, L.H.A. Correia, D.F. Macedo, J.C. Giacomin, and L.T. Andrade. Evaluation and avoidance of interference in WSN: A multi-radio node prototype using Dynamic Spectrum Allocation. In *IFIP Wireless Days (WD)*, pages 1–3, November 2013.

[167] Zhou Xiaoguang and Long Wei. The research of network architecture in warehouse management system based on RFID and WSN integration. In *IEEE International Conference on Automation and Logistics (ICAL)*, pages 2556–2560, September 2008.

[168] Wenyuan Xu, Wade Trappe, and Yanyong Zhang. Defending Wireless Sensor Networks from Radio Interference Through Channel Adaptation. *ACM Transactions on Sensor Networks*, 4(4):18:1–18:34, September 2008.

[169] Feng Xue and P. R. Kumar. The Number of Neighbors Needed for Connectivity of Wireless Networks. *Wireless Networks*, 10(2):169–181, March 2004.

[170] Wan Yadong and Duan Shihong. Study on IEEE 802.15.4 link reliability in industrial environment. In *IEEE International Conference on Wireless for Space and Extreme Environments (WiSEE)*, pages 1–7, November 2013.

[171] Guang-Zhong Yang and Magdi Yacoub. Body sensor networks. 2006.

[172] Ehsan Tabatabaei Yazdi, Andreas Willig, and Krzysztof Pawlikowski. On Channel Adaptation in IEEE 802.15.4 Mobile Body Sensor Networks: What can be Gained? In *18th IEEE International Conference on Networks (ICON)*, pages 262–267, December 2012.

[173] Ehsan Tabatabaei Yazdi, Andreas Willig, and Krzysztof Pawlikowski. Shortening Orphan Time in IEEE 802.15.4: What can be gained? In *19th IEEE International Conference on Networks (ICON)*, pages 1–6, December 2013.

[174] Ehsan Tabatabaei Yazdi, Amirhossein Moravejosharieh, and Sayan Kumar Ray. Study of target tracking and handover in Mobile Wireless Sensor Network. In *28th IEEE International Conference on Information Networking (ICOIN)*, pages 120–125, February 2014.

[175] Ehsan Tabatabaei Yazdi, Amirhossein Moravejosharieh, Andreas Willig, and Krzysztof Pawlikowski. Coupling Power and Frequency Adaptation for Interference Mitigation in IEEE 802.15.4-Based Mobile Body Sensor Networks: Part II. In *Australasian Telecommunication Networks and Applications Conference (ATNAC)*, 2014. (Accepted).

[176] Ehsan Tabatabaei Yazdi, Andreas Willig, and Krzysztof Pawlikowski. Coupling Power and Frequency Adaptation for Interference Mitigation in IEEE 802.15.4-Based Mobile Body Sensor Networks. In *9th IEEE International Conference on Intelligent Sensors, Sensor Networks and Information Processing (ISSNIP)*, pages 1–6, April 2014.

[177] Ehsan Tabatabaei Yazdi, Andreas Willig, and Krzysztof Pawlikowski. Frequency Adaptation for Interference Mitigation in IEEE 802.15.4-Based Mobile Body Sensor Networks. *Computer Communications*, 53(0):102–119, 2014. ISSN 0140-3664. URL `http://www.sciencedirect.com/science/article/pii/S014036641400245X`.

[178] Wei Ye, J. Heidemann, and D. Estrin. An energy-efficient MAC protocol for wireless sensor networks. In *Proceedings of the 21st Annual Joint Conference of the IEEE Computer and Communications Societies (INFOCOM)*, volume 3, pages 1567–1576, 2002.

[179] Jennifer Yick, Biswanath Mukherjee, and Dipak Ghosal. Wireless sensor network survey. *Computer Networks*, 52(12):2292–2330, 2008.

[180] Hoi-Jun Yoo, Namjun Cho, and J. Yoo. Low energy wearable body-sensor-network. In *Annual International Conference of the IEEE Engineering in Medicine and Biology Society (EMBC)*, pages 3209–3212, September 2009.

[181] Dae Gil Yoon, Soo Young Shin, Wook-Hyun Kwon, and Hong Seong Park. Packet Error Rate Analysis of IEEE 802.11b under IEEE 802.15.4 Interference. In *63rd IEEE Vehicular Technology Conference (VTC)*, volume 3, pages 1186–1190, May 2006.

[182] DaeGil Yoon, SooYoung Shin, JaeHee Park, HongSeong Park, and WookHyun Kwon. Performance Analysis of IEEE 802.11b Under Multiple IEEE 802.15.4 Interferences. 4517:213–222, 2007.

[183] S.B. Young. Evaluation of pedestrian walking speeds in airport terminals. *Transportation Research Record: Journal of the Transportation Research Board*, 1674:20–26, 1999.

[184] Hongqiang Zhai, Jianfeng Wang, Yuguang Fang, and Dapeng Wu. A dual-channel MAC protocol for mobile Ad Hoc networks. In *IEEE Global Telecommunications Conference Workshops (GlobeCom)*, pages 27–32, November 2004.

[185] Z. Zhao, G.-H. Yang, Q. Liu, V.O.K. Li, and L. Cui. Implementation and application of a multi-radio wireless sensor networks testbed. *IET Wireless Sensor Systems*, 1(4):191–199, December 2011.

[186] Xie Zhijun, He Wei, Lv Linghong, and He Jiaming. The implement of warehouse Management system based on RFID and Wireless Sensor Network. In *IET International Conference on Wireless Sensor Network (IET-WSN)*, pages 98–103, November 2010.

[187] M. Zuniga and B. Krishnamachari. Analyzing the transitional region in low power wireless links. In *1st Annual IEEE Communications Society Conference on Sensor and Ad Hoc Communications and Networks (SECON)*, pages 517–526, October 2004.

[188] Zhang Zuojing and Zhang Haihui. Design of Wireless Monitoring and Warning System for Protected Agriculture Environment. In *6th International Conference on Wireless Communications Networking and Mobile Computing (WiCOM)*, pages 1–5, September 2010.

A. Re-generating the IEEE 802.11 Transmit Spectral Mask

Using equation $\frac{SinX}{X}$ given in Figure 3.2, the different transmit-power between four simultaneous WiFi packets is calculated using a simple Matlab code. Having f_c equal to 2412. The following Matlab command-set generates the desired IEEE 802.11 transmit spectral mask illustrated in Figure A.1.

```
x=-360:0.1:360;
x=(x/720)*4*pi;
Fc=2412;
w=abs(sinc(x));
y=10*log(w);
plot((x*11)+Fc,y,'b');
grid;
```

By zooming in between frequencies 2400 and 2425, similar to Figure A.2, it is observed that for frequencies 2405, 2410, 2415 and 2420, which represent the first four channels of the IEEE 802.15.4 standard, the transmit spectral value in dB would be -7.8746, -0.5498, -1.2549 and -11.0632, respectively.

Considering the transmit spectral mask for all 11 channels of IEEE 802.11 and 16 channels of IEEE 802.15.4, it is possible to calculate all the different TX-powers for all operating frequencies. Table A.1 illustrates all the interference levels caused by

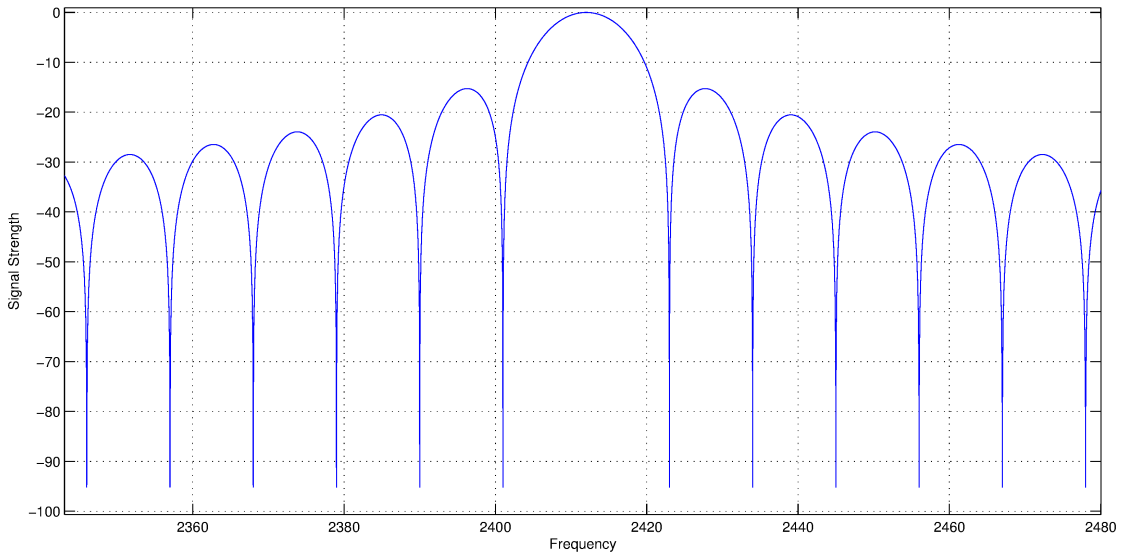

Figure A.1.: Re-generated IEEE 802.11 transmit spectral mask with $f_c = 2412$.

the WiFi Transceiver on different WSN channels when the WiFi's Transmit power is 0 dB.

Channels WSN \ WiFi	2412	2417	2422	2427	2432	2437	2442	2447	2452	2457	2462
2405	-7.875	-24.985	-15.903	-377.834	-20.529	-34.794	-24.525	-30.995	-28.770	-29.781	-34.049
2410	**-0.550**	-7.875	-24.985	-15.903	-377.834	-20.529	-34.794	-24.525	-30.995	-28.770	-29.781
2415	-1.255	**-0.550**	-7.875	-24.985	-15.903	-377.834	-20.529	-34.794	-24.525	-30.995	-28.770
2420	-11.063	-1.255	**-0.550**	-7.875	-24.985	-15.903	-377.834	-20.529	-34.794	-24.525	-30.995
2425	-19.268	-11.063	-1.255	**-0.550**	-7.875	-24.985	-15.903	-377.834	-20.529	-34.794	-24.525
2430	-17.319	-19.268	-11.063	-1.255	**-0.550**	-7.875	-24.985	-15.903	-377.834	-20.529	-34.794
2435	-31.491	-17.319	-19.268	-11.063	-1.255	**-0.550**	-7.875	-24.985	-15.903	-377.834	-20.529
2440	-20.893	-31.491	-17.319	-19.268	-11.063	-1.255	**-0.550**	-7.875	-24.985	-15.903	-377.834
2445	-377.834	-20.893	-31.491	-17.319	-19.268	-11.063	-1.255	**-0.550**	-7.875	-24.985	-15.903
2450	-23.946	-377.834	-20.893	-31.491	-17.319	-19.268	-11.063	-1.255	**-0.550**	-7.875	-24.985
2455	-37.748	-23.946	-377.834	-20.893	-31.491	-17.319	-19.268	-11.063	-1.255	**-0.550**	-7.875
2460	-27.127	-37.748	-23.946	-377.834	-20.893	-31.491	-17.319	-19.268	-11.063	-1.255	**-0.550**
2465	-33.321	-27.127	-37.748	-23.946	-377.834	-20.893	-31.491	-17.319	-19.268	-11.063	-1.255
2470	-30.873	-33.321	-27.127	-37.748	-23.946	-377.834	-20.893	-31.491	-17.319	-19.268	-11.063
2475	-31.700	-30.873	-33.321	-27.127	-37.748	-23.946	-377.834	-20.893	-31.491	-17.319	-19.268
2480	-35.813	-31.700	-30.873	-33.321	-27.127	-37.748	-23.946	-377.834	-20.893	-31.491	-17.319

Table A.1.: Different transmit-power off-set for different frequencies.

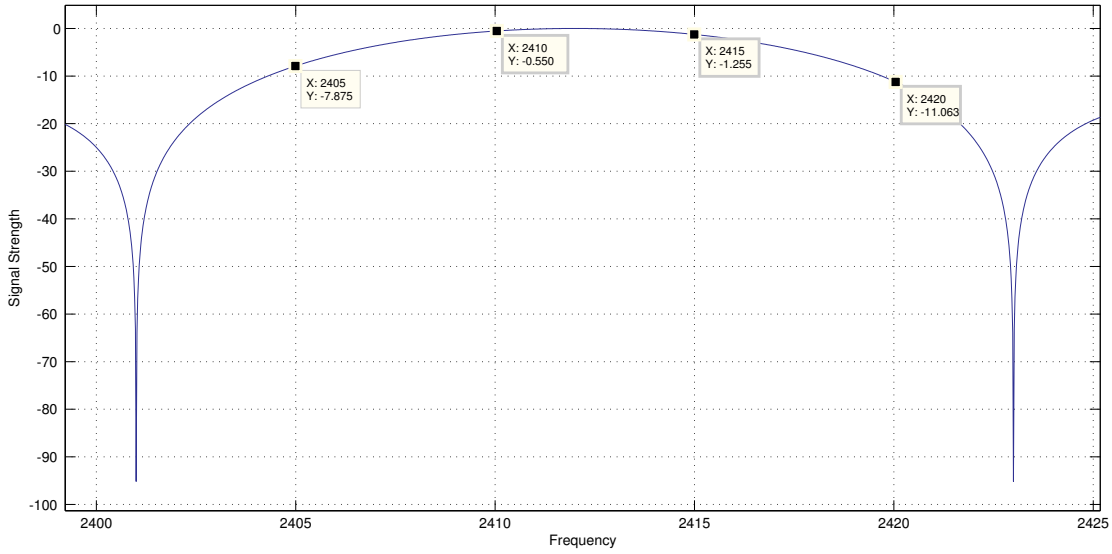

Figure A.2.: A close-up of the IEEE 802.11 transmit spectral mask with $f_c = 2412$.

B. Consumed energy calculations and examples

The formula for calculating the total consumed energy, E_{total} is given in Equation B.1; which is the sum of Power used in state i multiplied by the duration of Time spent in state i.

$$E_{total} = \sum_{i=1}^{S} P_i * T_i \tag{B.1}$$

Equation B.2 calculates the power used at a given transceiver state. P_i is equal to the current drawn from the battery at that transceiver state C_i multiplied by the Voltage of the battery V.

$$P_i = C_i * V \tag{B.2}$$

As an example: the consumed energy of a coordinator node using the IEEE 802.15.4 standard CAP scheme (non-adaptive CAP) for a total simulation time of 864 second (the time that takes a human carrier to walk at a constant speed of 5 km/h from one side of the field to the other) is roughly calculated, assuming that the active period and the super-frame duration are set to 61.44 and 122.88 ms, respectively. This assumption infers that the coordinator spends 50% of its time in sleep state and the rest is spent in active state (either RX or TX mode). Since, it is difficult to know exactly the proportion of the time that the coordinator spends in

RX or TX mode in the active state, and its proportion varies depending on many factors, namely interference and data packet inter-arrival time, etc., only the state with maximum current drainage is considered. Considering Tables 3.1 and 3.2 and Equations B.1 and B.2 the energy consumption of the coordinator is calculated as follows:

$$
\begin{aligned}
&TotalSimulationTime = 864\ s \\
&MaxCurrentatSleepState = 426\ \mu A \\
&MaxCurrentatActiveState = 19.7\ mA
\end{aligned}
$$

$$
\begin{aligned}
P_{Active} &= C_{Active} * V_{Active} \\
&= 19.7\ mA * 3.3\ V = 65.01\ mW \\
P_{Sleep} &= C_{Sleep} * V_{Sleep} \\
&= 426\ \mu A * 3.3\ V = 1.4058\ mW \\
E_{Max} &= \sum_{i=1}^{S} P_i * T_i \\
&= P_{Active} * T_{Active} + P_{Sleep} * T_{Sleep} \\
&= 65.01\ mW * 432\ s + 1.4058\ mW * 432\ s \\
&= 28691.6256\ mJ = 28.7\ Joule
\end{aligned}
$$

Looking at the Maximum consumed energy calculation that was carried out for the non-adaptive CAP scheme of the coordinator node, and the result illustrated in Figure 4.2a indicate that the values are roughly similar. Please, note that this calculation does not consider the guard time[1].

To breakdown the energy and switching costs for scanning all 16 channels the following equations are shown:

[1]The "guard time" is the fraction of time that the coordinator wakes up earlier and before the beginning on the next super-frame and continues listening after the active period is finished. These extra time that the coordinator spends in active state is also considered in the actual simulation results.

$$Time needed for one RSSI measurement = 256\ \mu s$$

$$Time needed to switch to a different channel (PPL) = 192\ \mu s$$

$$Power needed to perform one channel switch = 65.01\ mW$$

$$Power needed to perform one RSSI measurement = 65.01\ mW$$

$$Number of RSSI samples per channel = 8$$

$$\begin{aligned} E_{RSSI\_measurement} &= P_{RSSI\_measurement} * T_{RSSI\_measurement} \\ &= 65.01\ mW * 0.256\ ms = 16.64256\ \mu J \end{aligned}$$

$$\begin{aligned} E_{Channel\_Switch} &= P_{Channel\_Switch} * T_{Channel\_Switch} \\ &= 65.01\ mW * 0.192\ ms = 12.48192\ \mu J \end{aligned}$$

$$\begin{aligned} E_{\substack{Total Consumed Energy For \\ Scanning All 16 Channels}} &= (E_{RSSI\_measurement}) * 8 * 16 \\ &+ (E_{Channel\_Switch}) * 16 \\ &\approx 2.33\ mJ \end{aligned}$$

C. The Influence of Packet Size on Performance

The influence of packet size on the successful reception of data packets in environments with varying interferer traffic intensity λ and density Δ is evaluated in this section. This section selects the no-adaptation scheme proposed in Section 4.1.1 as our baseline schemes. New data packets are generated every second with varying payload size depending of the scheme.

The no-adaptation scheme with **MIN payload**, is the scheme in which the packet payload size is fixed to zero – resulting a packet size of 13 Bytes including the MAC header and CRC Fields. The no-adaptation scheme with **MAX payload**,is a scheme where the maximum payload is selected – resulting a packet size of 127 Bytes. The no-adaptation scheme with **RAN payload**, is the scheme where the length of the generated packet, represent an IID random variable, generated by an uniform distribution between 64 and 102 bytes.

For each combination of *lambda* and Δ, a minimum of 100 replication are performed to reach a maximum relative error of 5% or less, at a 95% confidence level. This simulation uses the same simulation scenario explained in Section 3.2. Our main Performance measure is the success rate, which represents the percentage of data packets successfully transmitted from the sensor node to the corresponding coordinator node and the sensor has successfully received an acknowledgement of that packet from its coordinator node.

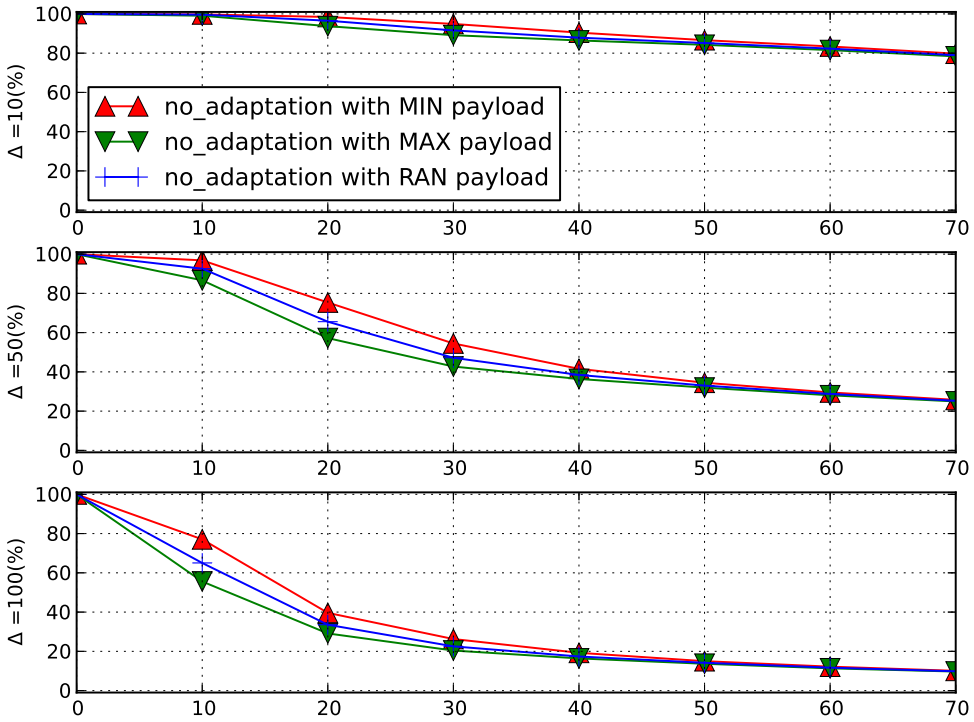

Figure C.1.: The influence of packet size on success rate where Δ=10, 50 and 100.

Looking at the results presented in Figure C.1, it can be clearly seen that scheme with minimum payload size achieves a substantially higher success rate than the scheme with maximum payload size. This noticeable difference in creases as the interferer density Δ increases. However, this this difference is only visible when the interferer intensity is reasonable low – between 10% to 40%. One reason is that as the intensity of the interferers increase the probability of the transmuted data packets being transmitted between the inter-arrival time of the WiFi packets narrows.